# Rate Constants for Abstraction of H from the Fluoromethanes by H, O, F, and OH

(iD) **Donald R. Burgess and** (iD) **Jeffrey A. Manion**

View Online          Export Citation          CrossMark
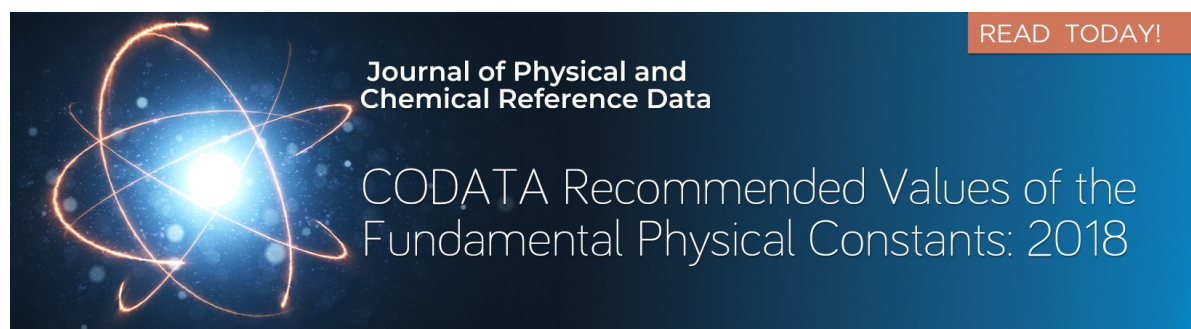
## ARTICLES YOU MAY BE INTERESTED IN

Journal of Physical and
Chemical Reference Data

READ TODAY!

CODATA Recommended Values of the
Fundamental Physical Constants: 2018

AIP Publishing

# Rate Constants for Abstraction of H from the Fluoromethanes by H, O, F, and OH EP

Donald R. Burgess Jr.[a] ID and Jeffrey A. Manion ID

## AFFILIATIONS

Chemical Sciences Division, National Institute of Standards and Technology, Gaithersburg, Maryland 20899, USA

[a]Author to whom correspondence should be addressed: dburgess@nist.gov

## ABSTRACT

In this work, we compiled and critically evaluated rate constants from the literature for abstraction of H from the homologous series consisting of the fluoromethanes ($CH_3F$, $CH_2F_2$, and $CHF_3$) and methane ($CH_4$) by the radicals H atom, O atom, OH, and F atom. These reactions have the form RH + X → R + HX. Rate expressions for these reactions are provided over a wide range of temperatures (300–1800 K). Expanded uncertainty factors $f(2\sigma)$ are provided at both low and high temperatures. We attempted to provide rate constants that were self-consistent within the series—evaluating the system, not just individual reactions. For many of the reactions, the rate constants in the literature are available only over a limited temperature range (or there are no reliable measurements). In these cases, we predicted the rate constants in a self-consistent manner employing relative rates for other reactions in the homologous series using empirical structure–activity relationships, used empirical correlations between rate constants at room temperature and activation energies at high temperatures, and used relative rates derived from *ab initio* quantum chemical calculations to assist in rate constant predictions.

## CONTENTS

## List of Tables

## List of Figures

# 1. Introduction and Background

## 1.1. Hydrofluorocarbon chemistry

In this work, we have compiled, evaluated, and recommended rate constants for a homologous series of reactions for the abstraction of H from the fluoromethanes (and methane) by the radicals H atom, O atom, F atom, and OH. Reactions for methane are included as benchmarks for each series. These series of reactions can be described by the set R–H + X → R + HX,

$$CH_4 + X \rightarrow CH_3 + HX,$$

$$CH_3F + X \rightarrow CH_2F + HX,$$

$$CH_2F_2 + X \rightarrow CHF_2 + HX,$$

$$CHF_3 + X \rightarrow CF_3 + HX,$$
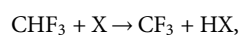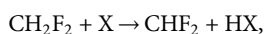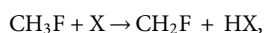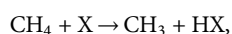
where X = (H, O, OH, F) and HX = (H$_2$, OH, H$_2$O, and HF).

These reactions involving the fluoromethanes are an important set of reference reactions for larger hydrofluorocarbons (HFCs), particularly the fluoroethanes used as refrigerants. They can also be used as references of hydrofluoroolefins (HFOs), hydrofluoroethers (HFEs), and brominated HFCs (used in a variety of applications as refrigerants, fire suppressants, blowing agents, and cleaning solvents). Uses of these chemical classes of compounds are regulated because of their global warming potential (GWP), and uses of the brominated compounds are regulated because of their ozone depletion potential (ODP).[1,2]

A number of common refrigerant agents that are used are difluoromethane (CH$_2$F$_2$, R32), 1,1-difluoroethane (CH$_3$CHF$_2$, R-152a), 1,1,1-trifluoroethane (CH$_3$CF$_3$, R-143a), 1,1,2-trifluoroethane (CH$_2$FCHF$_2$, R-134a), pentafluoroethane (CHF$_2$CF$_3$, R-125), 1,1,1,3,3,3-hexafluoropropane (CF$_3$CH$_2$CF$_3$, HFC-236fa), 1,1,1,2,3,3,3-heptafluoropropane (CF$_3$CHFCF$_3$, HFC-227ea), 2,3,3,3-tetrafluoropropene (CF$_3$CF=CH$_2$, HFO-1234yf), pentafluoroethyl methyl ether (CF$_3$CF$_2$OCH$_3$, HFE-245mc), heptafluoropropyl methyl ether (CF$_3$CF$_2$CF$_2$OCH$_3$, HFE-7000), and 2-bromotrifluoropropene (CF$_3$CBr=CH$_2$, 2-BTP).

The above agents are often used in various blends to achieve specific physicochemical properties optimized for specific applications. The physicochemical properties include such properties as critical temperature, enthalpy of vaporization, thermal conductivity, and vapor density. Additional property considerations are toxicity and flammability. Flammability of the components and blends is a significant safety concern in the context of engineering and regulatory needs. In the absence of individual empirical testing of all possible formulations and conditions, a daunting if not impossible task, predictive detailed kinetic models provide a valuable and more-rapid screening tool. Such flammability models require accurate knowledge of the kinetic properties at high temperatures. Kinetic information at lower temperatures relevant to the troposphere and stratosphere is likewise necessary to understand and minimize the GWPs and ODPs of the formulations.

The temperatures considered in the present evaluation range from near-ambient to those relevant to combustion. In general, there are more kinetic studies at the lower temperatures and a focus of this work is extrapolation of the rate constants to the higher temperatures necessary for flammability models of refrigerants. Indeed, it was the absence of reliable self-consistent data at higher temperatures that was a primary motivation for undertaking this work. The reactions described pertain to fluorinated C$_1$ species. Such species will naturally arise at some level during the breakdown of larger fluorinated compounds at high temperatures. The results will thus apply to combustion models of most refrigerants. Despite our primary motivation being the kinetics at high temperatures, we have critically considered data from lower temperatures and our recommendations are also applicable to atmospheric chemistry. As noted, self-consistent rate constants for these reactions comprise a valuable training set that can subsequently be used to, e.g., validate future quantum chemical calculations or structure–activity rules used to predict the reactivity of more complex agents including the fluoroethanes,[3,4] fluoropropanes,[5,6] fluoroalkenes,[7–12] and fluoroethers.[13–18]

## 1.2. Rationale for evaluation and estimation methodology

When evaluating chemical kinetic data, it is often found that the quality of the available information is highly variable. Ideally, the reactions under consideration will all have been studied by several researchers using different techniques over a wide range of temperatures and conditions. This is rarely the case, however. More often, one is faced with sparse, incomplete data of variable quality, obtained with methods ranging from crude estimates to highly sophisticated techniques. Even if a reliable measurement exists, each method spans a limited temperature range and the data will have to be extrapolated to cover all conditions of interest. If reactions are considered individually, such realities can lead to large uncertainties in the rate parameters. Fortunately, the experimental information can usually be placed in a broader context that will considerably constrain the possibilities. In the present work, we do this in several ways.

For example, transition state (TS) theory allows one to relate kinetic parameters and thermodynamic properties. If one considers a series of related reactions, one usually finds that barrier heights and TS entropies (related to pre-exponential factors) vary in a regular way with properties such as reaction enthalpy or electronic characteristics of substituents. Such behavior has been known for many decades and forms the basis of thermochemical kinetics and many predictive structure–activity relationships (SARs). More recently, high-level quantum chemical calculations, if available, provide improved methods of quantifying behavior. Although quantum calculations may not provide quantitatively exact rate constants, they usually capture trends with high accuracy. In the present evaluations, we seek to establish networks that, for related reactions, bring together all available sources of information, including experimental measurements of absolute and relative rates, empirical relationships, and quantum chemical calculations. While the reader is referred to the evaluations for details, the general principle of our approach is to first establish within each reaction set the cases that have the best information and experimental measurements and then to use these data to set absolute rates and bounding behavior. The less-well-studied reactions are then considered in the context of broader information that establishes rate trends. This yields a self-consistent set of recommended values that we believe are the best presently available.

In any evaluation, it is necessary to select, among often-conflicting data, the results that are to be preferred and used to derive the final recommendation. A difficulty in the study of kinetics, as is well known, is that the most important errors are usually not random but rather systematic in nature. Furthermore, the sources of the systematic errors vary with the technique and are often unknown; indeed, had they been understood, the researchers would have accounted for them. There are various ways to deal with this problem. Ideally, one would assign to all determinations a correct statistical weighting that accounts for the systematic errors. However, the unknown nature of the errors makes this difficult to do in a consistent manner; weighting assignments thus easily become *ad hoc* justifications rather than statistically relevant assessments. In the present work, we have adopted what we believe is a more transparent approach of using only what we have deemed "preferred data" in deriving our recommended fits. The results not used directly in the fits remain valuable, however, and have been considered in our assignment of the overall uncertainties. For clarity, the tables split the results into "preferred data" and "excluded data." Assignment to the latter category is not meant to necessarily imply that we have dismissed these data or consider them to be unimportant. Details of the data selection process for specific reactions are found in the individual evaluations.

### 1.3. Some general characteristics of the reactions and rate expression

All of the reactions considered in this evaluation are direct bimolecular reactions that are abstraction reactions that have the form R–H + X → R + XH, where the reactants are the stable (full valence) molecules R–H = ($CH_4$, $CH_3F$, $CH_2F_2$, $CHF_3$) and the radicals X = (H, O, OH, F) with the products being the corresponding radicals R = ($CH_3$, $CH_2F$, $CHF_2$, $CF_3$) and the stable molecules HX = ($H_2$, OH, $H_2O$, HF).

This reaction type can also be written in the form R–H + X → [R–H–X]‡ → R + XH where the intermediate entity is the TS [R–H–X]‡ corresponding to the highest point on the potential energy surface (PES) that connects reactants and products along the reaction coordinate. The overall reaction is usually exothermic, and the products are at lower energies than the reactants, leading to the generic PES illustrated in Fig. 1. Note that the reactions of $CH_4$ and $CHF_3$ with H are slightly exothermic. This moves the products above the reactants in energy, but does not change the general shape of the potential energy curves.

The bimolecular reaction rate can be written as

$$r = k[RH][X] = -d[RH]/dt,$$

where $k$ is the rate constant and [RH] and [X] are the concentrations of the reactants. Throughout this paper, we use the units mol, kJ, $cm^3$, s, and K. Consequently, the concentrations [M] are given in mol $cm^{-3}$, the rate of reaction is given in mol $cm^{-3}$ $s^{-1}$, and the rate constants $k$ are given in $cm^3$ $mol^{-1}$ $s^{-1}$.

Rate constants $k(T)$ are normally well-described over moderate temperature ranges by the simple two-parameter Arrhenius expression $k = A$ $e^{-E_a/RT}$, where $A$ is a pre-exponential factor ($cm^3$ $mol^{-1}$ $s^{-1}$), $E_a$ is the activation energy (kJ $mol^{-1}$), $T$ is temperature (K), and $R$ is the gas constant (8.314 J $mol^{-1}$ $K^{-1}$). For the broad range of temperatures considered in the present evaluation, a more accurate representation of $k(T)$ is given by the three-parameter extended Arrhenius expression
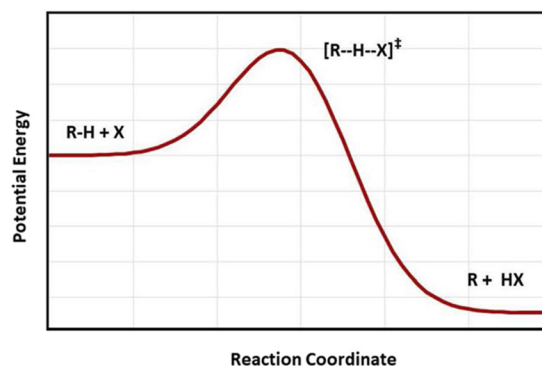


**FIG. 1.** Potential energy as a function of reaction coordinate for R–H + X → R + XH bimolecular abstraction reaction.

($k = A$ $T^n$ $e^{-E/RT}$), where $n$ is an additional temperature exponent coefficient and $E$ is an exponential temperature coefficient (it is not an "activation energy" $E_a$). The three-parameter expression allows one to better account for factors that lead to curvature in standard Arrhenius plots of log $k$ vs $1/T$, such as tunneling or temperature-dependent changes in the TS properties. There is no required relationship between corresponding $A$ and $E$ values in fits using the two- and three-parameter expressions; in addition, the values of $A$, $E$, and $n$ are highly correlated in the extended expression and the fits do not necessarily relate in a straightforward way to thermodynamic properties in the context of TS theory. When considering a limited subset of temperatures, we therefore sometimes use the simpler form $k = A$ exp($-E_a/RT$) in order to highlight relationships involving $A$ or $E$. The simpler rate expression $k(A, E_a)$ is also useful when comparing rate expressions in a homologous reaction series or optimizing the agreement of models with a series of observables.

## 2. Overview of Available Experimental Data and Analysis

### 2.1. Availability of data

As mentioned above, there are no experimental determinations of rate constants for all of the H abstraction reactions over a wide range of temperatures (200–2000 K). The rate constants for H abstractions by OH at lower temperatures (200–400 K) are pertinent to atmospheric chemistry and have been extensively measured (cited later). Rate constants at higher temperatures (1200–2000 K) are pertinent to combustion chemistry and flammability. Because of their importance in hydrocarbon combustion, the reactions of H, O, and OH have seen much study. F atoms are not present in most fuels, however, and little-to-no work has been done on their reactions at high temperatures. The reactivity of F atoms with HFCs is nonetheless important in the flammability of the neat refrigerants, where the absence of hydrocarbon fuel makes conditions relatively hydrogen-poor and fluorine-rich.

In Table 1, we briefly characterize the available data for the considered reactions. More details are provided in the subsequent corresponding reviews, which include comprehensive lists of the

**TABLE 1.** Counts of available data for the fluoromethanes + X → fluoromethyls + HX reactions, where X = H, O, OH, F. Only reliable data (<3σ) are included in the counts. "High T" denotes data at intermediate to high temperatures (500–2000) K, while "Low T" denotes near room temperature measurements (<300–500) K. "Calc." denotes data from quantum chemical calculations. The last column contains estimated expanded uncertainty factors $f$ (2σ) in the experimental measurements at high and low temperatures, with the low-temperature values given in parentheses

| Species | Expt. High T | Expt. Low T | Calc. | $f$ |
|---|---|---|---|---|
| R–H + H → R + H$_2$ | | | | |
| CH$_4$ | 9 | 1 | 5 | 1.4 (1.6) |
| CH$_3$F | 1 | 0 | 3 | 1.5 (1.8) |
| CH$_2$F$_2$ | 1 | 0 | 3 | 1.6 (1.8) |
| CHF$_3$ | 3 | 1 | 7 | 1.1 (2) |
| R–H + O → R + OH | | | | |
| CH$_4$ | 5 | 2 | 12 | 1.18 (1.5) |
| CH$_3$F | 0 | 9 | 5 | 1.4 (2) |
| CH$_2$F$_2$ | 0 | 0 | 2 | 1.4 (2) |
| CHF$_3$ | 2 | 0 | 1 | 1.7 (2.3) |
| R–H + OH → R + H$_2$O | | | | |
| CH$_4$ | 4 | 8 | 5 | 1.12 (1.05) |
| CH$_3$F | 0 | 9 | 9 | 1.5 (1.22) |
| CH$_2$F$_2$ | 0 | 8 | 6 | 1.5 (1.17) |
| CHF$_3$ | 1 | 7 | 6 | 1.3 (1.22) |
| R–H + F → R + HF | | | | |
| CH$_4$ | 0 | 9 | 6 | 1.35 (1.23) |
| CH$_3$F | 0 | 7 | 1 | 1.35 (1.24) |
| CH$_2$F$_2$ | 0 | 7 | 1 | 1.35 (1.35) |
| CHF$_3$ | 1 | 10 | 3 | 1.35 (1.20) |

measurements and calculations. In many cases, the data are sparse. By "High T" in Table 1, we mean moderate to high temperatures, roughly (500–2000) K, that is, substantially above the near-room-temperature measurements, which are denoted "Low T" and pertain to (<300–500) K. The case counts of Table 1 include only the "preferred experimental data"; there may be additional data not specifically used in the fits, but that was considered in the broader assessments of overall uncertainties (see Sec. 8 for each reaction). In a few instances, the counts include rate expressions for H abstractions by X that are derived from the reverse reaction (i.e., R + HX → R–H + X) using thermodynamics and detailed balance. For rate constants derived from computations, we include counts for all values without regard to perceived quality or accuracy. We note that in a number of cases, the rate constants from quantum chemical calculations differed substantially (an order of magnitude or more) from the recommended rate constants (and each other); see, for example, CHF$_3$ + H → CF$_3$ + H$_2$. More typically, however, they differed by factors of (1.3–2.5) and (2–4) at high and low temperatures, respectively, and outside our assigned uncertainties.

Our recommended rate expressions are derived (for the most part) from fits to the available data. Some data were excluded from the fits (as mentioned above) for several reasons since they would introduce bias to the recommended rate expressions because (a) the data were simply revised measurements made by the same research group and method; (b) the rate constants were substantially outside our recommended uncertainties; (c) the data were derived from

models where the values were dependent upon assumptions that were not reported, ill-defined, or more generally uncertain; and (d) the data showed incorrect temperature dependencies (differing substantially from the recommended values) and, consequently, would inappropriately skew the temperature dependence. In all cases, the recommended uncertainties that we provide take into account these outliers using appropriate weighting, and in all cases, we provide the deviations of the excluded data from the recommended values.

## 2.2. Data analysis and least-squares fit with additional constraints

The problem at hand is to develop self-consistent fits to rate data in a situation where the experimental data are often sparse, of variable quality, possibly conflicting, and not available over the full temperature range of interest. In a few cases, there are no experimental data. In the above circumstances, a simple least-squares fit to individual datasets would yield a multitude of possible parameters with equal statistical uncertainties in the fits. In addition, the derived Arrhenius parameters (A, n, E) would be unphysical: the resultant rate expression might accurately represent the rate constants in the limited temperature ranges but would be inaccurate at all other temperatures. We therefore apply additional information that will further constrain the kinetic parameters such as A-factors and activation energies. In particular, all the considered reactions are simple abstractions and each reaction set is comprised of a homologous series having a similar generic PES. It is expected that the functional similarities will lead to regular trends in the kinetic parameters. A key point is that there are usually good experimental data for (CH$_4$ + X) and (CHF$_3$ + X), the two reactions that are expected to bound the high and low rate constants in each homologous series. Some form of interpolation is therefore expected to yield reliable results for the other reactions.

The solution to this problem of fitting datasets where the data are sparse is straightforward: a least-squares fit to the data with additional constraints—an optimization that fits the experimental data while ensuring that deviations from objective functions involving other properties are minimized. This numerical analysis method is widely used in all fields of engineering in solving practical problems.[19] In our case for rates of reactions, given the scarcity of the data, a model employing just an extended Arrhenius expression is insufficient to find solutions that can be extrapolated with any certainty. Fortunately, one can relatively easily construct a more expansive model employing the concept of SARs, which is widely used in chemistry (and other fields).[20–27] The reactions studied here are a set of homologous reactions where the PESs for the reactions are functionally the same and, hence, SARs should work relatively well. This concept goes by many names and has been implemented in different ways in the field of chemical kinetics including SARs,[17,28–30] valid kinetic parameter range analysis,[31] group additivity kinetics,[32–35] rate constant rules,[36] reaction classes,[37–46] hierarchical classes,[47] isodesmic reactions for TSs,[48,49] graph theory for reactions,[50,51] and even reaction symbolic computing,[52] deep learning of activation energies,[53] and genetic algorithm-based method for kinetics.[54]

For each homologous series, the following assumptions were included as constraints in developing our fits:

1. **log(A/n$_H$) ∼ n$_H$.** The log of the normalized A factors (per H atom) at high temperatures (we chose 1200–1800 K) should vary roughly

linearly with the number of H atoms. The simplest assumption would be to make the normalized $A$-factors identical, but this is not the case for a number of reasons—the partition functions will change with increasing fluorine substitution, the PES will change due to polarizability changes, and for the reaction with OH, the degree of hindrance in the OH rotor in the TS will change. Consequently, the reaction coordinate will vary in a regular way across a homologous series of reactions, which will slightly impact the TS entropies and hence the $A$-factors. This criterion is applied at high temperatures to avoid interference from tunneling. As will be illustrated and discussed in Sec. 8, the uncertainties in the optimized $A$ factors of about $f = 1.1 \pm 0.1$ are substantially less than the assigned expanded uncertainty factors ($2\sigma$) of about $f = 1.4 \pm 0.2$, and thus, the normalized $A$ factors are highly correlated with the number of H atoms.

2.  $E_a \sim \Delta_r H$. The activation energy $E_a$ at high temperatures should vary roughly linearly with the heat of reaction $\Delta_r H$. This is an expression of the well-known Evans–Polanyi relationship.[40,55–58] We have qualified this to apply at high temperatures because tunneling is expected to cause the activation energy (an empirical quantity) to deviate at low temperatures from the relevant thermodynamic energy barrier, whereas tunneling plays only a minor role at high temperatures (see Sec. 8.4 for a further discussion of tunneling). One thus expects a better correlation at high temperatures. No particular assumptions were made about the slope in this correlation, but the value is approximately determined by the behavior and data for the bounding reactions. As will be illustrated and discussed in Sec. 8, the uncertainties in the optimized activation energies $E_a$ of about (3–7)% (excluding a few outliers) that correspond to an expanded uncertainty factor $f$ ($2\sigma$) of about (1.2–1.3) for the rate constants at high temperatures are less than the assigned expanded uncertainty factors $f(2\sigma)$ of about $f = 1.4 \pm 0.2$, and thus, the optimized activation energies $E_a$ are well correlated with the heats of reactions.

3.  $n \sim E_a$. The temperature coefficient $n$ should vary roughly linearly with the activation energy $E_a$ at high temperatures. This reflects the well-known kinetic compensation effect between the Arrhenius parameters $[A \exp(-E_a/RT) = (A'T^n) \exp(-E/RT)]$: a rate expression in order to go through the same rate constants would require a higher $A$ factor along with a higher activation energy $E_a$ and similarly would require a higher temperature coefficient $n$ along with a higher exponential energy coefficient $E$. The extended Arrhenius format accounts for an upward curvature in Arrhenius plots over an extended temperature range. Such a curvature is partly related to temperature-dependent changes in the thermodynamic properties of the TS, but tunneling also significantly increases the rate over the base non-tunneling value at near-ambient temperatures. The larger the barrier, the greater the relative contribution of tunneling at lower temperatures, leading to a greater curvature and a larger required $n$. In deriving our rate constant fits, we found that only modest changes in $n$ were required for each reaction partner (H, O, OH, F) and that assuming a roughly linear dependence on $E_a$ at high temperatures gave good results. As will be illustrated and discussed in Sec. 8, we estimate expanded uncertainty factors $f(2\sigma)$ of about $f = 1.25$ for rate constants (based on a derived empirical uncertainty of about 10% in the temperature coefficient $n$) using the correlation between $n$ and $E_a$, which is less than our assigned uncertainty factors of $f = 1.4 \pm 0.2$, demonstrating that the kinetic compensation effect is a good assumption.

4.  $\Delta E_a \sim \Delta E_a(ab\ initio)$. The relative activation energies at high temperatures for the different reactions in each set of reactions (R–H + X → R + HX) should roughly scale with those from *ab initio* calculations. In this work, we employed the rate expressions from Matsugi and Shiina[59] who carried out high-level calculations for (X = H, O, OH). We do not expect the computations to be quantitatively exact but do consider the relative rate constants to be good initial guesses. We do not provide a graphical characterization of this correlation but do briefly discuss it in each section of homologous reactions.

5.  $E_a(T_{low}) \sim E_a(T_{high})$. There is an exact relationship between $E_a$ at high and low temperatures that can be analytically derived from an extended Arrhenius expression, $E_a(T_{high}) - E_a(T_{low}) = nR(T_{high} - T_{low})$, where $R$ is the gas constant and $n$ is the temperature coefficient. Thus, the uncertainty in $E_a$ at low temperatures relative to that at high temperatures should be on the order of the uncertainty in the temperature coefficient $n$ or about 10% (see above). We illustrate and discuss this correlation in Sec. 8. We estimate expanded uncertainty factors $f(2\sigma)$ of about $f = 1.25$ for rate constants (based on a derived empirical uncertainty of about 10% in the temperature coefficient $n$) using the correlation between $n$ and $E_a$, which is less than our assigned uncertainty factors of $f = 1.4 \pm 0.2$. This demonstrates clearly that the kinetic compensation effect is a good assumption with regard to $E_a$ at high and low temperatures.

6.  $\log(k_{300}) \sim E_a$. Since there are correlations (see above) between the normalized $A$ factors (per H atom) and the number of H atoms, between the temperature coefficients $n$, and between the activation energies $E_a$ at high and low temperatures, there will also be a dependent correlation between the rate constants at low temperatures ($k_{300}$) and the activation energies $E_a$ at high temperatures. The log of the rate constant at room temperature (300 K) should vary roughly linearly with the activation energy $E_a$. For these reactions where an H atom is being abstracted, the rate constants at low temperatures are dominated by tunneling and the tunneling rate is, to first order, a direct function of the height of the barrier through which the H atom tunnels. It is also a function of the width and asymmetry in the barrier, but since we are considering a homologous set of reactions having PESs that are functionally the same, to first order, these will also scale roughly linearly. This correlation is illustrated and discussed in Sec. 8, although the uncertainty factor is on the order of $f = 2.0$—this is reflected in our assigned uncertainties at low temperatures (provided in tables in Secs. 4–7).

We note that because of high electronegativity of F, there will be some deviations from these linear correlations. We point out these instances in the discussion in Sec. 8.

This appears to be a complicated model requiring computer optimization, but in practical terms, it is not, and we optimized the parameters manually without much difficulty. Not all of the 3 Arrhenius parameters ($A, n, E$) for all of the 16 different reactions, RH + X → R + HX (RH = {CH$_4$, CH$_3$F, CH$_2$F$_2$, CHF$_3$}; X = {H, O, OH, F}), need to be simultaneously optimized. First, only $n$ and $E$ are independent parameters with $A$ being a dependent parameter determined through best agreement (least-squares fit) with the experimental data. We note that $E$ is essentially a first-order correction ("slope") to the rate expression, while $n$ is a second-order correction ("curvature"). Second, one only needs to optimize the parameters within each homologous series (X = {H, O, OH, or F}). Finally, the rate parameters for the

bounding cases RH = {CH$_4$ and CHF$_3$) are largely determined by experimental data that are for the most part available over wide temperature ranges, and thus, the parameters $n$ and $E$ for the rate expressions involving the intermediate species CH$_3$F and CH$_2$F$_2$ can be estimated fairly well through simple interpolation.

The optimization procedure was quite standard and fairly simple. First, initial guesses for the rate constants at high temperatures (1200–1800 K) were generated where the relative $A$ factors and relative activation energies $E_a$ were based on those from the *ab initio* calculations of Matsugi and Shiina[59] benchmarked to $A$ and $E_a$ of the bounding parameters (from fits to experimental data) for CH$_4$ and CHF$_3$. Second, initial guesses for the rate constants at low temperatures ($k_{300}$) were generated through interpolation of log($k_{300}$) vs $E_a$ at high temperatures from the bounding cases of CH$_4$ and CHF$_3$ and the initial estimate of $E_a$ at high temperatures for CH$_3$F or CH$_2$F$_2$. These estimated data at high and low temperatures plus the available experimental data were then fit to an extended Arrhenius expression to determine an initial guess for the parameters $A$, $n$, and $E$. This can be termed a "tight" optimization since the rate expression is forced to agree with the initial guesses including the parametric constraints from SARs. In contrast, a "loose" optimization is where the fit does not consider the parametric constraints.

The initial tight optimization was then iteratively made "looser" to generate more relaxed fits by adjusting the rate constants at high temperatures and/or at low temperatures and/or by adjusting the independent parameters $n$ and $E$. This process was then manually iterated a few times until a fully relaxed fit was obtained—that is, the data were fit to a least-squares regression to an extended Arrhenius expression *while the deviations from the structure–activity correlations were also minimized.* This is the same procedure as a formal (computer) optimization, which would, of course, find the "true" global minimum but would likely produce fits with uncertainties statistically similar to our recommended uncertainties. The figures and discussion in Sec. 8 show that the different parameters related to the 6 constraints above are well-correlated—the uncertainties in the parameters result in uncertainties in the rate constants that are less than our assigned uncertainties.

There are two caveats to the additional constraints. First, fluorine is highly electronegative and can change the PES in a non-linear fashion, especially at high fluorine substitution (i.e., CHF$_3$). Second, abstraction by OH has a hindered rotor in the TS. Consequently, the effective barrier to the hindered rotation will change significantly with addition of highly electronegative fluorine atoms and will become both sterically hindered and strongly temperature-dependent. Instances of these exceptions will be discussed in Sec. 8.

In each section for the homologous reactions RH + X → R + HX (X = H, O, OH, F), we provide tables and discussion regarding the goodness of these fits including statistically derived uncertainty factors $f$, $\Delta n$, and $\Delta E$. In Sec. 8, we also provide tables and discussion regarding the goodness of these fits, along with figures showing how well the parameters $A$, n, and $E$ and the rate constants at low temperatures ($k_{300}$) are correlated with the SAR constraints.

## 2.3. Network of related reactions

As discussed above, this reference series of reactions can be used to aid in determination of the reactivity of more complex agents. There are many agents where rate constants have not been measured, have only been measured in a restricted temperature range, or have been measured just at low temperatures but not at high temperatures (or vice versa). Rate constants are often (and best) determined by measuring the rate of one reaction relative to another reaction with well-established absolute rate constants. For some agents, reactivities (rate constants) have not been measured, and one can estimate fairly well the reactivities by interpolating using structure–activity relations (and energy relationships) such as the relative number of hydrogen and/or fluorine atoms or the relative bond strengths (equivalently, relative heats of reactions). In addition, high-level *ab initio* quantum chemical calculations can be used as an aid in determining relative rate constants and their temperature dependencies. Although the quantum calculations may not be completely accurate, they do very well in predicting relative rates.

For example, if TS calculations based on quantum chemical calculations predict that the magnitude of the relative rates of two reactions at high temperatures differs by about a factor of 6, then the actual (experimental) relative rates likely differ on the order of (4.5–8). Our recommended rate expressions show differences with the *ab initio* calculated relative values on the order of $f = 1.3$. Similarly, if quantum chemical calculations predict a relative barrier of about 1.25, the actual difference in barriers is likely on the order of (1.20–1.30). In short, the quantum chemical calculations often have modest differences when compared to experimentally derived rate constants, but these differences are largely systematic and hence lead to fairly precise relative rates.

Within a homologous series of reactions, the activation energies often correlate well with bond strengths (or equivalently, heats of reaction). This correlation is often termed Evans–Polanyi relationship.[55] For example, in the reactions considered here, a change in bond strength of 10 kJ mol$^{-1}$ results in a change of about 3.6 kJ mol$^{-1}$ ($\pm 6\%$) in the activation energy. See figures and discussion about this correlation in Sec. 8.

Since all of these reactions involve H atom transfer, the rates of reaction at low temperatures are dominated by quantum chemical tunneling. There is a strong correlation between tunneling rates and barriers to reaction, and the tunneling rate is, to first order, a direct function of the height of the barrier through which the H atom tunnels (it is also a function of the width and asymmetry of the barrier). Consequently, both experimental data and quantum chemical calculations for other similar reactions can be used to assist in predicting relative tunneling rates using this correlation.

At low temperatures, the rates of these H abstraction reactions are dominated by tunneling. These tunneling rate constants can be predicted (scaled) using *ab initio* barriers and curvature in the energy potentials. Although the tunneling calculations may not be accurate, there will be systematic differences with the actual (experimental) rate constants. For example, if the effective barrier, or activation energy ($E_a$), at high temperatures (e.g., 1500–1800 K) between two homologous reactions changes by about 10 kJ mol$^{-1}$, then the effective activation energy at low temperatures (e.g., 300 K) might differ on the order of 8.5 kJ mol$^{-1}$ ($\pm 15\%$). The tunneling roughly scales with the barrier because the shape of the energy potential along the reaction coordinate changes only slightly. See figures and discussion about this correlation in Sec. 8.

In short, the accuracy in the determination of absolute rate constants over a range of temperatures for all H abstraction reactions

involving a set of HFCs can be significantly increased by utilizing the more precise relative rates in a *network of self-consistent reactions* using correlations based on SARs and assigning uncertainties based on bracketing of the relative rates.

## 2.4. Overview of classes of reactions

The evaluations are divided into four sections, one for each reaction class, R–H + X → R + HX (X = H, O, OH, F). These sections are then followed by a discussion section that provides an overview of this critical evaluation and then analyzes the trends in $A$ factors, energies $E_a$ or $E$ (temperature dependencies), and tunneling with fluorine substitution, as well as the trends with regard to the attacking radical (H, O, OH, F). Within each section, an overview of the available data and evaluations is first provided for the homologous series with increasing fluorine substitution ($CH_4$, $CH_3F$, $CH_2F_2$, $CHF_3$) and this includes a table of recommended rate expressions for the series. These overviews are then followed by subsections for each of the compounds containing tables of available data from the literature (reviews, experimental, and theoretical), figures with the data and our fits, and a discussion of the evaluation for each individual reaction. In all cases, we have done our best to provide a good uncertainty estimate, $2\sigma$ (type B, a level of confidence of approximately 95%).[60] We note that uncertainties for the rate constants are often not provided in the literature for both experimental and (especially) theoretical values. In addition, in cases where uncertainties are provided, they are generally simply precision estimates and do not include systematic uncertainties, and the coverage ($1\sigma$ or $2\sigma$) is often not specified.

We note that a column "Method" is provided in the tables. This is a brief characterization of the methods used to determine the rate constants. The acronyms and abbreviations used for "Methods" are more fully specified in Sec. 10.

We now provide a brief overview for each of the four classes of reactions R–H + X → R + HX (X = H, O, OH, F). For all of these abstraction reactions, note that the available *ab initio* calculations, our (recommended) parameterization of the rate constants, and all available experimental data for abstraction reactions involving H, O, F, and OH suggest that the difference in barriers between abstraction reactions for $CH_3F$ and $CH_2F_2$ are on the order of $(2–3)$ kJ mol$^{-1}$ and that the differences in rate constants at low and high temperatures are on the order of $f = (1.5–2.5)$. Consequently, the relative rate of an abstraction reaction from one fluoromethane can be estimated relatively well from the same reaction involving another fluoromethane because of relatively small differences.

**R–H + H → R + H₂.** For the reactions involving H abstraction by H atoms from the fluoromethanes, there are reliable data for $CH_4$ and $CHF_3$ at both high and low temperatures and usually a single measurement each at intermediate temperatures for $CH_3F$ and $CH_2F_2$. There are possible conflicting data (about a factor of $f = 1.8$) at high temperatures for the reaction $CHF_3 + H → CF_3 + H_2$. We address this in our evaluation. In all cases, our recommended rate expressions agree with the available (reliable) experimental data (within uncertainties) at the midpoint of their limited temperature ranges. The temperature dependencies of the recommended rate expressions were determined by benchmarking the experimental data while considering trends in the series for the rate parameters $A$, $n$, and $E$ and relative values from *ab initio* calculations.

**R–H + O → R + OH.** For the reactions involving H abstraction by O atoms from the fluoromethanes, there are reliable data for $CH_4$ over a wide range of temperatures and rate constants for $CHF_3$ at intermediate and high temperatures, but none at room temperature for $CHF_3$. There are possible conflicting data at high temperatures for the $CHF_3 + O$ reaction, which we address in our evaluation. For the reaction of O atoms with $CH_3F$, there is a single measurement at high temperatures. In that same work, the reaction of O atoms with $CHF_3$ was determined (as well as the reaction with $CH_4$)—providing an excellent set of relative values that can be used. There are no reliable measurements for the reaction of the O atom with $CH_2F_2$ at any temperature. We provide a recommended rate expression for $CH_2F_2$ considering trends within the homologous series in the rate parameters $A$, $n$, and $E$ along with relative values from *ab initio* calculations.

**R–H + OH → R + H₂O.** There are extensive measurements for the reaction of OH with the fluoromethanes (and other HFCs) near room temperature (above and below) because of the importance of these reactions in atmospheric chemistry that impact global warming. Reliable rate constants for the reaction of OH with both methane and $CHF_3$ are available at high temperatures, but none for $CH_3F$ or $CH_2F_2$. The recommended rate constants at high temperatures for these two compounds were determined by considering trends within the homologous series in the rate parameters $A$, $n$, and $E$ along with relative values from *ab initio* calculations.

**R–H + F → R + HF.** There are a few reliable rate constants that have been measured for the reaction of F atoms with methane and all of the fluoromethanes at low (near room temperature) and intermediate temperatures, but unfortunately no measurements at high temperatures where the rate constants are important in the combustion of refrigerants. Rate constants for the reactions involving $CH_4$ and $CHF_3$ have been measured from about 200 K up to about $(450–550)$ K, while rate constants involving $CH_3F$ and $CH_2F_2$ have only been measured in the range $(200–300)$ K.

Unfortunately, many of the researchers who carried out *ab initio* calculations for these reactions did not report rate constants at *higher* temperatures where the rate constants are not known—they instead focused on rate constants at *lower* temperatures where the rate constants *are well-established*.

### 2.4.1. Estimation and interpolation

Where rate constants for R–H + X → R + HX in the series of reactions are unavailable, or only available over a limited temperature range, we loosely utilized the high-level *ab initio* quantum chemical calculations of Matsugi and Shiina[59] to guide the estimation and interpolation of rate constants in the different homologous series of reactions. (We did not repeat these calculations at other levels of theory because we believe their results are adequate as relative values.) Unfortunately, for some reactions, they did not provide their original calculations but instead provided "adjusted rate expressions" to agree with low-temperature measurements where tunneling is important. Because the exact adjustments are uncertain, we used the trends to guide our fits, but did not take the relative rates to be exact.

For abstractions involving OH, we utilized the relative rate constants from the *ab initio* quantum calculations of Schwartz *et al.*,[61] rather than those of Matsugi and Shiina, because the latter reported "adjusted" rate constants for these reactions instead of their original

values. Based on our inspection of these *ab initio* calculations and also considering them relative to the available experimental data, we believe that the relative rate constants from the *ab initio* calculations with regard to their magnitude ($A$ factor), temperature dependence ($E$), and curvature including tunneling ($T^n$) can be used fairly well to aid as interpolation and extrapolation tools when viewed in context of SARs, the relative number of hydrogen and fluorine atoms, and relative heats of reactions in these homologous series of reactions. Quantifying this, we believe that the uncertainty in this parametric estimation is on the order of the experimental uncertainties. The network of self-consistent rate constants based on all the experimental data in conjunction with parametric constraints leads to relatively accurate rate constants—certainly within less than a factor of $f = 2.0$ where little data are available but with uncertainties on the order of a factor of $f=(1.3–1.5)$ where more data are available.

## 3. Thermochemical Data

In Table 2, we provide standard enthalpies of formation for reactant and product species involved in H abstraction from the fluoromethanes by the radicals H, O, F, and OH. The enthalpies of formation provided are single high-quality values taken from original sources. We did not use evaluated sources that were weighted averages of different values yielding yet another value that is largely statistically indistinguishable from the single high-quality value. In some cases, we provide values from evaluated sources where the original sources were simply corrected using updated supplementary values (see the supplementary material). We also provide C–H bond dissociation energies (BDEs) for the fluoromethanes. These values are used in tables and figures in this paper.

## 4. Fluoromethanes + H → Fluoromethyls + H₂

In this section, we compile and evaluate rate constants for reactions involving the abstraction of H from C–H bonds by H atoms from methane and the fluoromethanes. Data are included from both

experimental determinations and quantum chemical calculations. Based on considering all of the data, we provide expanded uncertainty factors $f(2\sigma)$ that are generally a factor of about $f = (1.4–1.5)$ over the entire range.

Table 3 lists our recommended rate expressions for abstraction of H from fluoromethanes by H atoms. Preferred values for each reaction are subsequently discussed in Sec. 4 with each individual reaction. Two sets of rate expressions are provided in Table 3. The first set uses the three-parameter extended Arrhenius format ($k = A\,T^n\,e^{-E/RT}$) to specify values at temperatures of (300–1800) K. The second set uses the simpler two-parameter Arrhenius expression ($k = A\,e^{-E/RT}$) to describe the rate constants over a narrower range of temperatures more relevant to combustion (1200–1800 K). The latter expressions make it easier to inspect the parameters of related reactions for compatibility and are useful when adjusting rate parameters in models to optimize agreement with experimental observables such as ignition delays and burning velocities.

Both the extended and simple rate expressions can be used at temperatures above 1800 K; however, validation data at such temperatures are limited and the reliability is not well-tested. We note that there exist in the literature many "recommended" rate expressions (usually based on *ab initio* calculations) that give (300–2500) K as the range. We think values at temperatures above 1800 K should be treated with caution.

When placed in a standard Arrhenius format, the pre-exponential $A$ factors that describe H abstraction from the fluoromethanes by H at high temperatures (1200–1800 K) for $CH_2F_2$, $CH_3F$, and $CH_4$, relative to that for $CHF_3$ (1.0) are 1.92, 2.85, and 3.84, respectively, and are very similar to the reaction path degeneracies (the number of hydrogen atoms) of 2, 3, and 4. These ratios are about (10–15)% larger than the ratio of $A$ factors from the rate expressions in the quantum chemical work of Matsugi and Shiina,[59] which were 1.80, 2.51, and 2.99, respectively. The effective barriers $E_a$ at high temperatures (1200–1800 K) for the recommended rate expressions

**TABLE 2.** Standard enthalpies of formation $\Delta_f H°$(298.15 K) and C–H BDEs used in this work. Units for enthalpies and uncertainties are kJ mol$^{-1}$. Expanded absolute uncertainties $U$ ($2\sigma$) as reported are provided. We also provide our estimates of the uncertainties (in parentheses)

| Species | $\Delta_f H°$(298 K) | $U$ | Reference | BDE(C–H) |
|---|---|---|---|---|
| $CH_4$ | −74.55 | 0.15 | 04RUS/PIN[62] | 439.1 ± 0.3 |
| $CH_3F$ | −235.55 | 0.70 (1.2) | 18GAN/KAL[63] | 423.2 ± 1.4 |
| $CH_2F_2$ | −451.66 | 0.68 (1.2) | 18GAN/KAL[63] | 426.2 ± 1.4 |
| $CHF_3$ | −697.45 | 0.65 (1.4) | 18GAN/KAL[63] | 446.4 ± 1.7 |
| $CH_3$ | 146.55 | 0.25 | 09BOD/JOH[64] | |
| | | | 93BLU/CHE[65] | |
| $CH_2F$ | −30.39 | 0.50 (0.8) | 18GAN/KAL[63] | |
| $CHF_2$ | −243.45 | 0.51 (0.8) | 18GAN/KAL[63] | |
| $CF_3$ | −469.06 | 0.52 (1.0) | 18GAN/KAL[63] | |
| $H_2$ | 0.0 | 0.0 | By definition | |
| $H_2O$ | −241.831 | 0.026 | 13RUS[66] | |
| HF | −272.72 | 0.05 | 06HU/HEP[67] | |
| H | 217.9979 | <0.0001 | 04ZHA/CHE[68] | |
| O | 249.229 | 0.002 | 13RUS/FEL[69] | |
| OH | 37.51 | 0.03 | 13BOY/KOS[70] | |
| F | 79.46 | 0.05 (0.10) | 05YAN/HAO[71,72] | |

**TABLE 3.** Recommended rate expressions for H abstraction from the fluoromethanes by the H atom and enthalpies of reaction. $k(T) = A T^n \exp(-E/RT)$. $k(T)$, temperature-dependent rate constant. $A$, pre-exponential factor. $n$, temperature coefficient. $E$, energy coefficient. $f(2\sigma)$, expanded uncertainty factors. $\Delta_r H_{298}$, standard enthalpy of reaction at 298 K. Units: $k$ ($cm^3\ mol^{-1}\ s^{-1}$), $E$ ($kJ\ mol^{-1}$), $T$ (K). Uncertainty factors $f$ are at high(low) temperatures. Uncertainty factors in parentheses "$(f)$" are at low temperatures (300–500) K. $A/A_{CHF3}$ is the ratio of the pre-exponential to that for $CHF_3$.

| Reaction | $A$ | $n$ | $E$ | $f$ | $T$ | $\log_{10}(k_{300})$ | $\Delta_r H_{298}$ |
|---|---|---|---|---|---|---|---|
| $CH_4 + H \rightarrow CH_3 + H_2$ | $9.01 \times 10^5$ | $2.41 \pm 0.31$ | $38.21 \pm 2.13$ | 1.4(1.6) | 300–1950 | 5.28 | 3.1 |
| $CH_3F + H \rightarrow CH_2F + H_2$ | $2.13 \times 10^5$ | $2.56 \pm 0.42$ | $31.98 \pm 2.34$ | 1.5(1.8) | 300–1800 | 6.11 | −12.8 |
| $CH_2F_2 + H \rightarrow CHF_2 + H_2$ | $8.29 \times 10^4$ | $2.63 \pm 0.45$ | $30.65 \pm 2.41$ | 1.6(1.8) | 300–1800 | 6.09 | −9.8 |
| $CHF_3 + H \rightarrow CF_3 + H_2$ | $2.89 \times 10^4$ | $2.95 \pm 0.28$ | $38.61 \pm 2.28$ | 1.1(2.0) | 300–1800 | 4.05 | 10.4 |
| | | | | | | $A/A_{CHF3}$ | |
| $CH_4 + H \rightarrow CH_3 + H_2$ | $4.99 \times 10^{14}$ | | 68.10 | 1.4 | 1200–1800 | 3.84 | |
| $CH_3F + H \rightarrow CH_2F + H_2$ | $3.71 \times 10^{14}$ | | 63.06 | 1.5 | 1200–1800 | 2.85 | |
| $CH_2F_2 + H \rightarrow CHF_2 + H_2$ | $2.49 \times 10^{14}$ | | 62.53 | 1.6 | 1200–1800 | 1.92 | |
| $CHF_3 + H \rightarrow CF_3 + H_2$ | $1.30 \times 10^{14}$ | | 72.45 | 1.5 | 1200–1800 | 1.00 | |

for $CH_4$, $CH_3F$, $CH_2F_2$, and $CHF_3$ are 6.0%, 3.7%, 4.2%, and 4.1% lower, respectively, than those derived from the Matsugi and Shiina rate expressions. There is relatively good agreement between our recommendations and the computed values, in terms of both absolute $A$ factors and the relative scaling of $A$ factors and effective barriers $E$; this provides a degree of validation that the rate expressions are self-consistent and accurate within the indicated uncertainties. This will be discussed further later in this section.

In Table 3, we have assigned an expanded uncertainty factor $f(2\sigma)$ to each of the rate constants at both high and low temperatures (the latter in parentheses). For the $CH_4 + H$ and $CHF_3 + H$ reactions, the uncertainties are based on scatter in the experimental measurements. We have, however, increased this uncertainty slightly for $CHF_3 + H$. This accommodates the relatively imprecise measurement by Takahashi et al.[73] that is at odds with the recommended rate expression; it likewise accounts for uncertainties in the equilibrium constants for $CHF_3 + H \rightarrow CF_3 + H_2$ and $CF_3 + CF_3 \rightarrow C_2F_6$ that were used to derive the rate constants at low temperatures. The deviations between the recommended rate expressions and the experimental data for $CH_3F + H$ and $CH_2F_2$ are about $f = 1.2$ and $f = 1.45$, respectively. However, we believe that higher uncertainties of $f = 1.5$ and $f = 1.6$, respectively, are appropriate, given uncertainties in the experimental measurements and our estimation methods. Uncertainties for these reactions at low temperatures are assigned in accord with that estimated for $CH_4 + H$, with a higher uncertainty for $CHF_3 + H$ because of the limited measurements.

### 4.1. $CH_4 + H \rightarrow CH_3 + H_2$

In Table 4, we present rate constants compiled from the literature for $CH_4 + H \rightarrow CH_3 + H_2$. This is one of the most studied reactions in chemical kinetics. Table 4 does not include all measurements but is rather a substantial and representative set of the data considered to be most reliable. The recommended rate expression is based on our fit to these data. The first set in this table is comprised of evaluated values, the second set is the data used in our fits, the third set is data excluded from our fits, and the fourth set is from ab initio quantum chemical calculations. Data were excluded from the fits if the magnitude of the rate constants differed substantially (well outside our recommended uncertainty), the temperature dependence was

inconsistent with the well-established temperature dependence by many other measurements (and calculations), and/or they were revised values from prior measurements (duplicates). We note that our fit is statistically equivalent to the 2001 fit by Sutherland et al.,[74] an often-cited evaluation based on their measurements at high temperatures along with their analysis of measurements by others including at intermediate and low temperatures. We utilized our rate expression in this work instead because (1) we have included more data in our fit, particularly at low temperatures, and (2) our rate expression yields an effective rate expression at high temperatures (1200–1800 K) that has an $A$ factor that is self-consistent with $A$ factors we find for the fluoromethanes (see Table 3 and the quantum chemical calculations of Matsugi and Shiina[59]). Our recommended rate expression differs from that of Sutherland et al. in that it agrees slightly better with the high-temperature experimental data of both Sutherland et al. and Baeck et al.[75,76] and also with the low-temperature experimental data of Marquaire et al.[77]

Figure 2 presents, from Table 4, the experimental data deemed reliable, the results of the ab initio calculations of Matsugi and Shiina, and the recommended fit. Note that the plotted experimental data points are smoothed values obtained from the reported rate expressions rather than the primary measurements. We estimate the uncertainty in the rate constant to be a factor of about $f = 1.4$ at high temperatures (1200–1800) K and about $f = 1.6$ at low temperatures (300–450) K based on the scatter in the experimental data and the different statistically similar fits that could be obtained. The recommended uncertainty factor includes consideration—with appropriate weighting—of rate constants excluded from the fit. Those data excluded from the fit deviated from the recommended value by generally factors of about 2–3 (or more) and most had temperature dependencies that were significantly different than derived from the recommended values—on the order of $\Delta E = (10–20)\ kJ\ mol^{-1}$. The residuals between the fitted expression and the data excluded from the fit are provided in Fig. 3 [note in $\ln(k)$ units].

### 4.2. $CH_3F + H \rightarrow CH_2F + H_2$ and $CH_2F_2 + H \rightarrow CHF_2 + H_2$

Rate expressions for abstraction of H from $CH_3F$ and $CH_2F_2$ by H atoms that we compiled from the literature are provided in Tables 5 and 6. There is only one reliable measurement for the H atom

**TABLE 4.** $CH_4 + H \rightarrow CH_3 + H_2$ rate expressions. $k(T) = A T^n \exp(-E/RT)$. $k(T)$, temperature-dependent rate constant. $A$, pre-exponential factor. $n$, temperature coefficient. $E$, energy coefficient. $f(2\sigma)$, expanded uncertainty factors. Units: $k$ ($cm^3\ mol^{-1}\ s^{-1}$), $E$ ($kJ\ mol^{-1}$), $T$ (K). Uncertainty factors $f$ are at high temperatures. Uncertainty factors $f$ in parentheses "($f$)" are our estimates at low temperatures (300–500) K. Uncertainty factors in square brackets "[$f$]" are the deviations from our recommended values. See Sec. 10 for definitions of acronyms and abbreviations in the Method column

| $A$ | $n$ | $E$ | $f$ | $T$ | Method | Reference |
|---|---|---|---|---|---|---|
| Evaluations | | | | | | |
| $9.01 \times 10^5$ | 2.41 | 38.21 | 1.4(1.6) | 300–1950 | Recommended | This work |
| $4.38 \times 10^{14}$ | | 67.37 | 1.4 | 1200–1800 | Recommended, high T fit | This work |
| $4.08 \times 10^3$ | 3.16 | 36.63 | [1.5] | 348–1950 | Review | 01SUT/SU[74] |
| $3.86 \times 10^6$ | 2.11 | 32.43 | [2(5)] | 400–1800 | Review | 91RAB/SUT[78] |
| $6.31 \times 10^{13}$ | | 52.71 | 2.0[3] | 350–2000 | Review | 67DIX/WIL[79] |
| Experimental (preferred data) | | | | | | |
| $1.77 \times 10^{14}$ | | 57.65 | 1.2 | 913–1697 | Fwd/rev rxn, shock, photol, H abs | 01SUT/SU[74] |
| $1.54 \times 10^{14}$ | | 57.15 | 1.35 | 748–1054 | Dischg flow, reson fluor | 01BRY/SLA[80] |
| $3.10 \times 10^{14}$ | | 63.19 | [1.2] | 1310–1820 | Rev rxn, shock, CH3 UV abs | 95BAE/SHI1[75] |
| $4.40 \times 10^{14}$ | | 65.19 | [1.2] | 1250–1950 | Rev rxn, shock, CH3 UV abs | 95BAE/SHI2[76] |
| $3.21 \times 10^{11}$ | | 33.92 | [1.3] | 348–421 | Dischg flow, ESR | 94MAR/DAS[77] |
| $1.07 \times 10^{14}$ | | 53.55 | 1.5 | 897–1730 | Flash photol, shock, H abs | 91RAB/SUT[78] |
| $1.82 \times 10^{14}$ | | 55.12 | 1.8 | 640–818 | Dischg flow, GC | 79SEP/MAR[81] |
| $3.20 \times 10^{12}$ | | | 1.2 | 1600 | Flame, MS | 73PEE/MAH[82] |
| $6.25 \times 10^{13}$ | | 48.56 | 1.3 | 474–732 | Dischg flow, ESR | 70KUR/HOL[83] |
| $4.00 \times 10^{10}$ | | | 1.5 | 900 | Flame, MS | 67DIX/WIL[79] |
| $3.31 \times 10^{14}$ | | 63.18 | [1.4] | 673–753 | Ignition LIB | 62GOR/NAL[84] |
| Experimental (excluded data) | | | | | | |
| $1.02 \times 10^7$ | | | 1.2[5] | 298 | Dischg fast flow, ESR | 86JON/MA[85] |
| $7.23 \times 10^{14}$ | | 63.0 | [2.5] | 1700–2300 | Model, flow, H reson abs | 75ROT/JUS[86] |
| $1.24 \times 10^{14}$ | | 49.80 | [3] | 298–753 | Rev rxn, static, thermal, GC | 71BAK/BAL[87] |
| $6.9 \times 10^{13}$ | | 49.37 | 1.09[1.7] | 426–747 | Flow, H dischg, H ESR | 69KUR/TIM[88] |
| $1.21 \times 10^{13}$ | | 44.32 | 1.7[2.5] | 843–933 | Thermal, ESR | 67AZA[89] |
| $3.44 \times 10^{13}$ | | 35.59 | [70] | 298–398 | Ultrasonic, GC | 66LAW/FIR[90] |
| $6.03 \times 10^{11}$ | | 30.93 | 2.4 | 500–787 | Fast flow, dischg, GC | 64JAM/BRO[91] |
| $2.00 \times 10^{14}$ | | 48.14 | 1.7[2.5] | 1200–1800 | Model, flame | 61FEN/JON[92] |
| $1.00 \times 10^{10}$ | | 18.62 | [3] | 372–436 | Thermal, H heat combin | 54BER/LER[93] |
| Theoretical | | | | | | |
| $4.50 \times 10^5$ | 2.57 | 41.65 | [1.2(1.8)] | 300–2000 | CBS-QB3 Eckart | 14MAT/SHI[59] |
| $2.82 \times 10^{14}$ | | 72.84 | [1.2] | 1200–1800 | CBS-QB3 Eckart, this work, High T fit | 14MAT/SHI[59] |
| $2.59 \times 10^4$ | 2.93 | 38.30 | [1.2(1.8)] | 300–2500 | CC/pVQZ Eckart | 97KON/KRA[94] |
| $1.07 \times 10^1$ | 3.78 | 30.76 | [2.0(2.0)] | 298–2500 | G2MP2 | 97BER/EHL[95] |
| $4.25 \times 10^{-8}$ | 6.51 | 15.47 | [1.5(4.0)] | 200–1000 | MP4 CVT/SCT | 99MAI/DUN[96] |

abstraction reaction for $CH_3F$, but none for $CH_2F_2$. The rate measurement for $CH_3F$ by Westenberg and DeHaas[97] is at intermediate temperatures (750–900) K. Note that in that work, the decay of $CH_3F$ was measured (products were not identified), and the authors incorrectly assumed that the F atom was being abstracted by analogy with the other halogenated methanes $CH_3Cl$ and $CH_3Br$ where the halogen (Cl or Br) is abstracted.[97,98] C–F bonds are much stronger (about $480\ kJ\ mol^{-1}$) than C–Cl (about $350\ kJ\ mol^{-1}$) and C–Br (about $300\ kJ\ mol^{-1}$) bonds; consequently, for $CH_3F$, it is the H atom rather than the F atom that is being abstracted. For more discussion of abstraction of halogens (C–X) by the H atom, see the work by Manion and Tsang.[99]

There is also a reasonable rate constant reported in the literature for $CH_2F_2 + H \rightarrow CHF_2 + H_2$ by Pritchard and Perona,[100] who measured the rate of the reaction in the reverse direction $CHF_2 + H_2$ $\rightarrow CH_2F_2 + H$. This measurement, however, was determined relative to the rate of combination $CHF_2 + CHF_2$, which is pressure- and temperature-dependent, and deriving the rate constant involved modeling of a set of reactions and some assumptions. We display the rate constants derived from these measurements but did not use them in determining our recommended rate expression (although they roughly agree). Note that we computed the equilibrium constant (from available thermochemical data) in the temperature range of this measurement (500–635 K), $K_{eq} = 42.2 * \exp(-46.9/T)$, and utilized this to determine the "forward" rates from the measured "reverse" rates. The equilibrium constant was computed using Burcat's thermochemical polynomials[101] with an adjustment to make them compatible with the enthalpies of formation given in Table 2.

There are also several unreliable measurements for these two reactions by Parsamyan and Azatyan,[102] Parsamyan and
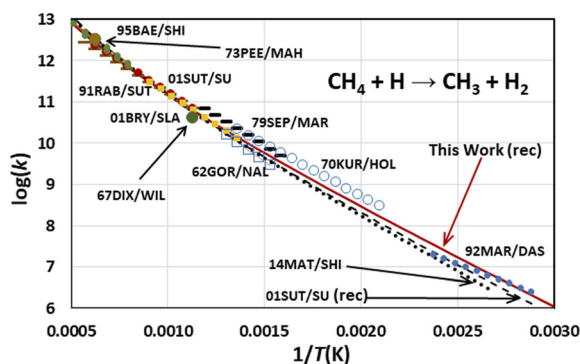
FIG. 2. $CH_4 + H \rightarrow CH_3 + H_2$ experimental data and fitted rate expression. Data: Evaluation 01SUT/SU,[74] Quantum 14MAT/SHI,[59] other experimental data as given in Table 4. $k$ ($cm^3$ $mol^{-1}$ $s^{-1}$). Note that other quantum chemical data rate expressions are not provided in this figure. Note that data points are not individual measurements but rather smoothed values obtained from the reported rate expression. Legend: This work (rec) recommendation (red line), 14MAT/SHI[59] (dotted line), 01SUT/SU[74] (rec, their recommended expression, dashed line), 01SUT/SU[74] (experimental, red dots), 01BRY/SLA[80] (yellow squares), 95BAE/SHI1[75,76] (green dots), 94MAR/DAS[77] (blue dots), 91RAB/SUT[78] (brown dashes), 79SEP/MAR[81] (black dashes), 73PEE/MAH[82] (large brown dot), 70KUR/HOL[83] (blue circles), 67DIX/WIL[79] (large green dot), and 62GOR/NAL[84] (blue squares).

Nalbandyan,[103] Hart and Grunfelder,[104] and Aders et al.[105] The reported rates are an order of magnitude (or more) different from that which is reasonable, and in some cases, in the papers, there are inconsistencies between the rate constants given in the tables and the reported rate expressions. In the evaluation by Baulch et al.,[106] they corrected the determination of the rate constant for $CH_3F + H$ by Parsamyan and Azatyan using correct values for relative reactions. The revised rate constant is in good agreement with that from Westenberg and DeHaas,[97] but we do not include it in the fit because of the many uncertainties in how it was derived.

There are also several rate expressions for these reactions based on *ab initio* quantum calculations, and these are provided in Tables 4–7. The rate constants from the work of Matsugi and Shiina,[59]
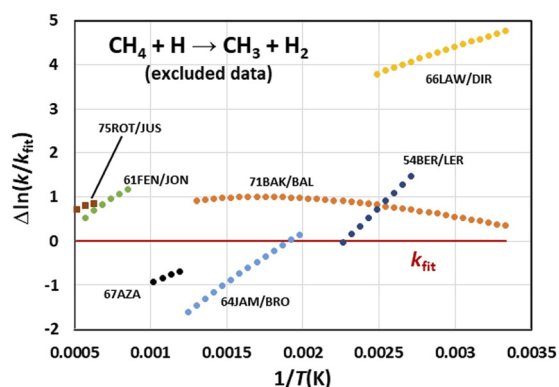


FIG. 3. $CH_4 + H \rightarrow CH_3 + H_2$ residuals for rate data excluded from fit. Note that not all of the excluded data are shown here because they either deviated much more than shown here or were revised measurements (duplicates).

however, are the only ones that are in relatively good agreement with the available experimental data.

In Fig. 4, we provide the experimental rate constants for $CH_3F + H$ and $CH_2F_2 + H$ that we think are relatively reliable, along with our recommended rate expressions and those from the quantum chemical calculations of Matsugi and Shiina. Note that in this figure, the curves for $CH_2F_2$ have been shifted up by a factor of 10 (1 $\log_{10}$ unit) for clarity because they overlapped with the curves for $CH_3F$. The actual rate constants for $CH_2F_2 + H$ are about 92% and 59% of the rate constants for $CH_3F$ at 300 K and 1800 K, respectively.

Our recommended rate expressions for $CH_3F + H$ and $CH_2F_2 + H$ given in Tables 5 and 6 and displayed in Fig. 4 were based on trial-and-error iterative parametric fits. The constraints were these: (1) The rate expression for $CH_3F + H \rightarrow CH_2F + H_2$ agrees with the midpoint of the single measurement for this reaction; (2) when combined with the data for $CH_4$ and $CHF_3$, the $A$ factors and activation energies $E_a$ at high temperatures (1200–1800) K should vary smoothly across the series $CH_4$, $CH_3F$, $CH_2F_2$, $CHF_3$; and (3) the effective $A$ and $E_a$ at high temperatures should roughly scale with those from the quantum chemical calculations of Matsugi and Shiina.[59] In short, we attempted to make the rate expressions self-consistent with other available data. Determined first in our procedure were the rate expressions for $CH_4$ and $CHF_3$ because these comprise the upper and lower rate bounds and both reactions have rate measurements extending from atmospheric to combustion temperatures; these bounding values were then used to help establish intermediate rates for the less-well-studied compounds $CH_3F$ and $CH_2F_2$.

## 4.3. $CHF_3 + H \rightarrow CF_3 + H_2$

### 4.3.1. Overview

We have compiled all available rate constants for $CHF_3 + H \rightarrow CF_3 + H_2$ from the literature. This includes both experimental and computational work and also rate constants for the reverse reaction $CF_3 + H_2 \rightarrow CHF_3 + H$. The forward rates in these cases were derived using the equilibrium constant for the reaction (see discussion below regarding computation of the equilibrium constant). The forward rates are given in Table 7, and the reverse rates are given in Table 8.

Our recommended rate expression is based on an unweighted fit to rate constants from four measurements at high temperatures (1000–1700 K) and one measurement at low temperatures (375–450 K). (See Table 7 and discussion below for details.) Other values were excluded in the fit because of their large deviation from others or lack reliability. The recommended rate expression along with almost all of the experimental data (included or excluded from the fit) is given in Fig. 5.

Based on all of the considerations, we assign an expanded uncertainty factor $f$ ($2\sigma$) of $f = 1.1$ for rate constants for our recommended rate expression at high temperatures and $f = 2$ at low temperatures.

In this section, we first provide the data for $CHF_3 + H \rightarrow CF_3 + H_2$ from the literature and the reverse reaction $CF_3 + H_2 \rightarrow CHF_3 + H$ in Tables 7 and 8, respectively, and rate constants in Fig. 5. This is followed by discussions of the data at both high temperatures and low temperatures. We then compare rate constants for $CHF_3 + H \rightarrow CF_3 + H_2$

**TABLE 5.** $CH_3F + H \rightarrow CH_2F + H_2$ rate expressions. $k(T) = A\,T^n \exp(-E/RT)$. $k(T)$, temperature-dependent rate constant. $A$, pre-exponential factor. $n$, temperature coefficient. $E$, energy coefficient. $f(2\sigma)$, expanded uncertainty factors. Units: $k$ ($cm^3\,mol^{-1}\,s^{-1}$), $E$ ($kJ\,mol^{-1}$), $T$ (K). The uncertainty factor is at high temperatures. The uncertainty $f$ in parentheses is at low temperatures (300–500) K

| $A$ | $n$ | $E$ | $f$ | $T$ | Method | Reference |
|---|---|---|---|---|---|---|
| Evaluations | | | | | | |
| $2.13 \times 10^5$ | 2.56 | 31.98 | 1.5(1.8) | 300–1800 | Recommended | This work |
| $3.71 \times 10^{14}$ | | 63.06 | 1.5 | 1200–1800 | Recommended, high T fit | This work |
| $2.3 \times 10^{13}$ | | 41.2 | 1.5 | 600–1000 | Review | 81BAU/DUX[106] |
| Experimental (preferred data) | | | | | | |
| $1.80 \times 10^{13}$ | | 39.33 | 1.2 | 750–900 | Dischg flow, ESR | 75WES/DEH[97] |
| Experimental (excluded data) | | | | | | |
| $6.30 \times 10^{13}$ | | 21.78 | 1.1[10] | 298–652 | Dischg flow, ESR | 75ADE/PAN[105] |
| $6.30 \times 10^{13}$ | | 34.27 | 1.7[5] | 870–1088 | Model, rel rate CH3Br, flame | 74HAR/GRU[104] |
| $1.38 \times 10^{12}$ | | 6.80 | 1.3[5] | 858–933 | Static | 67PAR/AZA[102] |
| Theoretical | | | | | | |
| $7.83 \times 10^4$ | 2.76 | 32.00 | [1.6(1.2)] | 200–1800 | CBS-QB3 Eckert | 14MAT/SHI[59] |
| $2.13 \times 10^{-6}$ | 5.94 | 8.44 | [2.5(5)] | 200–1000 | MP4 CVT/SCT | 99MAI/DUN[96] |
| $5.57 \times 10^{-2}$ | 4.40 | 18.95 | [1.5(2.0)] | 300–2500 | G2MP2 | 97BER/EHL[95] |

**TABLE 6.** $CH_2F_2 + H \rightarrow CHF_2 + H_2$ rate expressions. $k(T) = A\,T^n \exp(-E/RT)$. $k(T)$, temperature-dependent rate constant. $A$, pre-exponential factor. $n$, temperature coefficient. $E$, energy coefficient. $f(2\sigma)$, expanded uncertainty factors. Units: $k$ ($cm^3\,mol^{-1}\,s^{-1}$), $E$ ($kJ\,mol^{-1}$), $T$ (K). The uncertainty $f$ in parentheses is at low temperatures (300–500) K

| $A$ | $n$ | $E$ | $f$ | $T$ | Method | Reference |
|---|---|---|---|---|---|---|
| Evaluations | | | | | | |
| $8.29 \times 10^4$ | 2.63 | 30.65 | 1.6(1.8) | 300–1800 | Recommended | This work |
| $2.49 \times 10^{14}$ | | 62.54 | 1.6 | 1200–1800 | Recommended, high T fit | This work |
| Experimental (preferred data) | | | | | | |
| $2.72 \times 10^{14}$ | | 55.26 | 1.3[1.5] | 500–635 | This work, from rev rxn | 69PRI/PER[100] |
| Theoretical | | | | | | |
| $3.13 \times 10^4$ | 2.83 | 30.93 | [1.7(1.7)] | 200–1800 | CBS-QB3 Eckart | 14MAT/SHI[59] |
| $5.92 \times 10^{-6}$ | 5.74 | 7.59 | [2.5(5)] | 200–1000 | MP4 CVT/SCT | 99MAI/DUN[96] |
| $4.52 \times 10^{-2}$ | 4.39 | 18.44 | 1.5(2.0)] | 300–2500 | G2MP2 | 97BER/EHL[95] |

computed using quantum chemical methods—these data are provided in Table 7 and in Fig. 6.

We also provide here a discussion of systematic trends in rate constants for the entire homologous series fluoromethanes + H $\rightarrow$ fluoromethyls + H$_2$. It is shown that there appears to be strong relationships between the rate constant at room temperature ($k_{300}$) and the activation energy $E_a$ at high temperatures (1200–1800 K) and between the rate constant at high temperatures ($k_{1500}$) and C–H BDEs. We present these empirical correlations here because data for the present reaction CHF$_3$ + H $\rightarrow$ CF$_3$ + H$_2$ are the most reliable, and consequently, these systematic trends can be used for other fluoromethanes + H reactions employing CHF$_3$ + H $\rightarrow$ CF$_3$ + H$_2$ as the benchmark reaction.

Finally, at the end of this section, we also provide ancillary data in order to derive some of the rate expressions for CHF$_3$ + H $\rightarrow$ CF$_3$ + H$_2$ from the reverse reaction CF$_3$ + H$_2$ $\rightarrow$ CHF$_3$ + H. Table 9 provides

equilibrium constants for CHF$_3$ + H $\rightarrow$ CF$_3$ + H$_2$, and Table 10 provides rate constants for the reference reaction CF$_3$ + CF$_3$ $\rightarrow$ C$_2$F$_6$.

### 4.3.2. Rate constants at high temperatures

The three measurements included in the fit at high temperatures consist of two sets measured in the forward direction by Hranisavljevic and Michael[107] and Richter et al.[111,112] and one set measured in the reverse direction by Hranisavljevic and Michael[107] and Berces et al.[117] Although the rate constants from Richter et al. agree well with the other three sets of data, they are from flame measurements (and estimated flame temperatures) and are based on a model that required rate constants for abstraction of H by O atoms and OH radicals, as well as other reactions. The rate constants reported by Berces et al.[117] agree similarly well with the other rate expressions but were also derived using a complex model. Consequently, there is much more uncertainty in these data and the apparent good agreement may be
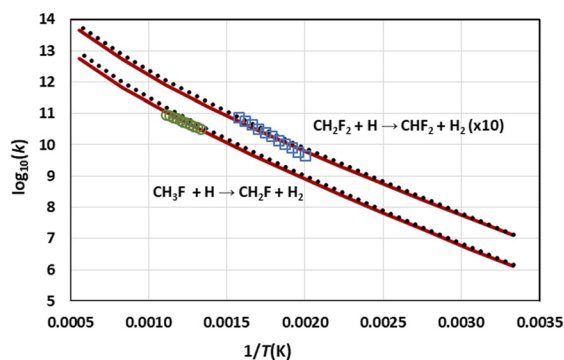
**FIG. 4.** $CH_3F + H \rightarrow CH_2F + H_2$ and $CH_2F_2 + H \rightarrow CHF_2 + H_2$ experimental data and rate expressions. The $CH_2F_2$ curves and points have been displaced upward by a factor of 10 for clarity. Rate constants $k$ (cm$^3$ mol$^{-1}$ s$^{-1}$). Note that data points shown simply represent the range of values and are not actual measured data points. Legend: This work recommended (red lines), 14MAT/SHI[59] (quantum, dotted lines), 69PRI/PER[100] (blue squares), and 75WES/DEH[97] (green circles).

coincidental—as a result, we excluded these two sets of data from our fit to the rate constants.

There are four additional rate constants at high temperatures reported by Skinner and Ringrose,[120,121] Hidaka et al.,[115] Fargash et al.,[119] and Westbrook[116] that were excluded from the fits because they differed by about an order of magnitude and the determinations had some significant uncertainties due to the lack of reported details and the use of complex model reaction systems to derive the reported rate expressions.

There is an additional 1997 measurement of this reaction (in the forward direction) at high temperatures by Takahashi et al.[73] that we did not weigh as strongly as the 1998 measurements of Hranisavljevic and Michael[107] even though we generally find both groups to provide reliable data and the methods used were similar. In agreement with Hranisavljevic and Michael, Takahashi et al. found much smaller rate constants than most early investigators (see Fig. 5); nonetheless, their values are about 1.8 times larger than those of Hranisavljevic and Michael and lie outside of the experimental uncertainties of each. In addition, the barrier of Takahashi et al. is about 20 kJ mol$^{-1}$ lower than that of Hranisavljevic and Michael, a discrepancy larger than expected. In considering the work of Takahashi et al., we note several issues: the H atom absorption coefficients did not follow a linear Beer–Lambert law; the H atom absorbance had to be corrected by subtracting absorbance by CHF$_3$; the relatively high concentration of CHF$_3$ could promote secondary chemistry; the decay traces were noisy in comparison to those of Hranisavljevic and Michael; the rate constants were derived using a model that required rate constants for the decomposition of the precursor C$_2$H$_5$I (used to produce the H atoms) as well as rate constants for the reaction of H atoms with the decomposition product CHF$_2$. We also find that the data of Takahashi et al. are inconsistent with the trends in Arrhenius parameters $A$, $n$, and $E$ observed for the other reactions in this series and, further, with the scaled rate parameters from the ab initio calculations of Matsugi and Shiina. The effective $A$ factor and activation energy $E_a$ at high temperatures (1200–1800 K) were higher than what one might expect, and the temperature coefficient ($T^n$) was much lower (flatter curve) than one would expect, $n = (2.1$–$2.2)$ vs $n = (2.5$–$3.0)$. For all these

reasons, we favor the results of Hranisavljevic and Michael and did not directly use the data of Takahashi et al. in deriving our fit.

In the work of Hranisavljevic and Michael, the H atom decay profiles showed precise single exponential decays with little noise (2%–5% uncertainty). The derived rate constants, however, showed significantly more variability—on the order of $(20$–$30)$% ($k = 1$) likely due to uncertainties in determining the temperatures and/or concentrations. Inspection of a scatter plot of the rate data relative to a best fit rate expression (for both forward and reverse reactions) seems to show that the deviations at the higher pressure measurements ($\sim$16 bar) were significantly larger and a significant proportion of data points were outside 3 sigma deviations of the mean. Eliminating just 9 outlier points of the 54 total data points significantly reduces the uncertainty ($k = 1$) from about $(25$–$30)$% to about $(13$–$18)$%.

Note that Hranisavljevic and Michael measured the rate constants for this reaction in both the forward and reverse directions. As with the other "reverse" rate constants, we employed the equilibrium constant to derive forward rates. The good agreement between the rate constants measured by Hranisavljevic and Michael in both directions is another confirmation of the validity of their data since these are essentially independent measurements. We compared the magnitude of the forward and reverse rate constants in the temperature range of 1100–1600 K and found that the equilibrium constant derived from the relative rates was within about a factor of $f = 1.35$ of the more accurate equilibrium constant computed from thermodynamic properties—a very good agreement for thermodynamic data derived from kinetics measurements.

When we examine the self-consistency of the recommended rate expression, we find that it is consistent with the effective rate expression at high temperatures (1200–1800 K) for the root reaction in this system $CH_4 + H \rightarrow CH_3 + H_2$, the effective $A$ factor being about 3.4 times less (the ratio of hydrogens is 4:1), and the effective barrier $E_a$ is 5.1 kJ mol$^{-1}$ higher, consistent with the difference of the BDEs of 5.3 kJ mol$^{-1}$. This fit is also consistent with slightly scaled rate parameters from the ab initio work of Matsugi and Shiina.[59]

Based on all of the considerations discussed, we assign an expanded uncertainty factor $f(2\sigma)$ of $f = 1.1$ for rate constants for our recommended rate expression at high temperatures (1500–1800 K)—there are five measurements that agree within this uncertainty (although two may be coincidental since they were derived using complex mechanisms).

### 4.3.3. Rate constants at low temperatures

As indicated in Tables 7 and 8, rate constants for $CHF_3 + H \rightleftharpoons CF_3 + H_2$ at lower temperatures have been measured in both the forward and reverse directions by several groups. However, some of these reported values are based on reworking earlier values or are based on estimates using BDEs. After consideration, we think the rate constants from the work of Ayscough et al.[113] and Kibby et al.[118] are most reliable. These two determinations measured the rate constant of CF$_3$ with H$_2$ relative to the rate of recombination of CF$_3$ to form C$_2$F$_6$. To convert these measurements to rate constants for $CHF_3 + H \rightarrow CF_3 + H_2$, we must know the equilibrium constant, $K_{eq} = k_{fwd}/k_{rev}$, and the rate constant for the reference reaction $CF_3 + CF_3 \rightarrow C_2F_6$.

There are two main issues to address here in order to derive rate constants for the reaction in the forward direction. First, the equilibrium constant must be calculated: $K_{eq} = k_{fwd}/k_{rev}$. We have done

**TABLE 7.** $CHF_3 + H \rightarrow CF_3 + H_2$ rate expressions. $k(T) = A T^n \exp(-E/RT)$. $k(T)$, temperature-dependent rate constant. $A$, pre-exponential factor. $n$, temperature coefficient. $E$, energy coefficient. $f(2\sigma)$, expanded uncertainty factors. Units: $A$ ($cm^3\,mol^{-1}\,s^{-1}$), $E$ ($kJ\,mol^{-1}$), $T$ (K). The uncertainty $f$ in parentheses is at low temperatures (300–500) K. See Fig. 5 showing an Arrhenius plot of the experimental rate expressions provided in this table, along with the recommended rate expression from a fit to the data

| A | n | E | f | T | Method | Reference |
|---|---|---|---|---|---|---|
| Evaluations | | | | | | |
| $2.89 \times 10^3$ | 2.95 | 38.61 | 1.1(2) | 300–1800 | Recommended | This work |
| $1.30 \times 10^{14}$ | | 72.45 | 1.1 | 1200–1800 | Recommended, high T fit | This work |
| $2.14 \times 10^1$ | 3.62 | 37.77 | [1.1(1.3)] | 300–1673 | Rev rxn, Fit w/$k_{300}$ = 2.0 × 10⁴ | 98HRA/MIC[107] |
| $3.20 \times 10^{12}$ | | 46.89 | [2] | 350–600 | Review | 67AMP/WHI[108] |
| $2.89 \times 10^{13}$ | | 38.07 | [5] | 219–447 | Review | 64PRI/FOO[109] |
| $1.05 \times 10^{13}$ | | 16.5 | [5] | 300–700 | Review | 72KON[110] |
| $3.39 \times 10^{14}$ | | 30.4 | [5] | 336–1300 | Review | 72KON[110] |
| Experimental (preferred data) | | | | | | |
| $3.69 \times 10^{13}$ | | 61.22 | [1.2] | 1111–1550 | Shock, H reson abs | 98HRA/MIC[107] |
| $1.78 \times 10^{14}$ | | 78.00 | [1.1] | 1168–1673 | Rev rxn, shock, H reson abs | 98HRA/MIC[107] |
| $1.16 \times 10^{14}$ | | 73.16 | [1.1] | 1050–1350 | Model, flame, MS | 94RIC/VAN[111,112] |
| $8.93 \times 10^{12}$ | | 52.47 | 2.3[1.1] | 375–447 | Static, this work rev rxn | 55AYS/POL[113] |
| Experimental (excluded data) | | | | | | |
| $9.54 \times 10^{13}$ | | 64.60 | 1.36[2] | 1100–1350 | Model, shock, H reson abs | 97TAK/YAM[73] |
| $3.76 \times 10^{13}$ | | 54.99 | 1.26[2] | 1100–1350 | Model, shock, H reson abs | 96YAM/TAK[114] |
| $2.75 \times 10^{14}$ | | 58.05 | [2] | 1000–1600 | Model, shock, IR, this work rev rxn | 93HID/NAK[115] |
| $5.01 \times 10^{12}$ | | 20.92 | [5] | 1400–1800 | Model, flame, MS | 83WES[116] |
| $7.08 \times 10^{12}$ | | 47.84 | 1.26[1.1] | 1029–1132 | Shock, this work rev rxn | 72BER/MAR[117] |
| $1.22 \times 10^{13}$ | | 53.68 | [3] | 333–550 | This work rev rxn | 68KIB/WES[118] |
| $4.20 \times 10^{14}$ | | 61.69 | [10] | 738–854 | This work rev rxn | 68FAR/MOI[119] |
| $5.00 \times 10^{12}$ | | 20.95 | [20] | 970–1300 | Model, shock, IR | 65SKI/RIN[120,121] |
| n/a | | | | | Rev rxn, rel rate | 56PRI/PRI[122] |
| Theoretical | | | | | | |
| $3.67 \times 10^4$ | 2.74 | 42.32 | [2.0(1.2)] | 200–1800 | CBS-QB3 Eckart | 14MAT/SHI[59] |
| $2.82 \times 10^{14}$ | | 75.58 | 2.0 | 1200–1800 | This work, fit high T | 14MAT/SHI[59] |
| $1.73 \times 10^5$ | 2.5 | 48.30 | [1.3(5)] | 200–2000 | CCSD/pVTZ, this work, extracted pts from figures, fit 200–2000 K | 13SHA/CLA[123] |
| $1.18 \times 10^{14}$ | 0 | 72.40 | [1.3] | 1000–1600 | CCSD/pVTZ, this work extracted pts from figures, fit 1000–1600 K | 13SHA/CLA[123] |
| $8.37 \times 10^6$ | 2.08 | 53.20 | [1.5(5)] | 300–2000 | G3B3, TST Wigner | 07ZHA/LIN[124] |
| $7.83 \times 10^6$ | 2.05 | 51.46 | [1.3(5)] | 300–2000 | CCSD/6-311G | 04LOU/GON[125] |
| $6.80 \times 10^{-6}$ | 5.26 | 21.32 | [1.1(1.3)] | 300–1700 | G2, adjusted E, Eckart | 98HRA/MIC[107] |
| $9.00 \times 10^3$ | 3.00 | 38.91 | [4] | 300–2000 | BAC-MP4 | 97BUR/ZAC[126] |
| $8.67 \times 10^1$ | 3.38 | 37.53 | [1.3(2)] | 300–2000 | CH | 97BER/EHL[95] |

this, and the equilibrium constants for $CHF_3 + H \rightarrow CF_3 + H_2$ and the reference reaction $CF_3 + CF_3 \rightarrow C_2F_6$ are derived, shown, and discussed later in this section in Tables 9 and 10, respectively. The biggest uncertainty here is the heat of reaction derived from the enthalpies of formation of $CHF_3$ and $CF_3$. The uncertainty in the heat of reaction (at 298 K) is about 2.6 kJ mol$^{-1}$ (see Table 2)—this translates into an uncertainty of about a factor of 2 at low temperatures.

Second, Ayscough et al. and Kibby et al. measured a relative rate constant and both workers employed a fixed equilibrium constant $K_{eq}$(400 K) for the reference reaction $CF_3 + CF_3 \rightarrow C_2F_6$ as determined by Ayscough et al. and did not consider the possible pressure dependence of this unimolecular reaction. Later determinations[129–131] showed that the value of Ayscough et al. was low by about a factor of 2.8. In addition, the theoretical work of Cobos et al.[131] showed that there was a small temperature dependence—it varied by about a factor of 1.15 over the

temperature range of the work by Ayscough et al. (375–447 K) and about a factor of 2.1 over the temperature range of Kibby et al. (333 K–870 K). Fortunately, Cobos et al. showed that there was no pressure dependence under the conditions used by Ayscough et al. Rate constants for the recombination of $CF_3$ ($CF_3 + CF_3 \rightarrow C_2F_6$) are given in Table 10.

At low temperatures, we utilized the corrected rate constants from Ayscough et al. in our fits. The reverse reaction was determined using the updated rate expression for the relative reference reaction of recombination of $CF_3$. The forward rate constants were then derived using the equilibrium constant for the reaction $CHF_3 + H \rightarrow CF_3 + H_2$ (see Table 10 and the discussion below). Although the rate constants from Kibby et al. are similar, we did not use them in the fits for several reasons: (1) significant uncertainties in both the equilibrium constants and the reference reaction; (2) the temperature dependence of the data being systematically weaker than that for Ayscough et al. and

**TABLE 8.** $CF_3 + H_2 \rightarrow CHF_3 + H$ rate expressions (reverse direction to $CHF_3 + H \rightarrow CF_3 + H_2$). $k(T) = A\,T^n \exp(-E/RT)$. $k(T)$, temperature-dependent rate constant. $A$, pre-exponential factor. $n$, temperature coefficient. $E$, energy coefficient. $f(2\sigma)$, expanded uncertainty factors. Units: $k$ ($cm^3\,mol^{-1}\,s^{-1}$), $E$ ($kJ\,mol^{-1}$), $T$ (K). The uncertainty $f$ in parentheses is at low temperatures (300–500) K

| $A$ | $n$ | $E$ | $f$ | $T$ | Method | Reference |
|---|---|---|---|---|---|---|
| Evaluations | | | | | | |
| $7.49 \times 10^{-1}$ | 3.70 | 27.29 | [1.1(1.3)] | 300–1673 | Fit w/$k_{300} = 2.0 \times 10^4$ | 98HRA/MIC[107] |
| Experimental (preferred data) | | | | | | |
| $1.54 \times 10^{13}$ | | 71.08 | [1.3] | 1168–1673 | Shock, H reson abs | 98HRA/MIC[107] |
| $1.13 \times 10^{13}$ | | 68.05 | [1.3] | 1111–1673 | Shock, fit to k1, k-1 | 98HRA/MIC[107] |
| $7.19 \times 10^{11}$ | | 39.74 | 2.3 | 375–447 | Photol, UV abs | 55AYS/POL[113] |
| Experimental (excluded data) | | | | | | |
| $2.2 \times 10^{13}$ | | 50.21 | [3.0] | 1000–1600 | Model, shock, IR | 93HID/NAK[115] |
| $5.01 \times 10^{11}$ | | 38.91 | [2.0] | 1029–1132 | Model, static, GC | 72BER/MAR[117] |
| $4.90 \times 10^{11}$ | | 15.82 | [2.5] | 1400–1800 | Model, flame | 83WES[116] |
| $8.91 \times 10^{11}$ | | 39.74 | [2.5] | 350–600 | Review | 78ART/BEL[127] |
| $2.45 \times 10^{11}$ | | 31.68 | [3.5] | 350–600 | Review | 75ART/DON[128] |
| $9.33 \times 10^{11}$ | | 40.84 | [3.5] | 333–870 | Rel rate, photol, MS | 68KIB/WES[118] |
| $2.52 \times 10^{13}$ | | 51.47 | [3.5] | 738–854 | photol, IR abs | 68FAR/MOI[119] |
| Theoretical | | | | | | |
| $1.26 \times 10^{-4}$ | 4.88 | 10.01 | [2.5(6)] | 200–1000 | MP4/pVTZ CVT/SCT | 99MAI/DUN[96] |
| $1.26 \times 10^{11}$ | | 25.86 | [3(6)] | 200–1000 | MP4/pVTZ CVT/SCT | 99MAI/DUN[96] |
| $6.80 \times 10^{-6}$ | 5.26 | 21.32 | [1.1(1.3)] | 300–1673 | Quant, G2, Eckart, adjusted E | 98HRA/MIC[107] |
| $2.54 \times 10^{11}$ | | 31.68 | [4] | 350–600 | Theory BEBO | 75ART/DON[128] |

our recommended expression; and (3) other possible systematic errors that are introduced because of the much wider temperature range in their measurements.

Based on the various considerations discussed above, we assign expanded uncertainty factors $f(2\sigma)$ of $f = 2$ for rate constants for our recommended rate expression at low temperatures (300–500 K)—this encompasses the difference in the measurements of Ayscouigh *et al.* and Kibby *et al.*

### 4.3.4. Quantum chemical calculations for CHF₃ + H

In Fig. 6, we present rate expressions from quantum chemical calculations for the reaction $CHF_3 + H \rightarrow CF_3 + H_2$. There are large differences between the different calculations that used different quantum chemical methods. These calculations also used different methods for predicting the dependence of the rate constant (increase) on tunneling at low temperatures. At high temperatures (1200–1800 K), the spread in rate constants from the different quantum chemical calculations is about a factor of 6, while at low temperatures (300–400 K), the spread is very large—about a factor of 60. Compared to the rate expression recommended in this work, the effective rate expressions at high temperatures from the quantum chemical calculations have pre-exponential $A$ factors mostly about (1.3–1.9) times higher,

**FIG. 5.** Rate constants for $CHF_3 + H \rightarrow CF_3 + H_2$. Open circles and open squares are high-temperature and low-temperature values, respectively, used in fit. All other rate constants were excluded (see Table 7 and text for details). Note that data points shown simply represent the range of values and are not actual measured data points. Legend: Recommended rates (red line); 68FAR/MOI[119] (green triangles); 93HID/NAK[115] (blue squares); 65SKI/RIN[120,121] (black asterisks); 83WES[116] (blue dots); 97TAK/YAM[73] (red dots); and 98HRA/MIC[107] and 94RIC/VAN[111,112] (blue circles).

**FIG. 6.** $CHF_3 + H \rightarrow CF_3 + H_2$. Rates from quantum chemical calculations. Rate constants $k$ ($cm^3\,mol^{-1}\,s^{-1}$). Deviations are on the order of factors of $f = 2.5$ and $f = 7.5$ at high and low temperatures, respectively. 97BUR/ZAC,[126] 97BER/EHL,[95] 04LOU/GON,[125] 07ZHA/LIN,[124] 13SHA/CLA,[123] and 14MAT/SHI.[59]

**TABLE 9.** Equilibrium constants for $CHF_3 + H \leftrightarrow CF_3 + H_2$. See text for details

| $T$ (K) | $K_{eq}$ |
|---|---|
| 300 | 0.282 |
| 400 | 0.751 |
| 500 | 1.393 |
| 600 | 2.123 |
| 700 | 2.870 |
| 800 | 3.584 |
| 900 | 4.238 |
| 1000 | 4.820 |
| 1100 | 5.324 |
| 1200 | 5.753 |
| 1300 | 6.114 |
| 1400 | 6.412 |
| 1500 | 6.656 |
| 1600 | 6.852 |
| 1700 | 7.006 |
| 1800 | 7.125 |
| 1900 | 7.213 |
| 2000 | 7.275 |

commensurate with temperature dependencies $E$ that are roughly (2.5–3.2) kJ mol$^{-1}$ higher (about 4%).

The rate expression from the work of Matsugi and Shiina[59] has the best agreement (within about 12%) with the experimental rate constants at low temperatures (not shown in Fig. 6 for clarity). This agreement, however, is because they adjusted the overall reaction barrier to match the low-temperature rate constants. This adjustment came "at a price"—their rate expression differs from our recommended value (based on high-temperature measurements) by a factor of 2. In the work of Matsugi and Shiina, they employed the CBS-QB3 quantum chemical method[132] using optimized structures with a high-quality DFT (density functional theory) method ωB97X-D[133] and corrected for tunneling using asymmetric Eckart potentials.[134] They computed rate expressions for the abstraction of H from methane and the fluoromethanes ($CH_4$, $CH_3F$, $CH_2F_2$, and $CHF_3$) not just by H but also by the radicals O atom and OH. There is relatively good agreement between these computed rate expressions and the limited

experimental data. Based on our analysis, however, there are modest systematic differences between the computed and experimentally derived rate constants. This is "good news" in the sense that the modest systematic differences enable using the relative values of the computed rates to help evaluate and predict rate expressions where experimental data are limited, not available, or in disagreement. For example, the effective pre-exponential $A$ factors that describe the computed rate expressions for the fluoromethanes + H reactions at high temperatures (1200–1800 K) for $CH_2F_2$, $CH_3F$, and $CH_4$ relative to that for $CHF_3$ are 1.8, 2.5, and 3.0, respectively, similar to (75%–90%) of the reaction path degeneracy (i.e., the number of hydrogen atoms) of 2, 3, and 4. This can provide a framework for generating self-consistent rate expressions among the fluoromethanes. The "bad news" is that any calculation that adjusts the overall reaction barrier to "hit" low-temperature data provides a bias and lowers the accuracy of the rate constants at high temperatures. The proper procedure would be to adjust the parameters for the tunneling potential parameters.

### 4.3.5. Discussion of systematic trends in fluoromethanes + H rate expressions

The tunneling (enhanced rate constants) at low temperatures is a function of a number of factors: barrier heights, barrier widths, and asymmetry in the potentials. For a homologous series of reactions where the potential energy reaction surfaces will be similar (but scaled), there should be a rough correlation between the tunneling rate constants (at low temperatures) and the barrier height. We have considered the barrier heights as characterized by the temperature dependence (effective activation energy) at high temperatures (1200–1800 K) compared to the rate constants at low temperatures (300 K). We considered both the experimentally derived recommended values from this work and those from the *ab initio* quantum chemical calculations by Matsugi and Shiina.[59] These comparisons are shown in Fig. 7. Note that in this figure, the rate constants are corrected for the number of hydrogen atoms (reaction path degeneracy). In Fig. 7, for $CH_4$, $CH_3F$, and $CH_2F_2$, there is a strong correlation (for both the experimental and *ab initio* values) between the rate constant at low temperatures ($k_{300}$) and the effective activation energy ($E_a$) at high temperatures. We calculated that the decrease in the rate constant at low temperatures with the barrier at high

**TABLE 10.** $CF_3 + CF_3 \longrightarrow C_2F_6$ rate constants. $k(T) = A T^n \exp(-E/RT)$. $k(T)$, temperature-dependent rate constant. $A$, pre-exponential factor. $n$, temperature coefficient. $E$, energy coefficient. Units: $k$ (cm$^3$ mol$^{-1}$ s$^{-1}$), $E$ (kJ mol$^{-1}$), $T$ (K). See text for discussion of uncertainties

| $A$ | $n$ | $E$ | $T$ | Method | Reference |
|---|---|---|---|---|---|
| $8.33 \times 10^{10}$ | 0.77 | 0.00 | 300–600 | Scaled 10COB/CRO | This work |
| $9.69 \times 10^{10}$ | 0.77 | 0.00 | 300–2000 | | 10COB/CRO[131] |
| $6.73 \times 10^{12}$ | | | 300 | From weighted average | This work |
| $8.44 \times 10^{12}$ | | | 400 | From weighted average | This work |
| $6.62 \times 10^{12}$ | | | 300 | | 08SKO/KHR[130] |
| $7.83 \times 10^{12}$ | | | 300 | | 10COB/CRO[131] |
| $5.96 \times 10^{12}$ | | | 300 | | 70OGA/CAR[141] |
| $9.77 \times 10^{12}$ | | | 400 | | 10COB/CRO[131] |
| $7.65 \times 10^{12}$ | | | 400 | | 08SKO/KHR[130] |
| $2.34 \times 10^{13}$ | | | 400 | | 56AYS[137] |
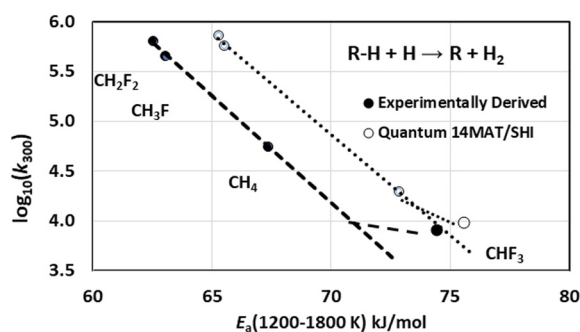
**FIG. 7.** Fluoromethanes + H rates (per H atom) at 300 K vs barriers at (1200–1800) K. Rate constants $k$ (cm$^3$ mol$^{-1}$ s$^{-1}$). $E_a$ for CHF$_3$ is about 3 kJ mol$^{-1}$ higher than the trend for other fluoromethanes. Filled circles and open circles are derived from experimental data and quantum chemical data (14MAT/SHI[59]), respectively.

temperatures is consistent with a change in the effective barrier at low temperatures that is about 1.7 of the change in the effective barrier at higher temperatures (suggestive of the barrier becoming proportionally wider). Likely, this effective relative decrease in the tunneling rate is due to the turning point in the reaction moving along the reaction coordinate—a higher barrier likely results in a later barrier (more product-like), a relatively wider barrier, and less tunneling possible.

The rate constant for CHF$_3$ + H → CF$_3$ + H$_2$, however, is not consistent with the trend for the other reactions, with the high-temperature barrier being about 3 kJ mol$^{-1}$ higher than that would be predicted (about 1 kJ mol$^{-1}$ higher for the *ab initio* value).

We can also consider this in the context of an Evans–Polanyi[55] type relationship[55] where the barrier to reaction in a homologous series of reactions should roughly scale with the heat of reaction or, equivalently, with the BDE. This correlation is represented in Fig. 8 where we plotted the rate constants at 300 and 1500 K vs the C–H BDEs for this series. Note that the rate constants are normalized to the number of H atoms (reaction path degeneracy). We see that the rate constants at both temperatures vary only slightly, except for CHF$_3$ where the rate constant is much lower at 300 K. These relative differences are consistent with a barrier for CHF$_3$ that is about (5–6) kJ mol$^{-1}$ higher than one might expect based on trends in BDEs.
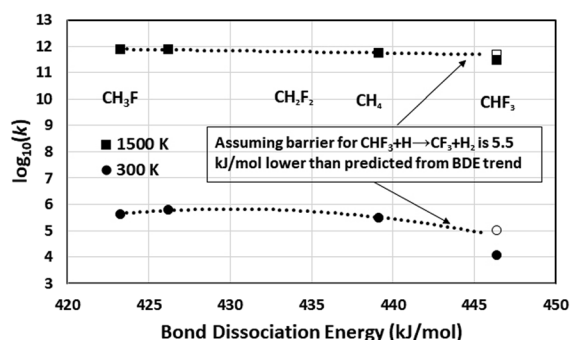


**FIG. 8.** Fluoromethanes + H rate constants (per H atom) vs BDEs. Rate constants $k$ (cm$^3$ mol$^{-1}$ s$^{-1}$). Open circles and squares were derived assuming the barrier for CHF$_3$ + H is 5.5 kJ mol$^{-1}$ lower than predicted using the trend in BDEs.

This anomaly for CHF$_3$ can be likely explained because of the extreme electronegativity of fluorine. In CH$_4$, the carbon is somewhat electronegative because of the electron-donating H atoms. With addition of fluorine, which is highly electron-withdrawing, the carbon becomes increasingly electropositive. In the case of CHF$_3$, the carbon is highly electropositive and the C–H bond involved in the reaction has a semi-ionic nature. Consequently, for CH$_4$, CH$_3$F, and CH$_2$F$_2$, the C–H bond breaking is largely covalent in nature. However, for CHF$_3$, there is an additional ionic contribution. The trends we observe suggest that the additional contribution to the barrier may be on the order of about (3–6) kJ mol$^{-1}$—not an unreasonable amount.

We would like to note here that we could generate fitted rate expressions with substantially different coefficients ($A$, $n$, $E$) but that were essentially statistically identical, because the experimental rate constants are only available in limited temperature ranges. We found differences that ranged from about factors of 1.3–1.5 for $A$, temperature coefficients $n$ ($T^n$) that ranged as much as a factor of 1.5, and barriers $E$ that ranged from 2 to 3 kJ mol$^{-1}$. In our fitting procedure, however, we selected intermediate values that were best consistent with trends in the parameters $A$, $n$, and $E$ and the rate constants at low and high temperatures.

### 4.3.6. Equilibrium constant for CHF$_3$ + H ↔ CF$_3$ + H$_2$

Equilibrium constants for this reaction at selected temperatures are given in Table 9 and were computed using Burcat's thermochemical polynomials[101] with a slight modification. Standard enthalpies of formation of CHF$_3$ and CF$_3$ were updated to −695.0 kJ mol$^{-1}$ and −467.6 kJ mol$^{-1}$, respectively. These revised enthalpies of formation are based on the iPEPICO measurements and thermochemical network analysis of Harvey *et al.*[135] and the high-level *ab initio* calculations by Cobos *et al.*[136] Burcat's thermochemical polynomials utilized −693.2 kJ mol$^{-1}$ and −467.4 kJ mol$^{-1}$ for the enthalpies of formation of CHF$_3$ and CF$_3$, respectively. The updated heat of reaction (at 298 K) is more endothermic by 1.6 kJ mol$^{-1}$ (9.5 kJ mol$^{-1}$ vs 7.9 kJ mol$^{-1}$). The resultant equilibrium constants are then about 0.52, 0.68, 0.83, and 0.90 times smaller at 300 K, 500 K, 1000 K, and 1800 K, respectively. The biggest impact is at low temperatures. The overall uncertainty in the heat of reaction is about 2.6 kJ mol$^{-1}$, based on the uncertainties in the enthalpies of formation for CHF$_3$ and CF$_3$ (see Table 2). Thus, the equilibrium constants computed using either set of enthalpies of formation are within the experimental uncertainties.

The equilibrium constants given in Table 9 can be described between 300 and 2000 K to within 1.0% by the following equation:

$$K_{eq}(T) = AT^n \exp(-E/RT)\exp(-T/T_1),$$

where $A = 5.11 \times 10^{-2}$, $n = 0.90$, $E = 8.02$ kJ mol$^{-1}$, and $T_1 = 1425$ K.

On a practical level, however, the uncertainty in the equilibrium constant at low temperatures is on the order of a factor of $f = 2.0$. Coupled with the uncertainty in the measurement of the rate of the reverse reaction CF$_3$ + H$_2$ → CHF$_3$ + H (estimated to be about a factor of $f = 1.5$), the calculated rate of the forward reaction CHF$_3$ + H → CF$_3$ + H$_2$ has an uncertainty on the order of a factor of about $f = 2.5$. We estimated the uncertainty in the reverse reaction by comparing the measurements of Ayscough[137] and Berces *et al.*[117]

We note that the equilibrium constants computed using $K = k_1/k_{-1}$ from the rate expressions provided by Hranisavljevic and

**TABLE 11.** Recommended rate expressions for H abstraction from the fluoromethanes by O atoms. $k(T) = A\,T^n \exp(-E/RT)$. $k(T)$, temperature-dependent rate constant. $A$, pre-exponential factor. $n$, temperature coefficient. $E$, energy coefficient. $f(2\sigma)$, expanded uncertainty factors. $\Delta_r H_{298}$, standard enthalpy of reaction at 298 K. Units: $k$ (cm$^3$ mol$^{-1}$ s$^{-1}$), $E$ (kJ mol$^{-1}$), $T$ (K). $A/A_{CHF3}$ is the ratio of each pre-exponential $A$ to that for CHF$_3$. Uncertainty factors $f$ in parentheses "$(f)$" are at low temperatures (300–500) K.

| Reaction | $A$ | $n$ | $E$ | $f$ | $T$ | $\log_{10}(k_{300})$ | $\Delta_r H_{298}$ |
|---|---|---|---|---|---|---|---|
| CH$_4$ + O → CH$_3$ + OH | $6.63 \times 10^6$ | $2.16 \pm 0.24$ | $31.42 \pm 1.91$ | 1.18(1.5) | 300–1800 | 6.70 | 9.4 |
| CH$_3$F + O → CH$_2$F + OH | $1.66 \times 10^6$ | $2.28 \pm 0.39$ | $26.34 \pm 2.44$ | 1.4(2.0) | 300–1800 | 7.28 | −6.6 |
| CH$_2$F$_2$ + O → CHF$_2$ + OH | $4.10 \times 10^5$ | $2.40 \pm 0.41$ | $27.19 \pm 2.52$ | 1.4(2.0) | 300–1800 | 6.72 | −3.5 |
| CHF$_3$ + O → CF$_3$ + OH | $2.70 \times 10^4$ | $2.65 \pm 0.58$ | $42.17 \pm 3.52$ | 1.7(2.3) | 300–1800 | 3.65 | 16.7 |
| | | | | | | $A/A_{CHF3}$ | |
| CH$_4$ + O → CH$_3$ + OH | $3.98 \times 10^{14}$ | | 57.55 | 1.18 | 1200–1800 | 4.26 | |
| CH$_3$F + O → CH$_2$F + OH | $2.70 \times 10^{14}$ | | 53.92 | 1.4 | 1200–1800 | 2.89 | |
| CH$_2$F$_2$ + O → CHF$_2$ + OH | $1.86 \times 10^{14}$ | | 56.32 | 1.4 | 1200–1800 | 1.99 | |
| CHF$_3$ + O → CF$_3$ + OH | $9.33 \times 10^{13}$ | | 74.27 | 1.7 | 1200–1800 | 1.00 | |

Michael[107] do not agree with the equilibrium constants we provide above nor those derived using the JANAF tables.[138–140] The equilibrium constants derived from their expressions *decrease* from $K = 7.8$ to $K = 5.0$ from 1000 K to 1600 K, while those provided above *increase* from $K = 5.8$ to $K = 7.7$, as one might expect. They indicated that they used equilibrium constants derived from the JANAF tables. We were unable to identify the source of this discrepancy (it is on the order of about 6 kJ mol$^{-1}$).

## 5. Fluoromethanes + O → Fluoromethyls + OH

### 5.1. Overview

In this section, we compile and evaluate rate constants from the literature and provide recommended rate expressions for reactions involving the abstraction of H from C–H bonds by O atoms from the fluoromethanes (and methane). The data for the fluoromethanes + O reactions are extremely limited. There are no experimental rate constants (except for CH$_4$) near room temperature. At medium to high temperatures (about 600–1600 K), there are two sets of relatively reliable rate constants for CHF$_3$, one reliable measurement for CH$_3$F, and none for CH$_2$F$_2$. There have been a number of rate constants for these series of reactions derived using *ab initio* quantum chemical methods that include tunneling. The work by Matsugi and Shiina[59] using the CBS-QB3 method for energies and Eckart potentials for tunneling is the best work employing quantum chemical calculations for the fluoromethanes + O reactions. There is somewhat of a disagreement (a factor of 1.8–2.2) between the two intermediate to high temperature (600–1300 K) measurements for CHF$_3$ + O, both by reliable groups.

In Table 11, we provide recommended rate expressions for abstraction of H from the fluoromethanes (and methane) by O atoms. This includes rate expressions (with three parameters $A$, $n$, and $E$) that are good over a wide temperature range (300 K–1800 K), as well as simpler rate expressions (with two parameters $A$ and $E$) to describe the rate constants at temperatures relevant to combustion (1200–1800 K). Also included in this table are relative $A$ factors at high temperatures. We see that the relative $A$ factors for the CHF$_3$, CH$_2$F$_2$, CH$_3$F, and CH$_4$ reactions from the recommended rate expressions (1.0, 1.89, 2.75, and 4.05) are roughly proportional to the number of hydrogen atoms in the molecules (reaction path degeneracy). The TS calculations from the *ab initio* quantum chemical work of Matsugi and Shiina also yielded relative $A$ factors (1.0, 1.55, 2.66, and 4.11) that are also roughly proportional to reaction path degeneracy. This analysis provides a measure of the self-consistency (estimated 20%–30%) of these recommended rate expressions at high temperatures.

The assigned expanded uncertainty factors $f(2\sigma)$ for CH$_4$ + O were determined from the scatter in the experimental measurements and the recommended rate expression. Although the measurements extend down to nearly 400 K, these are limited data, and consequently, a higher uncertainty is assigned. The uncertainty factors at high temperatures for CH$_3$F + O and CHF$_3$ + O were assigned based on experimental uncertainties from the work of Miyoshi *et al.*[142] and of Fernandez and Fontijn[143] and agreement between the two measurements for the CHF$_3$ + O reaction. At low temperatures, the uncertainty factors were increased to account for the uncertainty in tunneling based on the comparison of the calculated tunneling from Matsugi and Shiina[59] and that from the recommended expressions. The uncertainty factors for CH$_2$F$_2$ + O were assigned by analogy to CH$_3$F + O, which has nearly identical rate constants.

### 5.2. CH₄ + O → CH₃ + OH

We have compiled rate constants from the literature for CH$_4$ + O → CH$_3$ + OH—this is the benchmark reaction for analogous reactions for the fluoromethanes. Our recommended rate expression is based on a fit to six sets of measurements that range from about 400 to 1900 K. This recommended rate expression is largely statistically equivalent to a number of recommended rate expressions for this reaction in the literature. We, however, utilize our recommended rate expression for self-consistency in evaluating the other reactions (the fluoromethanes). Table 12 contains the rate expressions from the literature along with our recommended value. The rate expression from Miyoshi *et al.*[142] was not included in the fit since two other measurements by this group were included. Figure 9 shows the fit (solid curve) to the experimental rate constants (various symbols). For comparison, in Fig. 9, we also show the recommended rate expression of Sutherland *et al.*[144] and the quantum calculations of Matsugi and Shiina.[59] Figure 10 shows the deviations of the data not included in the

**TABLE 12.** $CH_4 + O \rightarrow CH_3 + OH$ rate expressions. $k(T) = A\,T^n \exp(-E/RT)$. $k(T)$, temperature-dependent rate constant. $A$, pre-exponential factor. $n$, temperature coefficient. $E$, energy coefficient. $f(2\sigma)$, expanded uncertainty factors. Units: $k$ ($cm^3\,mol^{-1}\,s^{-1}$), $E$ ($kJ\,mol^{-1}$), $T$ (K). Letters in the uncertainty factor $f$ column refer to quantum chemical data presented in Fig. 11. See Sec. 10 for definitions of acronyms and abbreviations in the Method column

| $A$ | $n$ | $E$ | $f$ | $T$ | Method | Reference |
|---|---|---|---|---|---|---|
| Evaluations | | | | | | |
| $6.63 \times 10^6$ | 2.16 | 31.42 | 1.18(1.5) | 300–1840 | Recommended | This work |
| $3.98 \times 10^{14}$ | | 57.55 | 1.18 | 1200–1800 | Recommended, high T fit | This work |
| $6.92 \times 10^8$ | 1.56 | 35.50 | [1.4] | 400–2250 | Review | 86SUT/MIC[144] |
| $4.90 \times 10^6$ | 2.2 | 31.76 | [1.3] | 420–1520 | Review | 86COH/WES[154] |
| $1.62 \times 10^6$ | 2.3 | 29.68 | [1.3] | 300–1800 | Review | 86COH[155] |
| $3.16 \times 10^{12}$ | 0.50 | 43.07 | [1.5(2.5)] | 475–2250 | Review | 81KLE/TAN[156] |
| $1.14 \times 10^7$ | 2.08 | 31.93 | [1.2] | 300–2200 | Review | 79ROT/JUS[157] |
| $2.1 \times 10^{13}$ | | 37.83 | 1.3 | 350–1000 | Review | 73HER/HUI[158] |
| $2.19 \times 10^{13}$ | | 37.08 | [1.6] | 300–1000 | Review | 69HER/HUI[159] |
| Experimental (preferred data) | | | | | | |
| $2.83 \times 10^{14}$ | | 54.13 | 1.52 | 980–1529 | Shock, flash photol, reson abs | 94MIY/TSU[160] |
| $5.01 \times 10^{14}$ | | 58.28 | 1.55 | 980–1520 | Shock, flash photol, reson abs | 93MIY/OHM[142] |
| $6.75 \times 10^{14}$ | | 64.44 | 1.86 | 1340–1840 | Shock, flash photol, reson abs | 92OHM/YOS[161] |
| $1.61 \times 10^8$ | 1.75 | 34.26 | 2.0 | 763–1760 | Shock, flash photol, reson abs | 87SUT/KLE[162] |
| $5.55 \times 10^5$ | 2.40 | 24.44 | 2.0 | 763–1760 | Shock, flash photol, reson abs | 86SUT/MIC[144] |
| $5.24 \times 10^5$ | 2.50 | 29.67 | 2.4 | 420–1670 | Fast flow, flash photol, reson fluor | 86FEL/MAD[163] |
| $1.21 \times 10^{14}$ | | 45.15 | 1.7 | 474–1160 | Dischg flow, reson fluor | 81KLE/TAN[156] |
| $7.60 \times 10^{12}$ | | 34.18 | [1.3] | 474–520 | Dischg flow, reson fluor | 81KLE/TAN[156] |
| $1.14 \times 10^7$ | 2.08 | 31.93 | 2.6 | 525–1250 | Flow, flash photol, reson fluor | 79FEL/FON[164] |
| $2.0 \times 10^{13}$ | | 38.50 | 1.12[1.7] | 400–900 | Fast dischg flow, ESR | 69WES/DEH[145] |
| $1.23 \times 10^{13}$ | | 36.03 | [1.3] | 363–605 | Refit 69WES/DEH | This work |
| Experimental (excluded data) | | | | | | |
| $4.0 \times 10^5$ | | | [10] | 293 | Static, photol | 73FAL/HOA[165] |
| $1.9 \times 10^{12}$ | | 30.51 | 1.5[5] | 350–1000 | Revised 65CAD/ALL | 73HER/HUI[158] |
| $1.26 \times 10^7$ | | | [3] | 300 | Fast dischg flow, ESR | 69WES/DEH[145] |
| $4.0 \times 10^8$ | | | [100] | 300 | Fast dischg flow, ESR | 68FRO[166] |
| $4.0 \times 10^{14}$ | | 41.82 | [10] | 375–576 | Stirred reactor, dischg, MS | 67WON/POT[167] |
| $7.0 \times 10^{12}$ | | 32.18 | 1.29[5] | 450–600 | Dischg flow, ESR | 67BRO/THR[168] |
| $3.30 \times 10^9$ | | | 1.5 | 295 | Dischg flow, O emiss | 65CAD/ALL[169] |
| $2.3 \times 10^{13}$ | | 27.6 | 1.5 | 295–533 | Dischg flow, O emiss | 65CAD/ALL[169] |
| $7.1 \times 10^{12}$ | | 30.51 | 1.5[10] | 295–533 | Dischg flow, oxygen emiss | 65CAD/ALL[169] |
| $2.00 \times 10^{12}$ | | 28.85 | 1.5[3] | 353–580 | Stirred reactor, MW dischg, MS | 63WON/POT[170] |
| Theoretical | | | | | | |
| $5.64 \times 10^{-4}$ | 5.20 | 12.97 | [3] x | 200–1000 | Quantum PES, our fit to data in tables | 16ZHA/WAN[171] |
| $1.87 \times 10^3$ | 3.24 | 24.86 | [1.6] a | 300–1800 | CBS-QB3 Eckart | 14MAT/SHI[59] |
| $8.68 \times 10^{14}$ | | 64.06 | [1.6] | 1200–1800 | This work; high T fit | 14MAT/SHI[59] |
| $6.78 \times 10^2$ | 3.27 | 23.15 | [1.3] b | 300–2500 | Quant PES; our fit to data in tables | 14GON/COR[147,148] |
| $2.09 \times 10$ | 4.01 | 18.65 | [1.3] c | 200–2500 | Quant PES; our fit to data in tables | 05TRO/GAR[149] |
| $5.62 \times 10^4$ | 2.70 | 28.06 | [1.7] d | 200–1000 | Quant PES; our fit to data in tables | 02HUA/MAN[151] |
| $8.12 \times 10^4$ | 2.60 | 26.32 | [1.7] e | 200–1250 | Quant PES | 00YU/NYM[152] |
| $3.63 \times 10^6$ | 2.17 | 30.09 | [1.3] f | 200–2500 | Quant PES | 00ESP/GAR[146] |
| $2.16 \times 10^9$ | 1.32 | 38.43 | [3.5] x | 300–1000 | Quant PES; our fit to data in figures | 99CLA[172] |
| $3.39 \times 10^{14}$ | | 51.8 | [2.0] x | 300–2500 | Quant PES | 98COR/ESP[173] |
| $5.38 \times 10^1$ | 3.65 | 22.95 | [1.3] g | 300–2000 | Quant PES | 90GON/MCD[150] |
| $2.13 \times 10^6$ | 2.21 | 27.11 | [1.3] h | 500–2500 | BEBO theory | 83MIC/KEI[153] |
| $5.12 \times 10^6$ | 2.00 | 26.94 | [1.4] i | 300–2500 | Semi-empirical | 78SHA[174] |
| $1.03 \times 10^{14}$ | | 38.58 | [4] x | 300–1000 | BEBO Theory | 68MAY/SCH[175,176] |
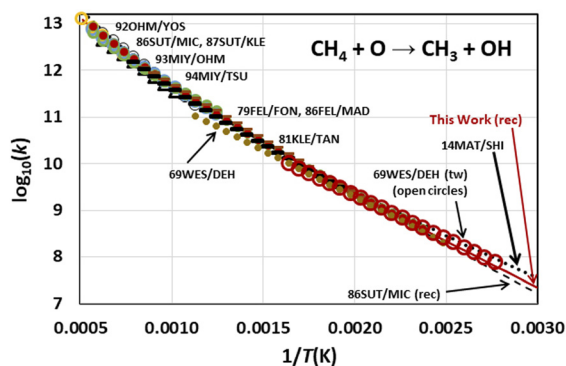
**FIG. 9.** $CH_4 + O \rightarrow CH_3 + OH$ rate constants and recommended rate expression. Rate constants $k$ ($cm^3$ $mol^{-1}$ $s^{-1}$). Legend: Red line (recommended), dotted line (14MAT/SHI[59]), dashed line (86SUT/MIC rec, their recommendation), black triangles (94MIY/TSU[160]), black circles (93MIY/OHM[142]), yellow circles (92OHM/YOS[161]), blue circles (87SUT/KLE[162]), green circles (86SUT/MIC[144]), red dots (86FEL/MAD[163]), brown dashes (81KLE/TAN[156]), black dashes (79FEL/FON[164]), brown dots (69WES/DEH[145]), and red circles (69WES/DEH[145] tw) were derived from our refitting of the original data.

fit from the recommended rate expression, and Fig. 11 shows the deviations for the quantum calculations.

The rate constants at intermediate to high temperatures (500–1800 K) are well established (within about 20%). At low temperatures (300–500 K), there is a single fairly reliable measurement by Westenberg and Dehaas.[145] There are, however, some inconsistencies in the data. First, the barrier from the reported rate expression (38 kJ $mol^{-1}$) is substantially lower than the effective temperature dependencies (44 kJ $mol^{-1}$) of measurements at intermediate temperatures (600–900 K) by other workers. Second, the reported rate expression is inconsistent with the individual rate constant data presented in the paper. In our fits, we utilized an intermediate temperature subset of the reported data (4 points from 363 K to 605 K) and ignored the lowest (297 K) and highest (904 K) data points—and our fit goes through roughly the midpoint (450 K) of these data.
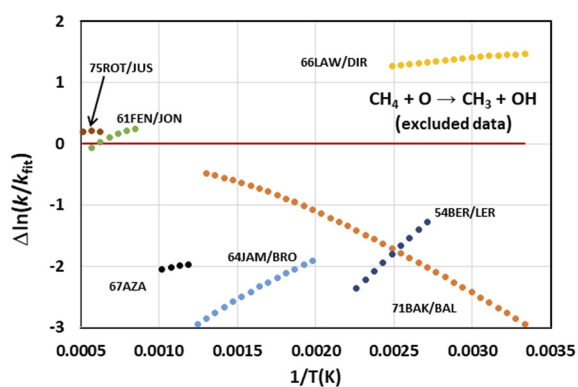


**FIG. 10.** Residuals for $CH_4 + O \rightarrow CH_3 + OH$ rate constants excluded from fit. Rate constants $k$ ($cm^3$ $mol^{-1}$ $s^{-1}$). Residuals in $\ln(k)$ units.
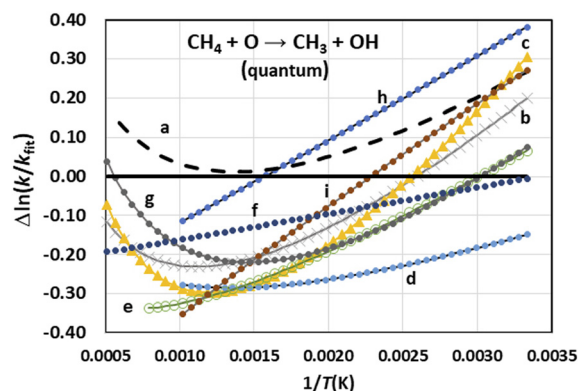


**FIG. 11.** Residuals for $CH_4 + O \rightarrow CH_3 + OH$ rate constants from quantum chemical calculations. Rate constants $k$ ($cm^3$ $mol^{-1}$ $s^{-1}$). Residuals in $\ln(k)$ units. See Table 12 for legend ("a" through "i" labels).

Figure 11 shows the deviations of the rate constants $\Delta \ln(k)$ for quantum calculations from the recommended rate expression. Note that several sets of rate constants are not included in this figure because they deviated by large amounts (these are denoted in Table 12 with "x" in the uncertainty factor column). Note also that identification of the rate expressions with the labels "a" through "i" is also denoted in this table.

Overall, the differences between the rate constants from quantum calculations and the recommended values are on the order of a factor of $f = 1.7$. The rate constants from the quantum calculations are on the average about 20% lower at high temperatures and about 10% higher at low temperatures compared to the recommended rate constants based on experimental data. The rate expression from quantum chemical calculations that is closest to the recommended expression is that of Espinosa-García and García-Bernáldez[146]—the temperature coefficients $n$ are virtually identical (2.17 vs 2.16), the temperature dependencies differ by under 1.5 kJ $mol^{-1}$, and the rate constants at 300 K differ by just 1.2%.

The rate constants at high temperatures from the calculations of González-Lavado et al.,[147,148] Troya and Garcia-Molina,[149] and Gonzalez et al.[150] agree satisfactorily (within about 25%) with the experimental values. The temperature dependencies at low temperatures from the quantum calculations agree satisfactorily (within about 2 kJ $mol^{-1}$) with that derived from the recommended rate expression in the work of Gonzalez-Lavado et al.,[147,148] Hurarte-Larranga and Manthe,[151] Yu and Nyman,[152] and Michael et al.,[153] although the absolute rate constants deviate by factors of $f=(1.3–2.0)$.

Other key things to note about the *ab initio* calculations are that the rate expression at high temperatures (1200–1800 K) from the work of Matsugi and Shiina has an $A$ factor about 2.2 times higher than the fitted recommended value and a temperature dependence $E$ that is about 11% higher. They adjusted their barrier so that their rate expression agreed with the low-temperature data, which then affects the rate constants at high temperatures. This is an incorrect procedure, and the tunneling parameters should have been adjusted. Other observations are that at 300 K, the predicted tunneling rate by Yu and Nyman is about 15% higher than that derived from the recommended rate expression, and the tunneling rate from Matsugi and Shiina is
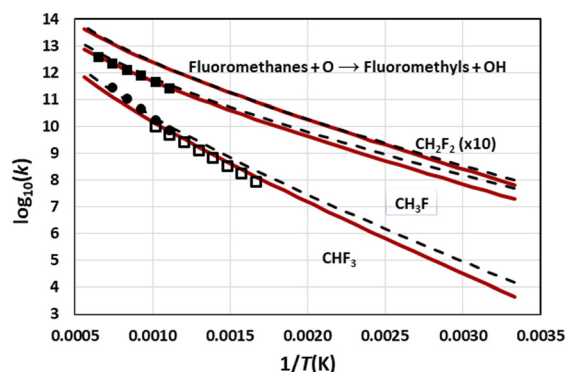
**FIG. 12.** Rates of reaction for H abstraction by O from $CH_3F$, $CH_2F_2$, and $CHF_3$. Rate constants $k$ (cm$^3$ mol$^{-1}$ s$^{-1}$). Circles and squares are experimental rate constants. Open squares (01FER/FON[143]), filled circles (93MIY/OHM[142]), and filled squares (adjusted 93MIY/OHM[142]). Solid curves are recommended rate expressions. Dotted curves are from quantum calculations of Matsugi and Shiina.[59] The rate constants for $CH_2F_2$, where no experimental data are available, were estimated by interpolating the rate expressions using the rate constants calculated by Matsugi and Shiina as a relative measure, as well as trends in $A$, $n$, and $E$ in this homologous series.

about 1.9 times higher. We will employ the latter difference to assist in estimating $k$(300 K) for the other fluoromethane + O reactions.

### 5.3. $CH_3F$ + O → $CH_2F$ + OH

There is one set of reliable experimental data for this reaction from the shock tube work of Miyoshi et al.[142] in the temperature range (920–1570) K. There are other reported rate constants, but they differ from the recommended and self-consistent rate expression by as much as an order of magnitude. In the work of Miyoshi et al., the authors measured rate constants for the abstraction of H by O atoms from $CH_4$, $CH_3F$, and $CHF_3$ (as well as other molecules). Consequently, these three sets of measurements provide a good measure of the relative rates of these reactions.

The rate constants for the homologous reaction $CH_4$ + O in the work of Miyoshi et al. are slightly different (about 15% higher) than the rate constants measured in other work for this reaction by the same group[160,161] and slightly different from the rate expression recommended in this work. The most recent work of Miyoshi et al.[142] reanalyzed/corrected the rate expression for $CH_4$ + O. Thus, we have also corrected the reported rate constants for the reaction $CH_3F$ + O → $CH_2F$ + OH by Miyoshi et al. by 15% (decreased) to account for this difference.

There are no measured rate constants for this reaction at low temperatures (i.e., near room temperature). In order to provide a rate expression valid over a range of temperatures (300–1800 K), we needed to fit the high-temperature data along with providing an estimate for the rate constant at low temperatures. We estimated $k$(300 K) for $CH_3F$ (and for $CH_2F_2$ and $CHF_3$) by extrapolating the rate constants at high temperatures with a fixed $k$(300 K) for $CH_4$. [Note that the high-temperature rate constants for $CH_2F_2$ were estimated by analogy to $CH_3F$ + O (see discussion for that reaction below).] We bracketed $k$(300 K) for the fluoromethanes that provided a range of reasonable parameters for the fitted rate

expressions using the systematic differences between the calculated tunneling rates from Matsugi and Shiina[59] and the fitted values. We then used intermediate values from the bracketing of $k$(300 K) for each fluoromethane. The procedure we used was iterative and systematic but manual (not computer optimization). [Note that by "reasonable parameters," we mean different sets of parameters ($A$, $n$, $E$) that gave statistically similar fits and were constrained by the correlations that we discuss in Sec. 8. For example, a temperature coefficient of $n$ = (2–3) is reasonable, while $n$ = (1 or 4) is not.]

The resultant fit to the experimental rate constants of Miyoshi et al. and the estimated $k$(300 K) from bracketing are shown in Fig. 12. Rate expressions from the literature are given in Table 13. The fitted rate expression not only agrees very well with the rate constants at high temperatures but also displays the same effective activation energy (temperature dependence) at high temperatures. From inspection of the raw data of Miyoshi et al., we estimated an uncertainty factor of $f$ = 1.4 at high temperatures. Considering the uncertainties inherent in the bracketing methodology to estimate a rate constant at low temperatures (along with the uncertainties in the rate constants at high temperatures), we estimate an uncertainty factor of $f$ = 2.0 for $k$(300 K).

### 5.4. $CH_2F_2$ + O → $CHF_2$ + OH

There are no reliable experimental measurements for this reaction. The reported values by Parsamyan and Nalbandyan[103] are off by an order of magnitude from what would be reasonable. In order to provide a rate expression, we utilized estimated rate constants at both high and low temperatures. An initial guess for the rate constants at high temperatures was estimated using the recommended rate expression for $CH_3F$ + O and then scaling the rate constants by the ratio of the constants from the ab initio calculations of Matsugi and Shiina.[59] An initial guess for the low-temperature $k$(300 K) rate constant was estimated by bracketing reasonable values for the temperature coefficient $n$ (2.2–2.5)—considering the trend in temperature coefficients $n$ for the other molecules $CH_4$, $CH_3F$, and $CHF_3$, as well as considering the derived activation energy at low temperatures to be about 60% of the derived activation energy at high temperatures. See Sec. 8 for figures and discussion regarding these correlations. These parameters were manually adjusted to obtain a best relaxed fit while maintaining the relative rate constants for the reactions involving $CH_3F$ and $CH_2F_2$ from the ab initio calculations of Matsugi and Shiina. The resultant estimated rate constants are shown in Fig. 12, and the rate expressions are provided in Table 14. As before, we estimated expanded uncertainty factors $f$ (2$\sigma$) of $f$ = 1.5 and $f$ = 2.0 at high and low temperatures, respectively.

Note that the rate constants in Fig. 12 for $CH_2F_2$ + O are displaced upward by an order of magnitude (one log$_{10}$ unit) for clarity. The absolute values for the $CH_2F_2$ + O rate constants are about 1.8 times lower at high temperatures and about 2.9 times lower at low temperatures than those for $CH_3F$ + O.

### 5.5. $CHF_3$ + O → $CF_3$ + OH

There are two relatively reliable measurements of the reaction of O with trifluoromethane ($CHF_3$) by Fernandez and Fontijn[143] and Miyoshi et al.[142] They are, however, in disagreement by a factor of about (1.8–2.2) and outside their respective expanded uncertainty

**TABLE 13.** $CH_3F + O \rightarrow CH_2F + OH$ rate expressions. $k(T) = A T^n \exp(-E/RT)$. $k(T)$, temperature-dependent rate constant. $A$, pre-exponential factor. $n$, temperature coefficient. $E$, energy coefficient. $f(2\sigma)$, expanded uncertainty factors. Units: $k$ (cm$^3$ mol$^{-1}$ s$^{-1}$), $E$ (kJ mol$^{-1}$), $T$ (K)

| $A$ | $n$ | $E$ | $f$ | $T$ | Method | Reference |
|---|---|---|---|---|---|---|
| Evaluations | | | | | | |
| $1.66 \times 10^6$ | 2.28 | 27.19 | 1.4(2.0) | 300–1800 | Recommended | This work |
| $2.70 \times 10^{14}$ | | 53.92 | 1.4 | 1200–1800 | Recommended, high T fit | This work |
| Experimental (preferred data) | | | | | | |
| $1.48 \times 10^{14}$ | | 47.47 | 1.1 | 920–1570 | Adjusted 93MIY/OHM[142] | This work |
| Experimental (excluded data) | | | | | | |
| $1.70 \times 10^{14}$ | | 47.47 | 1.3 | 920–1570 | Shock, laser photol, O reson abs | 93MIY/OHM[142] |
| $7.83 \times 10^{12}$ | | 40.57 | [7] | 858–933 | Static | 67PAR/AZA[102] |
| **Theoretical** | | | | | | |
| $3.01 \times 10^3$ | 3.13 | 20.45 | [1.7(3.0)] | 300–1800 | CBS-QB3 Eckart | 14MAT/SHI[59] |
| $5.76 \times 10^{14}$ | | 58.44 | [1.7] | 1200–1800 | This work, high T fit | 14MAT/SHI[59] |
| n/a | | 51.25 | | 298 | G2M | 01KRE/SEY[177] |
| $7.5 \times 10^6$ | | | | 298 | G2M | 01KRE/SEY[177] |
| $2.54 \times 10^{-3}$ | 4.80 | 10.08 | | 200–3000 | G2MP2 | 99WAN/HOU[178] |

factor $f(2\sigma)$ of $f = 1.3$ and $f = 1.5$. Both measurements were made by reliable researchers who have obtained essentially the same rate constants (within <10%) for the reference reaction $CH_4 + O \rightarrow CH_3 + OH$, as well as having made reliable measurements for other reactions.

The limited data for this reaction are given in Table 15. The rate constants from the literature and our recommended rate expression are presented in Fig. 12 along with the rate expression from the *ab initio* calculations of Matsugi and Shiina.[59] The other values in the table not considered are in significant disagreement with the expression recommended here.

We have examined the measurements of this reaction by Fernandez and Fontijn and by Miyoshi *et al.* and see no obvious *a priori* reason to consider one or the other to be in error. In order to discriminate between the two measurements, we utilized the *ab initio* calculations of Matsugi

and Shiina combined with parametric fits to the data and also self-consistency with the other rate expressions. We found that utilizing the rate constants of Miyoshi *et al.* yielded fitted rate expressions with $A$ factors at high temperatures (1200–1800 K) that closely scaled with the $A$ factors derived from the TS/quantum chemical calculations of Matsugi and Shiina and that these rate expressions yielded exponential temperature coefficients ($T^n$) that were more reasonable, $n = (2.0–2.5)$, and relaxed (not a forced fit). On the other hand, the activation energy in the temperature range of interest from the fitted curve was consistent with the measured temperature dependence of Fernandez and Fontijn, while the data of Miyoshi *et al.* showed a higher activation than the trend from the fitted curve. Consequently, we used both of these sets of data to determine the recommended rate expression with the data of Fernandez and Fontijn and Miyoshi *et al.* a factor of about 1.35 lower and 1.65 higher at the midpoint of their respective temperature ranges than the recommended

**TABLE 14.** $CH_2F_2 + O \rightarrow CHF_2 + OH$ rate expressions. $k(T) = A T^n \exp(-E/RT)$. $k(T)$, temperature-dependent rate constant. $A$, pre-exponential factor. $n$, temperature coefficient. $E$, energy coefficient. $f(2\sigma)$, expanded uncertainty factors. Units: $k$ (cm$^3$ mol$^{-1}$ s$^{-1}$), $E$ (kJ mol$^{-1}$), $T$ (K)

| $A$ | $n$ | $E$ | $f$ | $T$ | Method | Reference |
|---|---|---|---|---|---|---|
| Evaluations | | | | | | |
| $4.10 \times 10^5$ | 2.49 | 27.19 | 1.4(2) | 300–1800 | Recommended | This work |
| $1.86 \times 10^{14}$ | | 56.32 | 1.4 | 1200–1800 | Recommended, high T fit | This work |
| Experimental (preferred data) | | | | | | |
| NONE | | | | | | |
| Experimental (excluded data) | | | | | | |
| $2.65 \times 10^{12}$ | | 36.83 | 1.14[10] | 873–953 | Static | 68PAR/NAL[103] |
| Theoretical | | | | | | |
| $1.20 \times 10^3$ | 3.17 | 22.61 | [1.8] | 300–1800 | CBS-QB3 Eckart | 14MAT/SHI[59] |
| $3.28 \times 10^{14}$ | | 61.08 | [1.6(1.13)] | 1200–1800 | This work, high T fit | 14MAT/SHI[59] |
| n/a | | 54.48 | | 298 | G2M | 01KRE/SEY[177] |
| $2.7 \times 10^6$ | | | | 298 | G2M | 01KRE/SEY[177] |
| $2.24 \times 10^{-4}$ | 5.03 | 9.30 | | 200–3000 | G2MP2 | 99WAN/HOU[178] |

**TABLE 15.** $CHF_3 + O \rightarrow CF_3 + OH$ rate expressions. $k(T) = A T^n \exp(-E/RT)$. $k(T)$, temperature-dependent rate constant. $A$, pre-exponential factor. $n$, temperature coefficient. $E$, energy coefficient. $f(2\sigma)$, expanded uncertainty factor. Units: $k$ ($cm^3$ $mol^{-1}$ $s^{-1}$), $E$ ($kJ$ $mol^{-1}$), $T$ (K)

| $A$ | $n$ | $E$ | $f$ | $T$ | Method | Reference |
|---|---|---|---|---|---|---|
| Evaluations | | | | | | |
| $2.70 \times 10^4$ | 2.65 | 42.17 | 1.7(2.3) | 300–1800 | Recommended CHN | This work |
| $9.33 \times 10^{13}$ | | 74.27 | 1.7 | 1200–1800 | Recommended, high T fit CHN | This work |
| $3.07 \times 10^{14}$ | | 79.28 | | 630–1330 | Review | 01FER/FON[143] |
| Experimental (preferred data) | | | | | | |
| $4.57 \times 10^{14}$ | | 81.80 | 1.6 | 956–1328 | Shock, laser photol, O reson abs | 93MIY/OHM[142] |
| $3.98 \times 10^{14}$ | | 81.80 | [1.65] | 956–1328 | Adjusted 93MIY/OHM | This work |
| $1.51 \times 10^{13}$ | | 60.16 | [1.35] | 630–940 | Fast flow, VUV flash photol, O reson abs | 01FER/FON[143] |
| Experimental (excluded data) | | | | | | |
| $1.50 \times 10^{11}$ | | 24.94 | 1.25[5] | 500–750 | Flow, photol, LIF | 97MED/FLE[179] |
| $1.10 \times 10^{12}$ | | 13.30 | [7] | 920–1150 | Model, flame | 94RIC/VAN[111] |
| $4.88 \times 10^{12}$ | | 45.15 | [6] | 298–600 | Plasma excit, MS | 77JOU/POU[180] |
| Theoretical | | | | | | |
| $1.51 \times 10^2$ | | 36.58 | [1.2(2)] | 300–1800 | CBS-QB3 Eckart | 14MAT/SHI[59] |
| $2.11 \times 10^{14}$ | | 77.48 | [1.2] | 1200–1800 | High T fit | 14MAT/SHI[59] |

rate expression, respectively. We note that in the small temperature range (940–956 K) where the two sets of data overlap, they differ by (20–30)%, diverging at higher and lower temperatures.

In the fitting procedure, while utilizing the experimental high-temperature data, it was necessary to estimate $k(300\ K)$ for $CHF_3$. To do this, we used a bracketing procedure (as discussed earlier) based on extrapolating the rate constants from high temperature, using $k(300\ K)$ for $CH_4$, and utilizing the differences between calculated tunneling rates by Matsugi and Shiina and that obtained through fits of the experimental data. This was not a rigorous procedure but rather (manually) iteratively adjusting $k(300\ K)$ to obtain a range of reasonable fit parameters. See Secs. 2 and 8 for discussion and figures regarding this optimization procedure where the experimental data are fit subject to constraints involving correlations due to SARs.

In summary, the recommended rate expression is based on the rate constants of Fernandez and Fontijn and Miyoshi *et al.* at high temperatures and an estimated $k(300\ K)$. Based on the uncertainties in the experimental data and the uncertainty in the parametric fit to the data, we estimate an expanded uncertainty factor $f(2\sigma)$ of about a factor $f = 1.7$ to the rate constant at high temperatures and about $f = 2.3$ at 300 K.

## 6. Fluoromethanes + OH → Fluoromethyls + H₂O

### 6.1. Overview

All of the fluoromethanes and methane have many reliable measurements for the abstraction of H by OH radicals at low temperatures, both below and above room temperatures (250–500 K). The extent of the number of these measurements is because the lifetimes of these molecules in the upper atmosphere are important to radiative forcing and global warming.[1] High-temperature measurements (1000–2000 K) related to the combustion of these molecules have been made only for $CH_4$ and $CHF_3$, but not for $CH_3F$ or $CH_2F_2$. However, the rates of these two latter reactions at low temperatures (up to about 500 K) are due to tunneling and the curvature in the rate expressions (characterized by the temperature exponent $T^n$) is a constraint on the rate constant at high temperatures.

The recommended rate expressions for the reaction of OH with methane and the fluoromethanes are collected in Table 16. The relative $A$ factors at high temperatures for abstraction by OH do not follow the reaction path degeneracy (number of hydrogen atoms) like they roughly do for abstraction by H and O atoms—1.0, 3.0, 4.3, and 10.9 vs 1, 2, 3, and 4 for $CHF_3$, $CH_2F_2$, $CH_3F$, and $CH_4$, respectively. This is likely because the TS has a hindered rotor; this is discussed in more detail in the discussion near the end of this paper.

### 6.2. CH₄ + OH → CH₃ + H₂O

In Table 17, we provide rate expressions compiled from the literature for the reaction $CH_4 + OH \rightarrow CH_3 + H_2O$. These include evaluations/review, experimental measurements, and quantum chemical calculations. We fit the experimental data from 9 different measurements to provide a recommended rate expression with expanded uncertainty factors $f(2\sigma)$ of about $f = 1.15$ at higher temperatures (1000–2000 K) and $f = 1.07$ at low temperatures (200–500 K), respectively. Although we assign an uncertainty of 7% at low temperatures, we note that at (300–400) K Bryukov *et al.*,[181] Bonard *et al.*,[13] Dunlop and Tully,[182] Gierczak *et al.*,[183] Vaghjiani and Ravishankara,[184] Amedro *et al.*,[185] and Overend *et al.*[186] all agree to within about 3% of the recommended values. For more discussion of the low-temperature data for this reaction, see Burkholder *et al.*[187] The recommended rate expression by Burkholder *et al.* agrees with our recommended rate expression (and the experimental data) to within about 5% in the temperature range (200–350) K but diverges rapidly above about 400 K.

The data excluded from our fit deviated from the recommended expression by factors of $f = (1.2–5.0)$, and almost all of these data had rate constants that were higher than the recommended values. In addition, many of these had temperature dependencies that were inconsistent with the recommended rate expression. In general, the data included had residuals on the order of (3–13)%, while the data excluded had residuals of about (20–70)%. Figure 13 shows the experimental rate data along with the recommended rate expression.

**TABLE 16.** Recommended rate expressions for H abstraction from the fluoromethanes by OH radicals. $k(T) = A T^n \exp(-E/RT)$. $k(T)$, temperature-dependent rate constant. $A$, pre-exponential factor. $n$, temperature coefficient. $E$, energy coefficient. $f(2\sigma)$, expanded uncertainty factor. $\Delta_r H_{298}$, standard enthalpy of reaction at 298 K. Units: $k$ (cm$^3$ mol$^{-1}$ s$^{-1}$), $E$ (kJ mol$^{-1}$), $T$ (K). $A/A_{CHF_3}$ is the ratio of each pre-exponential $A$ to that for CHF$_3$.

| Reaction | $A$ | $n$ | $E$ | $f$ | $T$ | $\log_{10}(k_{300})$ | $\Delta_r H_{298}$ |
|---|---|---|---|---|---|---|---|
| $CH_4 + OH \rightarrow CH_3 + H_2O$ | $6.19 \times 10^5$ | $2.23 \pm 0.09$ | $9.84 \pm 1.54$ | 1.12(1.05) | 200–2025 | 9.62 | −58.2 |
| $CH_3F + OH \rightarrow CH_2F + H_2O$ | $1.06 \times 10^6$ | $2.04 \pm 0.26$ | $5.70 \pm 1.93$ | 1.5(1.22) | 240–1800 | 10.08 | −74.2 |
| $CH_2F_2 + OH \rightarrow CHF_2 + H_2O$ | $3.29 \times 10^6$ | $1.86 \pm 0.24$ | $7.52 \pm 1.90$ | 1.5(1.17) | 220–1800 | 9.82 | −71.1 |
| $CHF_3 + OH \rightarrow CF_3 + H_2O$ | $1.20 \times 10^6$ | $1.85 \pm 0.19$ | $13.71 \pm 1.78$ | 1.3(1.22) | 250–1800 | 8.27 | −51.1 |
| | | | | | | $A/A_{CHF_3}$ | |
| $CH_4 + OH \rightarrow CH_3 + H_2O$ | $6.12 \times 10^{13}$ | | 35.33 | 1.12 | 1200–1800 | 10.9 | |
| $CH_3F + OH \rightarrow CH_2F + H_2O$ | $2.40 \times 10^{13}$ | | 30.44 | 1.5 | 1200–1800 | 4.26 | |
| $CH_2F_2 + OH \rightarrow CHF_2 + H_2O$ | $1.68 \times 10^{13}$ | | 30.09 | 1.5 | 1200–1800 | 2.98 | |
| $CHF_3 + OH \rightarrow CF_3 + H_2O$ | $5.64 \times 10^{12}$ | | 36.15 | 1.2 | 1200–1800 | 1.00 | |

Figures 14 and 15 show the deviations of the included and excluded data, respectively, in ln($k$) units from the recommended expression. There have been many precise measurements at lower temperatures for this reaction but only one at high temperatures by Srinivasan et al.[188] This is reflected in an uncertainty at high temperatures that is about 2 times higher than at low temperatures (15% vs 7%). We note that our fit is statistically similar to the recommended rate expression (not their experimental one) by Srinivasan et al. (see Table 17) based on their fit to available data with their rate expression being about 5% and 14% higher at low and high temperatures, respectively. Our fit is slightly different because we consider other data and use different weightings. Note that we excluded the data from flame measurements.

### 6.3. (CH$_3$F, CH$_2$F$_2$, CHF$_3$) + OH → (CH$_2$F, CHF$_2$, CF$_3$) + H$_2$O

We can estimate (in a relative fashion) the rate constants for CH$_3$F + OH and CH$_2$F$_2$ + OH at high temperatures (1200–1800 K) utilizing the low-temperature measurements and extrapolating and bracketing considering the relative activation energies from ab initio calculations (benchmarked to that for CH$_4$ + OH and CHF$_3$ + OH), considering a range of temperature exponents by analogy to CH$_4$ and CHF$_3$, and considering that the $A$ factors should vary (roughly) uniformly from that for CH$_4$ to that for CHF$_3$.

Using the low-temperature data and extrapolating based on a range of temperature exponents ($n = 1.95 \pm 0.10$), we find that the activation energies for CH$_3$F + OH and CH$_2$F$_2$ + OH should be about 6.8 ± 0.8 kJ mol$^{-1}$ and 5.5 ± 0.8 kJ mol$^{-1}$ lower, respectively, than that for CHF$_3$ + OH. Using the relative activation energies from TSs computed in the quantum chemistry work of Schwartz et al.[61] and Matsugi and Shiina,[59] the activation energies for CH$_3$F + OH and CH$_2$F$_2$ + OH should both be about 6.9 ± 0.3 kJ mol$^{-1}$ lower than that for CHF$_3$ + OH. There is some uncertainty in the relative activation energies from the work of Matsugui and Shiina because they arbitrarily adjusted the barriers (at 0 K) in order to make their tunneling calculations agree with the experimental rate constants at low temperatures (and do not report the unadjusted rate constants)—hence, we increase the uncertainty and estimate the activation energies for CH$_3$F + OH and CH$_2$F$_2$ + OH as 6.9 ± 0.3 kJ mol$^{-1}$ lower than that for CHF$_3$. Concurrent with the lower activation energies, the rate constants ($k$) at high temperature should be about 6.2 ± 0.3 and 5.1 ± 0.3 times higher for CH$_3$F + OH and CH$_2$F$_2$ + OH compared to

CHF$_3$ + OH, and $A$ factors should be about 3.9 ± 0.3 and 2.9 ± 0.3 times higher, respectively.

Our recommended rate expressions for CH$_3$F + OH and CH$_2$F$_2$ +OH are based on bracketing the rate parameters $A$, $n$, and $E$ using the recommended rate expressions for CH$_4$ + OH and CHF$_3$ + OH as benchmarks and interpolating using the ab initio calculations as a measure. The uncertainties provided in square brackets "[]" for the rate constants in Table 18 are based on deviations for the experimental measurements at low and high temperatures. We have assigned uncertainty factors of $f = 1.4$ for both CH$_3$F + OH and CH$_2$F$_2$ + OH based on our bracketing estimate. This corresponds to an uncertainty in the activation energy of 4.2 kJ mol$^{-1}$ at 1500 K.

Tables 17–19 list the rate constants compiled from the literature for the reactions of OH with CH$_3$F, CH$_2$F$_2$, and CHF$_3$, and Figs. 15–17 present the recommended rate constants along with the selected data for these three reactions. Figure 19 is a summary comparing the temperature dependence of the recommended rate constants with reactions involving CH$_3$F and CH$_2$F$_2$ being similar, while CHF$_3$ + OH has a much stronger temperature dependence.

Table 18 provides rate constants from the literature for CH$_3$F + OH → CH$_2$F + H$_2$O, and Fig. 16 compares the experimental rate constants to our recommended rate expression. The only experimental rate constant data that exists for this reaction CH$_3$F + OH → CH$_2$F + H$_2$O is at low temperatures between about 240 and 500 K. The scatter in the experimental data is about a factor of $f = 1.3$. In this range, our recommended rate expression agrees with the recommended values from the NASA/JPL Kinetics Panel Evaluation[187] to within about (6–8)% (see the dashed line in Fig. 16). We assign an uncertainty to our rate expression in this range of $f = 1.2$.

Table 19 provides rate constants from the literature for CH$_2$F$_2$ + OH → CHF$_2$ + H$_2$O, and Fig. 17 compares the experimental rate constants to our recommended rate expression. There are no experimental data above about 500 K. The majority of the data are between about 220 and 400 K. There are two sets of data that extended slightly above 400 K (420 and 490 K). The agreement between the experimental data at low temperatures is good, and we assign an uncertainty factor $f = 1.17$. Because of the uncertainty in extrapolating the rate constants to high temperatures, we assign an uncertainty factor $f = 1.5$ in this range.

The recommended rate expressions provided here for the reactions of OH with CH$_3$F and CH$_2$F$_2$ are based on fits to the

**TABLE 17.** $CH_4 + OH \rightarrow CH_3 + H_2O$ rate expressions. $k(T) = A T^n \exp(-E/RT)$. $k(T)$, temperature-dependent rate constant. $A$, pre-exponential factor. $n$, temperature coefficient. $E$, energy coefficient. Expanded uncertainty factor $f(2\sigma)$. Units: $k$ (cm³ mol⁻¹ s⁻¹), $E$ (kJ mol⁻¹), $T$ (K). See Sec. 10 for definitions of acronyms and abbreviations in the Method column

| $A$ | $n$ | $E$ | $f$ | $T$ | Method | Reference |
|---|---|---|---|---|---|---|
| Evaluations | | | | | | |
| $8.68 \times 10^5$ | 2.18 | 9.98 | 1.15(1.07) | 200–2025 | Recommend | This work |
| $6.12 \times 10^{13}$ | | 35.33 | 1.25 | 1200–1800 | Recommend, high T fit | This work |
| $1.69 \times 10^{10}$ | 0.67 | 13.09 | 1.1[1.2] | 243–480 | Review | 15BUR/SAN[187] |
| $1.48 \times 10^{12}$ | | 14.76 | 1.1[1.2] | 243–480 | Review, our fit | 15BUR/SAN[187] |
| $1.00 \times 10^6$ | 2.18 | 10.24 | 1.2 | 195–2025 | Review | 05SRI/SU[188] |
| $2.46 \times 10^3$ | 3.04 | 7.65 | 1.05[1.12] | 195–1234 | Review | 02BON/DAE[13] |
| $1.57 \times 10^7$ | 1.83 | 11.64 | 1.41[1.23] | 250–2500 | Review | 92BAU/COB[189] |
| $1.93 \times 10^5$ | 2.40 | 8.81 | 1.4[1.1] | 300–2500 | Review | 86TSA/HAM[190] |
| $5.72 \times 10^6$ | 1.96 | 11.04 | [1.17] | 268–1512 | Review | 86FEL/MAD[163] |
| $1.90 \times 10^5$ | 2.40 | 8.81 | 2.0[1.08] | 240–3000 | Review | 83COH/WES[191] |
| $1.55 \times 10^6$ | 2.13 | 10.26 | [1.13] | 250–2000 | Review | 78ERN/WAG[192] |
| Experimental (preferred data) | | | | | | |
| $3.61 \times 10^9$ | | | 1.03[1.06] | 296 | Flow, laser photo, LIF | 12AME/MIY[185] |
| $5.70 \times 10^{13}$ | | 34.37 | 1.17 | 840–2025 | Shock, OH abs | 05SRI/SU[188] |
| $2.30 \times 10^5$ | 2.38 | 9.45 | 1.05[1.03] | 298–1009 | Laser photol, OH LIF | 04BRY/KNY[181] |
| $3.40 \times 10^3$ | 3.01 | 7.97 | 1.09[1.03] | 295–668 | Laser photol, OH LIF | 02BON/DAE[13] |
| $1.12 \times 10^4$ | 2.82 | 8.21 | 1.06[1.03] | 196–420 | Laser photol, OH LIF | 97GIE/TAL[183] |
| $1.54 \times 10^{12}$ | | 14.63 | 1.67[1.1] | 233–343 | Laser photol, OH LIF | 94MEL/TET[193] |
| $5.83 \times 10^4$ | 2.58 | 8.98 | 1.05[1.03] | 293–800 | Laser photol, OH LIF | 93DUN/TUL[182] |
| $1.71 \times 10^{12}$ | | 14.72 | [1.06] | 378–422 | Dischg flow, OH EPR LIB | 92LAN/LEB[194] |
| $2.41 \times 10^{12}$ | | 16.13 | 1.4[1.06] | 278–378 | Dischg flow, OH res fluor | 92FIN/EZE[195] |
| $9.59 \times 10^3$ | 2.84 | 8.13 | 1.12[1.03] | 223–420 | Laser photol, OH LIF | 91VAG/RAV[184] |
| $1.81 \times 10^{12}$ | | | 1.07 | 1240 | Flow, laser pyrolysis, LIF | 85SMI/FAI[196] |
| $4.61 \times 10^9$ | | | 1.08[1.14] | 300 | Flash photol, reson fluor | 81HUS/PLA[197] |
| $4.20 \times 10^9$ | | | 1.01[1.09] | 296 | Flash photol, reson fluor | 80SWO/HOC[198] |
| $4.58 \times 10^9$ | | | 1.12 | 298 | Rel rate, flow, chemilum | 76COX/DER[199] |
| $3.92 \times 10^9$ | | | 1.04 | 295 | Flash photo, UV abs | 75OVE/PAR[186] |
| Experimental (excluded data) | | | | | | |
| $1.70 \times 10^{12}$ | | | 1.19[1.3] | 1072–1139 | Shock, OH abs | 12HON/DAV[200] |
| $5.82 \times 10^{11}$ | | 11.81 | [1.25] | 178–298 | Laser photol, OH LIF | 93SHA/SMI[201] |
| $1.62 \times 10^{12}$ | | | [1.5] | 1030 | Flame, GC, model | 92YET/DRY[202] |
| $2.60 \times 10^{12}$ | | | 1.19[1.5] | 1200 | Shock, OH abs | 89BOT/COH[203] |
| $1.55 \times 10^7$ | 1.83 | 11.64 | 1.16[1.3] | 298–1510 | Fast flow, flash photol, reson fluor | 85MAD/FEL[204] |
| $2.23 \times 10^{13}$ | | 21.2 | 1.25[1.7] | 340–1250 | Flow disch, OH res fluor | 84JON/MUL[205] |
| $1.55 \times 10^6$ | 2.13 | 10.23 | 1.1[1.2] | 403–696 | Photol, GC | 83BAU/CRA[206] |
| $3.37 \times 10^{12}$ | | 16.38 | 1.27 | 278–473 | Flow disch, OH res fluor | 82JEO/KAU[207] |
| $7.96 \times 10^6$ | 1.92 | 11.31 | 1.13[1.3] | 298–1020 | Flash photo, reson fluor | 80TUL/RAV[208] |
| $2.5 \times 10^{12}$ | | | 1.3 | 1300 | Shock, flash photol, OH reson abs | 78ERN/WAG[192] |
| $3.47 \times 10^3$ | 3.08 | 8.4 | 1.2[1.6] | 300–900 | Flash photo, reson fluor | 76ZEL/STE[209] |
| $5.73 \times 10^9$ | | | 1.15[1.4] | 296 | Dischg flow, LMR | 76HOW/EVE[210] |
| $2.33 \times 10^{12}$ | | 15.46 | [1.5] | 300–700 | Flash photo, reson fluor | 75STE/ZEL1[211] |
| $2.8 \times 10^{12}$ | | 15.48 | [1.3] | 300–480 | Flash photo, reson fluor | 75STE/ZEL2[211] |
| $2.31 \times 10^{12}$ | | 15.3 | 1.05[1.22] | 290–440 | Flow disch, OH res fluor | 74MAR/KAU[212] |
| $1.42 \times 10^{12}$ | | 14.22 | 1.09[1.16] | 240–373 | Flash photo, reson fluor | 74DAV/FIS[213] |
| $3.60 \times 10^{13}$ | | 25.11 | 1.2[1.5] | 1100–1900 | Model, flame, MS LIB | 73PEE/MAH[82] |
| $2.52 \times 10^{13}$ | | 20.95 | 1.38[2.3] | 298–753 | Rev rxn, photol, GC | 71BAK/BAL[87] |
| $3.97 \times 10^{12}$ | | 15.8 | 1.25[1.7] | 301–492 | Flash photo, OH abs | 70GRE[214] |
| $6.5 \times 10^9$ | | | 1.23[1.5] | 300 | Dischg flow, OH ESR | 67WIL/WES[215] |
| $5.01 \times 10^{13}$ | | 20.92 | [4] | 298–423 | Static, flash photo, OH abs | 67HOR/NOR[216] |
| $3.00 \times 10^{12}$ | | | 1.33[1.4] | 1280 | Flame, MS, model | 67DIX/WIL[79] |
| $1.43 \times 10^{14}$ | | 27.19 | [4] | 372–1340 | Flame, model, MS LIB | 63FRI[217] |

**TABLE 17.** (Continued.)

| A | n | E | f | T | Method | Reference |
|---|---|---|---|---|---|---|
| $3.5 \times 10^{14}$ | | 37.66 | 1.7[5] | 1200–1800 | Flame, model, MS | 61FEN/JON[92] |
| Theoretical | | | | | | |
| $6.62 \times 10^{4}$ | 2.56 | 9.15 | [1.4(1.08)] | 300–2000 | CBS-QB3 Eckart | 14MAT/SHI[59] |
| n/a | | 24.4 | | 200–1000 | CBS-RAD | 09BLO/HOL[218] |
| n/a | | 15.1 | | 0 | B3LYP/6–311 0 K barrier | 02KOR[219] |
| $4.64 \times 10^{5}$ | 2.30 | 11.47 | [1.3] | 200–1500 | CCSD VTST | 01MAS/GON[220] |
| n/a | | 16.6 | | 298 | MP2/6-31 | 01ELT[221] |
| n/a | | 19.7 | | 280–420 | G2 | 99KOR/KAW[222] |
| $8.37 \times 10^{2}$ | 3.21 | 6.59 | [1.5] | 200–2500 | G2 Eckart | 98SCH/MAR[61] |
| n/a | | 10.0 | | 0 | B3LYP/6–311 0 K barrier | 96JUR[223] |
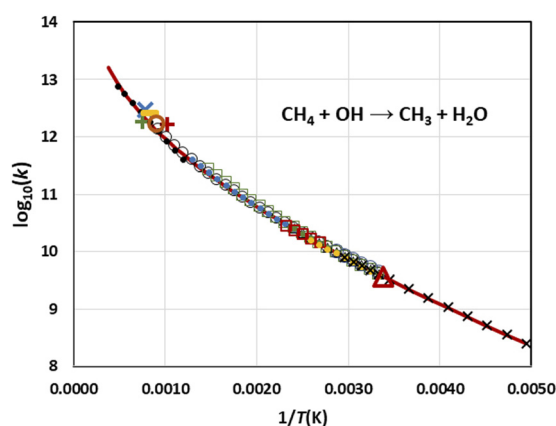


**FIG. 13.** $CH_4 + OH \rightarrow CH_3 + H_2O$ rate constants and recommended rate expression. Rate constants $k$ ($cm^3$ $mol^{-1}$ $s^{-1}$). Legend: Black dots (05SRI/SU[188]), black circles (04BRY/KNY[181]), green squares (02BON/DAE[13]), black triangles (97GIE/TAL[183]), blue circles (94MEL/TET[193]), blue dots (93DUN/TUL[182]), green dots (91VAG/RAV[184]), red squares (92LAN/LEB[194]), yellow dots (92FIN/EZE[195]), black X's (15BUR/SAN[187] evaluation), red plus (92YET/DRY[202]), blue X (67DIX/WIL[79]), green plus (85SMI/FAI[196]), yellow dash (89BOT/COH[203]), brown circle (12HON/DAV[200]), and red triangle (12AME/MIY[185]). Note that only data within about $3\sigma$ of the recommended rate expression are included in this figure. Note also that all of the experimental data below room temperature are represented by the recommended rate expression from the evaluation by Burkholder et al.[187] (using black X's).



**FIG. 14.** $CH_4 + OH \rightarrow CH_3 + H_2O$ rate constant residuals relative to the recommended rate expression. Rate constants $k$ ($cm^3$ $mol^{-1}$ $s^{-1}$). Legend: Black dots (05SRI/SU[188]), black circles (04BRY/KNY[181]), green squares (02BON/DAE[13]), black triangles (97GIE/TAL[183]), blue circles (94MEL/TET[193]), blue dots (93DUN/TUL[182]), green dots (91VAG/RAV[184]), brown squares (92LAN/LEB[194]), yellow dots (92FIN/EZE[195]), black X's with line (15BUR/SAN[187] evaluation), blue asterisks (92FIN/EZE[195]), red X (81HUS/PLA[197]), blue square (76COX/DER[199]), red diamond (80SWO/HOC[198]), blue triangle (75OVE/PAR[186]), green plus (85SMI/FAI[196]), red triangle (12AME/MIY[185]).

experimental data at low temperatures and extrapolation to higher temperatures using parametric correlations that we developed (see the discussion in Sec. 8). The rate constants at high temperatures for these two reactions were interpolated between those for $CH_4$ and for $CHF_3$ (experimental data exist for both of these reactions at high temperatures). The interpolation was determined by considering the relative A factors and activation energies from the quantum chemical study of Matsugi and Shiina,[59] trends in A factors with fluorine substitution, and correlations between the rate constants at room temperature and the activation energies at high temperatures for this and other homologous series (fluoromethanes + X → fluoromethyls + HX). This procedure provides a relatively self-consistent set of rate expressions. We assign uncertainties of $f = 1.5$ for these two rate constants at high temperatures by considering a range of parameters that are consistent with our empirical correlations.

Table 20 lists rate constants compiled from the literature for $CHF_3 + OH \rightarrow CF_3 + H_2O$, and Fig. 18 shows the recommended rate expression along the experimental rate constants used in the fits. This reaction, unlike those for $CH_3F$ and $CH_2F_2$, has rate data at high temperatures. There are also a fair amount of reliable rate constants at low temperatures—six that are individual points at room temperature and four with temperature dependencies. Because of the extent of the data and good agreement, we assign expanded uncertainty factor $f$ ($2\sigma$) $f = 1.3$ and $f = 1.22$ at high and low temperatures, respectively. Finally, Fig. 19 compares the recommended rate constants for the reaction of OH with the three fluoromethanes, showing that the rate constant for $CHF_3 + OH$ has a much stronger temperature dependence than those for $CH_3F$ and $CH_2F_2$.

## 7. Fluoromethanes + F → Fluoromethyls + HF

### 7.1. Overview

In this section, we compile rate constants from both experimental and quantum chemical studies for the reaction of F atoms with
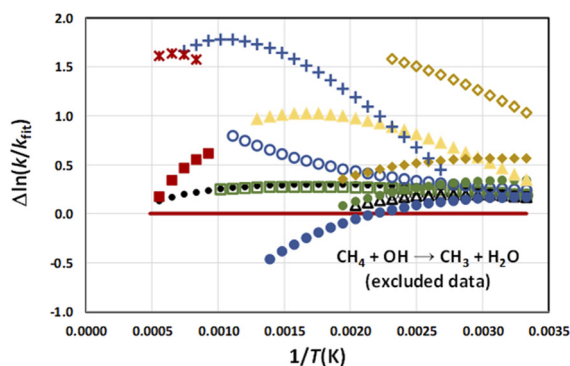
**FIG. 15.** $CH_4 + OH \rightarrow CH_3 + H_2O$ rate constant residuals for excluded data relative to the recommended rate expression. Legend: Black dots (86FEL/MAD[163]), black circles (83BAU/CRA[206]), black open triangles (82JEO/KAU[207]), green squares (80TUL/RAV[208]), blue circles (76ZEL/STE[209]), blue dots (75STE/ZEL1[211]), green dots (75STE/ZEL2[211]), red squares (73PEE/MAH[82]), yellow filled triangles (71BAK/BAL[87]), brown filled diamonds (70GRE[214]), brown open diamonds (67HOR/NOR[216]), blue plus signs (63FRI[217]), and red asterisks (61FEN/JON[92]). Note that not all of the excluded data provided in Table 17 are included here.

the fluoromethanes (and methane) that abstract H atoms. Based on our analysis and fitting procedures, we recommend rate expressions for these reactions over a wide range of temperatures. Experimental rate constants are only available at lower temperatures (about 200–550 K). We extend these rate constants to higher temperatures employing quantum chemical calculations (done by others) as frameworks and empirical correlations (see discussion later). A summary of the recommended rate expressions is given in Table 21.

Individual rate constants and expressions for H abstraction by F atoms from the fluoromethanes are given in the following tables: $CH_4$ (Table 22), $CH_3F$ (Table 23), $CH_2F_2$ (Table 24), and $CHF_3$ (Table 25). Figure 20 provides an Arrhenius plot of the experimental data for these four compounds along with the recommended rate expressions. The rate expressions are represented by $k(T) = A\ T^n \exp(-E/RT)$, where $A$, $n$, and $E$ (pre-exponential factor, temperature coefficient, and energy coefficient, respectively) are given in the tables. Expanded uncertainty factors $f(2\sigma)$ are also provided. The uncertainty factors are as provided in the original works. Uncertainty factors that we assigned are 2-sigma coverage. The range of temperatures for the rate expressions are given, as is a short description of the method used to determine the rate constants. Along with the experimental and computed rate constants, we provide recommended rate expressions for these reactions over a range of temperatures. Two sets of recommended expressions are provided: the first are extended Arrhenius expressions with $A$, $n$, and $E$ that are good from about 200 to 2000 K and the second are simple Arrhenius expressions with just $A$ and $E$ that are good at high temperatures from about 1200 to 1800 K—relevant to combustion chemistry. We also provide a rate constant for each reaction at room temperature (298 K) based on a weighted average of the experimental measurements—although we would recommend values at 298 K from our rate expressions.

Unfortunately, there are no measurements at high temperatures for H abstraction from the fluoromethanes by F atoms where this chemistry is very important in describing the decomposition of the agents. The flammability of the neat agents in combustion processes

in air is extremely dependent upon the hydrogen content. For neat agents, where there is no hydrocarbon fuel present, the flames become hydrogen-poor and fluorine-rich. The only rate measurements for these reactions are at low temperatures. For $CH_4$ and $CHF_3$, rate constants are available in the range of about 200–550 K, while for $CH_3F$ and $CH_2F_2$, it is a much more limited range just below room temperature (from about 200 to 300 K). For each of the reactions, there are multiple determinations of the rate constant at room temperature (300 K) but only a few temperature-dependent measurements. However, these temperature-dependent measurements are deemed reliable.

A summary of the rate constants for this series of reactions is provided in Fig. 20. The many single room-temperature measurements are not shown for clarity. There also are a few temperature-dependent measurements that are not shown—they are inconsistent with the other measurements and the recommended rate expressions. The experimental data are represented by points (circles and squares). The solid lines represent the recommended rate expression. In addition, dashed lines represent the variational transition state theory calculations by Wang et al.[247,248] using a PES determined from ab initio quantum chemical calculations using coupled cluster theory. Other rate expressions from ab initio calculations are not shown in Fig. 20 for clarity.

We now discuss in more detail the experimental data and the recommended rate expressions for this homologous series of reactions.

There are many studies measuring the rate of H abstraction by F atoms at room temperatures. The experimental data for temperature-dependent rate constants, however, are more limited. Persky has measured the rate constants at below room temperature (189–298 K) for $CH_3F$ and $CH_2F_2$ and at below and above room temperature (184–406 K) for $CH_4$.[249–253] Wagner et al.[254] and Beiderhase et al.[255] have measured the rate constants at below room temperature (220–312 K) for $CH_4$ and $CH_3F$, respectively. There have been three measurements from below room temperature to slightly higher temperatures (>400 K) of the rate constants for $CHF_3 + F \rightarrow CF_3 + HF$ by Louis and Sawerysyn,[256] Maricq and Szente,[257] and Clyne et al.[258] Wang and coworkers have used quantum chemical methods to compute rate expressions for the reaction of F atoms with methane and all of the fluoromethanes.[247,248,259] Other work using quantum chemical methods is listed in the tables.

We fitted our rate expressions to the low-temperature data and then utilized empirical trends in the derived $A$ factors at high temperatures, activation energies vs heats of reaction, and temperature coefficients $T^n$ to extrapolate the rate expressions to higher temperatures in a self-consistent manner (see Sec. 8 about this parameterization). We also considered the predicted temperature dependence from quantum calculations.

We benchmarked our rate expression for $CH_4 + F$ to the experimental data of Persky and found that it agrees with our recommended values to within about 20%. Note that Persky revised his expression in 2008 from that reported in 2006 using an updated expression for the rate constant of $H_2 + F$ (relative rate constants were measured in this work).[249,250] We note that the temperature dependence at low temperatures for the data of Persky is weaker than that from our recommended expression (we calculated effective activation energies of 1.8 kJ mol$^{-1}$ vs 2.5 kJ mol$^{-1}$), and the

**TABLE 18.** $CH_3F + OH \rightarrow CH_2F + H_2O$ rate expressions. $k(T) = AT^n \exp(-E/RT)$. $k(T)$, temperature-dependent rate constant. $A$, pre-exponential factor. $n$, temperature coefficient. $E$, energy coefficient. $f(2\sigma)$, expanded uncertainty factor. Units: $k$ ($cm^3\ mol^{-1}\ s^{-1}$), $E$ ($kJ\ mol^{-1}$), $T$ (K). Uncertainty factors when reported in the literature are given in the table. In addition, we provide deviations (uncertainty factors $f$) from our recommended rate constants in square "[$f$]" brackets with the uncertainty factor at low temperatures given in parentheses "($f$)."

| $A$ | $n$ | $E$ | $f$ | $T$ | Method | Reference |
|---|---|---|---|---|---|---|
| Evaluations | | | | | | |
| $1.06 \times 10^6$ | 2.04 | 5.70 | 1.5(1.22) | 240–1800 | Recommend | This work |
| $2.40 \times 10^{13}$ | | 30.44 | 1.5 | 1200–1800 | Recommend, high T fit | This work |
| $1.32 \times 10^{12}$ | | 11.64 | 1.1[1.1] | 243–480 | Review | 15BUR/SAN[187] |
| Experimental (preferred data) | | | | | | |
| $2.65 \times 10^{12}$ | | 13.8 | [1.2] | 308–398 | Photol, FTIR | 96DEM[224] |
| $1.32 \times 10^{12}$ | | 12.06 | [1.15] | 298–363 | Photol, FTIR | 95HSU/DEM[225] |
| $1.05 \times 10^{12}$ | | 10.81 | [1.1] | 243–373 | Laser photol, LIF | 93SCH/TAL[226] |
| $4.93 \times 10^{12}$ | | 15.71 | 1.08[1.4] | 292–480 | Dischg flow, reson fluor | 82JEO/KAU[207] |
| Experimental (preferred data, 298 K) | | | | | | |
| $1.16 \times 10^{10}$ | | | [1.3] | 298 | Ultrasonic, UV abs | 98KOW/JOW[227] |
| $9.04 \times 10^9$ | | | 1.07[1.3] | 298 | Photol, FTIR | 93WAL/HUR[228] |
| $1.03 \times 10^{10}$ | | | 1.14[1.2] | 298 | Pulse radiolysis, reson abs | 88BER/HAN[229] |
| $1.31 \times 10^{10}$ | | | 1.08[1.1] | 297 | Flash photo, reson abs | 79NIP/SIN[230] |
| $9.64 \times 10^9$ | | | 1.22[1.3] | 296 | Dischg flow, LMR | 76HOW/EVE[210] |
| Experimental (excluded data, all duplicates) | | | | | | |
| $1.01 \times 10^{10}$ | | | [1.2] | 298 | Photol, FTIR | 96DEM[224] |
| $1.02 \times 10^{10}$ | | | [1.15] | 298 | Photol, FTIR | 95HSU/DEM[225] |
| $1.34 \times 10^{10}$ | | | [1.1] | 298 | Laser photol, LIF | 93SCH/TAL[226] |
| $8.64 \times 10^9$ | | | [1.4] | 298 | Dischg flow, reson fluor | 82JEO/KAU[207] |
| Theoretical | | | | | | |
| $1.93 \times 10^5$ | 2.37 | 6.15 | [2(1.2)] | 300–2000 | CBS-QB3 Eckart | 14MAT/SHI[59] |
| $4.03 \times 10^{10}$ | | | [3] | 300 | DFT KKMLYP/6–311 Wigner | 12PET/HAR[231] |
| $1.91 \times 10^6$ | 2.15 | 8.92 | | 200–700 | CC/cbs CVT/SCT, our fit | 08MAR/GRU[232] |
| $4.12 \times 10^4$ | 2.60 | 5.72 | | 200–1500 | mPW1PW91/6–31 CVT/μOMT | 06ALS/SWA[233] |
| n/a | | 9.6 | | 0 | B3LYP/6–311 0 K barrier | 02KOR[219] |
| $2.21 \times 10^6$ | 2.03 | 7.66 | | 200–1000 | MP2/6–31 CVT/μOMT, our fit | 01LIE/YOU[234] |
| n/a | | 21.34 | | 298 | CC/pVTZ | 01LIE/YOU[234] |
| $1.14 \times 10^{12}$ | | 13.18 | [2.5] | 250–400 | MP4/6–311G Wigner | 00LOU/GON[235] |
| $2.28 \times 10^2$ | 3.35 | 3.06 | [4(1.3)] | 300–2000 | G2 Eckart | 98SCH/MAR[61] |
| $4.44 \times 10^3$ | 4.78 | −4.52 | | 200–1000 | CVT/μOMT | 98ESP/COI[236] |
| n/a | | 0.4 | | 0 | B3LYP/6–311 0 K barrier | 96JUR[223] |

temperature dependence from Foon and Reid is even weaker (1.2 kJ mol$^{-1}$). Given this uncertainty in the temperature dependence of the rate expression, we assign an uncertainty of a factor of $f = 1.4$ at high temperatures.

Our recommended rate expressions for reaction of F atoms with $CH_3F$ and $CH_2F_2$ agree well with the data of Persky to within 2% and 4%, respectively. We excluded the data of Beiderhase for $CH_3F$ because they had a temperature dependence (activation energy) that was inconsistent with the temperature dependence (5.0 kJ mol$^{-1}$ vs 3.5 kJ mol$^{-1}$) from our self-consistent rate expressions developed for the fluoromethanes + F homologous series. We benchmarked the rate constants for $CHF_3$ at low temperatures with the data of Louis and Sawerysyn and Maricq and Szente with our recommended values and found that they agree to within 6% and 11%, respectively. We excluded the higher temperature data by Clyne *et al.* because they had a weak temperature dependence inconsistent with our self-consistent

rate expressions, resulting in a rate constant that was about 40% lower at the highest temperature (667 K).

## 7.2. Evaluation procedure

The recommended rate expressions were determined by fitting the low-temperature experimental data and the scaled rate constants at high temperatures (1200 K–1800 K) from the work of Wang *et al.*[247] The procedure was to first fit the *ab initio* rate expressions at $T = (1200–1800)$ K to determine $A$ and $E$ (simple Arrhenius expression). The values of $A$ and $E$ were then (iteratively) adjusted to arrive at scaled values that were best self-consistent with fits to the experimental data and the scaled rate constants. This procedure worked well for $CHF_3 + F$ and $CH_2F_2 + F$—where the *ab initio* and fitted curves are very similar in curvature. For $CH_3F + F$, however, there was some tension in the fitting procedure—where we obtained values for the temperature coefficient ($n$) that ranged from about 1.1 to 1.4. We

**TABLE 19.** $CH_2F_2 + OH \rightarrow CHF_2 + H_2O$ rate expressions. $k(T) = A T^n \exp(-E/RT)$. $k(T)$, temperature-dependent rate constant. $A$, pre-exponential factor. $n$, temperature coefficient. $E$, energy coefficient. $f(2\sigma)$, expanded uncertainty factor. Units: $k$ ($cm^3$ $mol^{-1}$ $s^{-1}$), $E$ ($kJ$ $mol^{-1}$), $T$ (K)

| $A$ | $n$ | $E$ | $f$ | $T$ | Method | Reference |
|---|---|---|---|---|---|---|
| Evaluations | | | | | | |
| $3.29 \times 10^6$ | 1.86 | 7.52 | 1.5(1.17) | 220–1800 | Recommend | This work |
| $1.68 \times 10^{13}$ | | 30.09 | 1.5 | 1500–1800 | Recommend, high T fit | This work |
| $1.02 \times 10^{12}$ | | 12.47 | 1.2 | 220–492 | Review | 15BUR/SAN[187] |
| Experimental (preferred data) | | | | | | |
| $1.08 \times 10^{12}$ | | 12.89 | 1.07 | 297–383 | Photol, FTIR | 95HSU/DEM[225] |
| $9.46 \times 10^{11}$ | | 12.22 | 1.13 | 220–380 | Flash photol, LIF | 91TAL/MEL[237] |
| $2.65 \times 10^{12}$ | | 14.72 | 1.08 | 250–492 | Dischg flow, reson fluor | 82JEO/KAU[207] |
| $3.89 \times 10^{12}$ | | 16.63 | 1.74 | 293–429 | Dischg, reson fluor | 79CLY/HOL[238] |
| Experimental (preferred data, 298 K) | | | | | | |
| $6.05 \times 10^9$ | | | 1.03 | 298 | Dischg flow, reson fluor LIB | 00SZI/DOB[239] |
| $5.30 \times 10^9$ | | | 1.16 | 298 | Pulse radiolysis, reson abs | 88BER/HAN[229] |
| $7.05 \times 10^9$ | | | 1.12 | 297 | Flash photol, reson abs | 79NIP/SIN[230] |
| $4.70 \times 10^9$ | | | 1.15 | 296 | Dischg flow, LMR | 76HOW/EVE[210] |
| Experimental (excluded data, 298 K, some duplicates) | | | | | | |
| $9.89 \times 10^9$ | | | [1.6] | 298 | Ultrasonics, UV abs | 98KOW/JOW[227] |
| $5.94 \times 10^9$ | | | 1.07 | 298 | Photol, FTIR | 95HSU/DEM[225] |
| $6.82 \times 10^9$ | | | 1.13 | 298 | Flash photol, LIF | 91TAL/MEL[237] |
| $6.97 \times 10^9$ | | | [1.17] | 298 | Dischg flow, reson fluor | 82JEO/KAU[207] |
| $4.73 \times 10^9$ | | | 1.74[1.2] | 298 | Dischg, reson fluor | 79CLY/HOL[238] |
| Theoretical | | | | | | |
| $1.32 \times 10^5$ | 2.35 | 6.40 | | 300–2000 | CBS-QB3 Eckart | 14MAT/SHI[59] |
| $3.77 \times 10^{10}$ | | | | 300 | DFT KKMLYP/6–311 Wigner | 12PET/HAR[231] |
| n/a | | 24.4 | | 298 | CBS-RAD | 09BLO/HOL[218] |
| $2.38 \times 10^4$ | 2.86 | 10.06 | | 200–1500 | mPW1PW91/6–31 CVT/µOMT | 07ALB/SWAa[240] |
| n/a | | 8.8 | | 0 | B3LYP/6–311 0 K barrier | 02KOR[219] |
| n/a | | 16.8 | | 298 | MP2/6–31 | 01ELT[221] |
| $3.25 \times 10^{12}$ | | 13.39 | | 250–400 | MP4/6–311G Wigner | 00LOU/GON[235] |
| $3.33 \times 10^{-5}$ | 5.43 | −5.13 | | 210–500 | CCSD/pVTZ VTST/LCT | 01GON/LIU[241] |
| $2.64 \times 10^2$ | 3.27 | 3.98 | | 300–2000 | G2 Eckart | 98SCH/MAR[61] |
| n/a | | 0.4 | | 0 | B3LYP/6–311 0 K barrier | 96JUR[223] |
| n/a | | 9.2 | | 298 | MP2/3–21 | 93BOT/POG[242] |
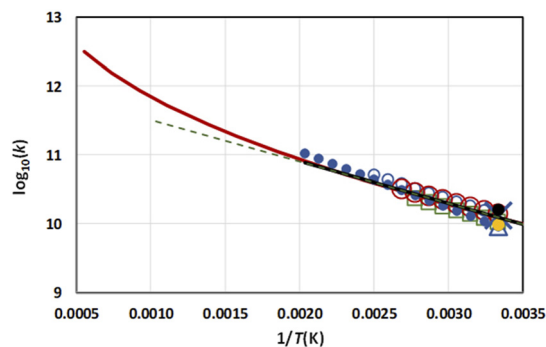


**FIG. 16.** $CH_3F + OH \rightarrow CH_2F + H_2O$. Rate constants $k$ ($cm^3$ $mol^{-1}$ $s^{-1}$). Red solid line (this work recommended), large black dot (98KOW/JOW[227]), open blue circles (96DEM[224]), green squares (95HSU/DEM[225]), large blue triangle (93WAL/HUR[228]), red circles (93SCH/TAL[226]), blue dots (82JEO/KAU[207]), large blue X (79NIP/SIN[230]), large yellow dot (76HOW/EVE[210]), and dashed line (15BUR/SAN[187] recommended).
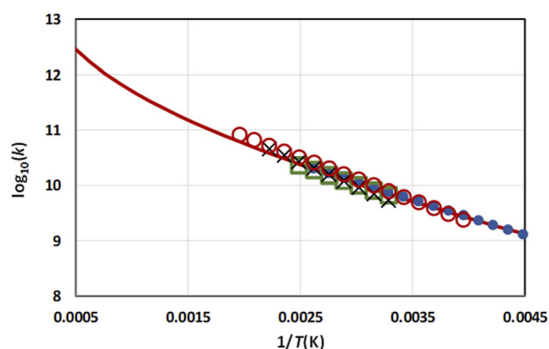


**FIG. 17.** $CH_2F_2 + OH \rightarrow CHF_2 + H_2O$. Rate constants $k$ ($cm^3$ $mol^{-1}$ $s^{-1}$). Red solid line (this work recommended), blue dots (91TAL/MEL[237]), green squares (95HSU/DEM[225]), black X's (79CLY/HOL[238]), and red circles (82JEO/KAU[207]).

**TABLE 20.** $CHF_3 + OH \rightarrow CF_3 + H_2O$ rate expressions. $k(T) = A T^n \exp(-E/RT)$. $k(T)$, temperature-dependent rate constant. $A$, pre-exponential factor. $n$, temperature coefficient. $E$, energy coefficient. $f(2\sigma)$, expanded uncertainty factor. Units: $k$ ($cm^3$ $mol^{-1}$ $s^{-1}$), $E$ ($kJ$ $mol^{-1}$), $T$ (K)

| $A$ | $n$ | $E$ | $f$ | $T$ | Method | Reference |
|---|---|---|---|---|---|---|
| Evaluations | | | | | | |
| $1.20 \times 10^6$ | 1.85 | 13.71 | 1.3(1.22) | 250–1800 | Recommend | This work |
| $5.64 \times 10^{12}$ | | 36.15 | 1.3 | 1200–1800 | Recommend, high T fit | This work |
| $3.67 \times 10^{11}$ | | 18.79 | chk | 253–500 | Review | 15BUR/SAN[187] |
| Experimental (preferred data) | | | | | | |
| $5.84 \times 10^{12}$ | | 36.56 | 1.22 | 995–1663 | Shock CH | 07SRI/SU[243] |
| $2.89 \times 10^{11}$ | | 18.13 | 1.27 | 253–343 | Rel rate, static, photol, GC | 03CHE/KUT[244] |
| $3.85 \times 10^{11}$ | | 19.54 | [1.1] | 298–383 | Photol, FTIR | 95HSU/DEM[225] |
| $4.18 \times 10^{11}$ | | 19.12 | [1.2] | 298–500 | Laser photol, LIF | 93SCH/TAL[226] |
| $1.82 \times 10^{12}$ | | 24.20 | 1.1 | 387–480 | Dischg flow, reson fluor | 82JEO/KAU[207] |
| $4.0 \times 10^{11}$ | | | 1.25 | 1350 | Shock, flash photol, OH reson abs | 78ERN/WAG[192] |
| 0.19 | | | | 1300 | Rel rate CH4+OH, shock, flash photol, OH reson abs | 76BRA/CAP[245] |
| Experimental (excluded data, some duplicates at 298 K) | | | | | | |
| $1.92 \times 10^8$ | | | 1.27 | 298 | Rel rate, static, photol, GC | 03CHE/KUT[244] |
| $6.62 \times 10^{11}$ | | 19.12 | [2] | 298–750 | Photol, LIF | 97MED/FLE[179] |
| $2.95 \times 10^8$ | | | [1.8] | 298–750 | Photol, LIF | 97MED/FLE[179] |
| $1.45 \times 10^8$ | | | [1.10] | 298 | Photol, FTIR | 95HSU/DEM[225] |
| $1.86 \times 10^8$ | | | [1.16] | 298 | Laser photol, LIF | 93SCH/TAL[226] |
| $1.39 \times 10^9$ | | | 1.17[9] | 298 | Pulse radiolysis, reson abs | 88BER/HAN[229] |
| $1.04 \times 10^8$ | | | 1.1 | 298 | Dischg flow, reson fluor | 82JEO/KAU[207] |
| $2.1 \times 10^8$ | | | 1.5 | 297 | Flash photo, reson abs | 79NIP/SIN[230] |
| $1.21 \times 10^8$ | | | 2 | 296 | Dischg flow, LMR | 76HOW/EVE[210] |
| Theoretical | | | | | | |
| $1.39 \times 10^3$ | 2.83 | 11.31 | | 300–2000 | CBS-QB3 Eckart | 14MAT/SHI[59] |
| $5.94 \times 10^7$ | | | | 300 | DFT KKMLYP/6–311 Wigner | 12PET/HAR[231] |
| $4.25 \times 10^3$ | 3.22 | 9.96 | | 298–2500 | G3B3 | 07ZHA/LIN[124] |
| $4.60 \times 10^3$ | 2.87 | 14.70 | | 200–1500 | mPW1PW91/6–31 CVT/μOMT | 07ALB/SWAb[246] |
| n/a | | 29.6 | | 298 | MP2/6–31 | 01ELT[221] |
| $1.20 \times 10^{12}$ | | 22.82 | | 250–400 | MP4/6–311G Wigner | 00LOU/GON[235] |
| $6.93 \times 10$ | 3.66 | 8.86 | | 300–2000 | G2 Eckart | 98SCH/MAR[61] |
| n/a | | 5.9 | | 0 | B3LYP/6–311 0 K barrier | 96JUR[223] |

selected an intermediate value of $n = 1.25$. As can be seen in Fig. 20, the calculated rate curve for $CH_3F + F$ shows much more curvature than the fitted curve. We speculate that the additional curvature is due to the inadequacy of variational transition-state theory to represent a complicated and multi-dimensional quantum dynamical PES (see discussion below). This is evident in the many quantum dynamics studies for the $CH_4 + F$ reaction (see Table 22), which disagree substantially on the degree of curvature—these studies found that the rate constants were extremely dependent upon fine details of the PESs used to determine the rates of reaction.

The recommended rate expression for the reaction $CH_4 + F$ is taken from the quantum dynamics study of Chu et al.[260] This rate expression agrees with the experimental data at low temperatures within the experimental uncertainties. Note that all of the other quantum calculations for $CH_4$ provided in Table 22 are also consistent with the experimental data. We chose the rate expression from Chu et al. for several reasons. It is one of the higher level calculations using a refined PES. The temperature coefficient ($n = 0.91$) from this

study was an intermediate value compared to other computations ($n = 0.53–1.57$). In addition, we found that the temperature coefficient ($n$) for the reaction series $CH_4$, $CH_3F$, $CH_2F_2$, and $CHF_3$ varied smoothly (with a slight quadratic curvature) as a function of $\log_{10}(k_{298})$ where $k_{298}$ is the rate constant for each reaction at 298 K.

In summary, we compiled rate expressions for H abstraction by F atoms from the fluoromethanes (and methane) and provide recommended rate expressions over a range of temperatures. These rate expressions agree with the experimental data at low temperatures, appear to be self-consistent with one another, and are generally consistent with rate expressions from quantum calculations.

### 7.3. Discussion of fluorine impact on rate constants

If we consider the rate parameters in Table 21, we first see that the effective A factors at high temperatures do not scale with the number of hydrogen atoms as found for abstraction by other radicals. In contrast, the effective activation energies at high temperatures scale
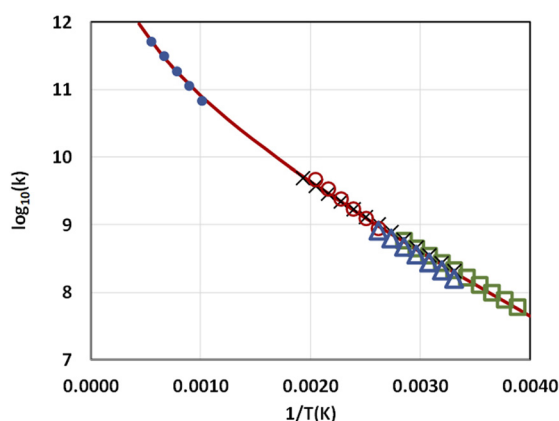
**FIG. 18.** $CHF_3 + OH \rightarrow CF_3 + H_2O$. Rate constants $k$ ($cm^3$ $mol^{-1}$ $s^{-1}$). Red solid line (this work recommended), blue dots (07SRI/SU[243]), blue triangles (95HSU/DEM[225]), green squares (03CHE/KUT[244]), black X's (93SCH/TAL[226]), and red circles (82JEO/KAU[207]).
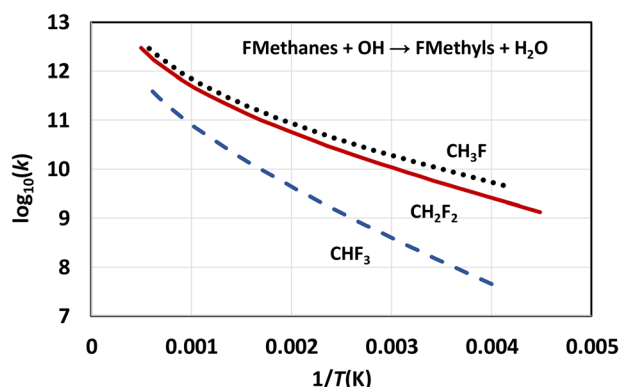


**FIG. 19.** Fluoromethanes + OH $\rightarrow$ fluoromethyls + $H_2O$. Recommended rate constants $k$ ($cm^3$ $mol^{-1}$ $s^{-1}$). See Figs. 15–17 for rate data and fits for individual reactions.

roughly with the C–H BDEs (see Table 2): $E_a$ and BDEs: $CH_3F$ < $CH_2F_2$ < $CH_4$ < $CHF_3$. In contrast, we see that both the curvatures as expressed by the temperature coefficients $n$ ($T^n$) and the rate constants at low temperatures scale well with the number of fluorine atoms in the molecule. We interpret this as a clear indication of semi-ionic contributions to the rates of these reactions in this extraordinary class of reactions involving the reaction of F atoms (highly electro-negative) with fluorinated methanes (electropositive carbon atom). These are nearly barrierless reactions, and thus, the strong curvature in the rate constants cannot be due to tunneling. The strong overall temperature dependence would be indicative of the turning point from products to reactants moving along the reaction coordinate and likely related to the charge on the central carbon atom. At low temperatures (low collision energies), semi-ionic forces may domi-nate the rate of reaction (related to the charge on the carbon atom). On the other hand, at high temperatures (high collision energies), the covalent nature of the bonding is dominant (evident by the barrier scaling with BDEs).

Much of the following discussion is based on that in earlier work by others.[247,248,259,260,268–271] A more complete and accurate dis-cussion of these quantum dynamical effects for F atom abstraction of H atoms can be found in the quantum chemical works referenced in the rate expression tables for these molecules (the quantum dy-namical studies of the $CH_4 + F \rightarrow CH_3 + HF$ provide the most information).

All of these reactions $CX_3H + F \rightarrow CX_3 + HF$ display a large change in rate constants with temperature and significant curvature to the Arrhenius rate expressions. These effects need to be explained because these reactions are barrierless reactions (or nearly) that are not classical abstraction reactions. Classical abstraction reactions essentially involve the intersection of two covalent bond-breaking PESs (e.g., C–H and H–F in the forward and reverse directions, respectively). In contrast, these reactions proceed essentially only on attractive potential surfaces with very early turning points. The high electronegativity of the F atom results in a more ionic and less covalent character to the bond breaking with polarization of the H–F bond and a charge separation. The largest temperature dependence is observed with the reaction $CHF_3 + F$, where electron withdrawal by the three fluorine atoms on $CHF_3$ leads to a much stronger C–H bond.

**TABLE 21.** Recommended rate expressions for H abstraction from the fluoromethanes by F atoms. $k(T) = A\,T^n \exp(-E/RT)$. $k(T)$, temperature-dependent rate constant. $A$, pre-exponential factor. $n$, temperature coefficient. $E$, energy coefficient. $f(2\sigma)$, expanded uncertainty factor. Units: $k$ ($cm^3$ $mol^{-1}$ $s^{-1}$), $E$ (kJ $mol^{-1}$), $T$ (K). $A/A_{CHF3}$ is the ratio of the pre-exponential to that for $CHF_3$. $\Delta_rH_{298}$, standard enthalpy of reaction at 298 K

| Reaction | $A$ | $n$ | $E$ | $f$ | $T$ | $\log_{10}(k_{300})$ | $\Delta_rH_{298}$ |
|---|---|---|---|---|---|---|---|
| $CH_4 + F \rightarrow CH_3 + HF$ | $2.93 \times 10^{11}$ | $0.91 \pm 0.21$ | $0.79 \pm 1.51$ | 1.35(1.23) | 180–1800 | 13.58 | −131.1 |
| $CH_3F + F \rightarrow CH_2F + HF$ | $1.91 \times 10^{10}$ | $1.25 \pm 0.29$ | $0.81 \pm 1.49$ | 1.35(1.24) | 180–1800 | 13.24 | −147.0 |
| $CH_2F_2 + F \rightarrow CHF_2 + HF$ | $2.05 \times 10^{8}$ | $1.79 \pm 0.25$ | $1.30 \pm 1.65$ | 1.35(1.35) | 180–1800 | 12.52 | −144.0 |
| $CHF_3 + F \rightarrow CF_3 + HF$ | $4.57 \times 10^{4}$ | $2.77 \pm 0.20$ | $3.00 \pm 1.47$ | 1.35(1.20) | 180–1800 | 11.00 | −123.8 |
| | | | | | | $A/A_{CHF3}$ | |
| $CH_4 + F \rightarrow CH_3 + HF$ | $5.81 \times 10^{14}$ | | 11.95 | 1.35 | 1200–1800 | 1.42 | |
| $CH_3F + F \rightarrow CH_2F + HF$ | $6.86 \times 10^{14}$ | | 6.87 | 1.35 | 1200–1800 | 1.68 | |
| $CH_2F_2 + F \rightarrow CHF_2 + HF$ | $5.54 \times 10^{14}$ | | 9.77 | 1.35 | 1200–1800 | 1.35 | |
| $CHF_3 + F \rightarrow CF_3 + HF$ | $4.09 \times 10^{14}$ | | 15.54 | 1.35 | 1200–1800 | 1.00 | |

**TABLE 22.** $CH_4 + F \rightarrow CH_3 + HF$ rate expressions. $k(T) = A\,T^n \exp(-E/RT)$. $k(T)$, temperature-dependent rate constant. $A$, pre-exponential factor. $n$, temperature coefficient. $E$, energy coefficient. $f(2\sigma)$, expanded uncertainty factor. Units: $k$ ($cm^3\,mol^{-1}\,s^{-1}$), $E$ ($kJ\,mol^{-1}$), $T$ (K). See Sec. 10 for definitions of acronyms and abbreviations in the Method column.

| $A$ | $n$ | $E$ | $f$ | $T$ | Method | Reference |
|---|---|---|---|---|---|---|
| Evaluations | | | | | | |
| $2.93 \times 10^{11}$ | 0.91 | 0.79 | 1.35(1.23) | 180–1800 | Recommend. Selected 09CHU/HAN[260] | This work |
| $5.81 \times 10^{14}$ | | 11.95 | 1.4 | 1200–1800 | Recommend, high T fit | This work |
| $7.71 \times 10^{13}$ | | 1.79 | 1.12 | 184–406 | Review | 06PER[252] |
| $4.09 \times 10^{13}$ | | | 1.2 | 298 | Review | 93WAL/HUR[228] |
| Experimental (preferred data) | | | | | | |
| $7.71 \times 10^{13}$ | | 1.79 | 1.12 | 184–406 | Corrected 96PER[249] | 98PER[250] |
| Experimental (preferred data, 298 K) | | | | | | |
| $3.78 \times 10^{13}$ | | | 1.26 | 298 | Average | This work |
| $3.73 \times 10^{13}$ | | | 1.1 | 298 | Rel rate, dischg flow, MS | 98PER[250] |
| $2.83 \times 10^{13}$ | | | 1.2 | 298 | Rel rate, photol, FTIR | 95MOO/SMI[261] |
| $3.19 \times 10^{13}$ | | | 1.1 | 294 | Rel rate, photol, FTIR | 94MOO/SMI[262] |
| $3.97 \times 10^{13}$ | | | 1.1 | 298 | Fast flow, MS | 89WOR/HEY[263] |
| $4.00 \times 10^{13}$ | | | [1.03] | 298 | Pulse photol, UV detect | 88PAG/MUN[264] |
| $3.44 \times 10^{13}$ | | | 1.05 | 298 | IR photodissoc, HF emission | 82FAS/NOG[265] |
| $4.52 \times 10^{13}$ | | | 1.2 | 298 | Dischg flow, atomic reson | 78CLY/NIP[266] |
| $4.30 \times 10^{13}$ | | | [1.1] | 298 | Laser photol, HF emission | 72KOM/WAN[267] |
| $3.49 \times 10^{13}$ | | | 1.15 | 298 | Rel rate, flow, GC | 71FOO/REI[253] |
| $4.74 \times 10^{13}$ | | | 1.5[1.3] | 298 | Fast flow, MS | 71WAG/WAR[254] |
| Experimental (excluded data) | | | | | | |
| $9.88 \times 10^{13}$ | | 2.20 | 1.1 | 184–406 | Rel rate, dischg flow, MS | 96PER[249] |
| $3.3 \times 10^{14}$ | | 4.81 | [1.5] | 250–312 | Fast flow, MS | 71WAG/WAR[254] |
| Theoretical | | | | | | |
| $2.63 \times 10^9$ | 1.57 | −1.74 | [1.07] | 184–404 | Quant dynamics, PES, CC/pVTZ | 13WAN/CZA[259] |
| $2.93 \times 10^{11}$ | 0.91 | 0.79 | selected | 180–400 | Quant dynamics, PES, CC/pVTZ | 09CHU/HAN[260] |
| $2.00 \times 10^{12}$ | 0.53 | 0.58 | [1.5] | 180–500 | Quant dynamics, PES, CC/pVTZ | 07ESP/BRA[268] |
| $1.27 \times 10^9$ | 1.70 | −1.58 | [1.5] | 200–2000 | CC/pVTZ, VTST | 05ROB/MAC[269] |
| $5.68 \times 10^{11}$ | 0.71 | −0.29 | [1.5] | 180–500 | Quant dynamics, PES, CC/pVTZ | 05RAN/NAV[270] |
| $7.07 \times 10^9$ | 1.30 | −1.92 | [2.0] | 200–500 | Quant dynamics, PES, CC/pVTZ | 04TRO/MIL[271] |

The strong temperature dependence of the rates of these reactions is due to a number of factors. Quantum chemical calculations reveal the existence of van der Waals adducts $X_3C$–H–F in the entrance channel (reactants) due to long-range forces. The quantum dynamical studies of these systems (supported by experimental evidence) suggest that rovibrational excitations coupled to the electronic PES result in reactive resonances that enhance the reactivity. Although there are essentially no "barriers" to these reactions, the turning point moves along the reaction path as a function of energy, leading to an entropic temperature dependence to the reaction rate. This effect requires the use of variational transition state theory or quantum dynamical studies to accurately predict reactivity in these systems. In addition, the ground state of the F atom is split into two states $^2P_{3/2}$ and $^2P_{1/2}$ with degeneracies of 4 and 2, respectively, and the higher state $^2P_{1/2}$ is separated by a spin–orbit splitting of 404.10 $cm^{-1}$ (4.83 kJ $mol^{-1}$). This leads to a change in effective electronic degeneracy (and rate constant) with temperature. In addition, the quantum dynamics studies suggest that the $^2P_{1/2}$ state may have a significantly higher reaction rate.

In summary, all of these factors contribute to the large change in rate constants as a function of temperature—even though these are barrierless reactions.

## 8. Discussion

### 8.1. Overview

In this work, we complied and evaluated rate constants for the abstraction of H from the fluoromethane homologous series ($CH_4$, $CH_3F$, $CH_2F_2$, $CHF_3$) by the radicals H atom, O atom, F atom, and OH and provided self-consistent recommended rate expressions for these reactions from room temperature to combustion temperatures (300–1800 K). There were limited experimental temperature-dependent rate constants for some of the reactions. In these cases, we predicted the rate constants using relative rates employing a combination of rate constants from *ab initio* calculations and self-consistent parametric fits considering all the reactions as a set of homologous reactions. In this work, the rate expressions we provided are consistent with all the reliable experimental data within reported uncertainties. Other rate

**TABLE 23.** $CH_3F + F \rightarrow CH_2F + HF$ rate expressions. $k(T) = A\,T^n \exp(-E/RT)$. $k(T)$, temperature-dependent rate constant. $A$, pre-exponential factor. $n$, temperature coefficient. $E$, energy coefficient. $f(2\sigma)$, expanded uncertainty factor. Units: $k$ ($cm^3\,mol^{-1}\,s^{-1}$), $E$ ($kJ\,mol^{-1}$), $T$ (K)

| $A$ | $n$ | $E$ | $f$ | $T$ | Method | Reference |
|---|---|---|---|---|---|---|
| Evaluations | | | | | | |
| $1.91 \times 10^{10}$ | 1.25 | 0.81 | 1.35(1.24) | 190–1800 | Recommend | This work |
| $6.86 \times 10^{14}$ | | 6.87 | 1.25 | 1200–1800 | Recommend, high T fit | This work |
| Experimental (preferred data) | | | | | | |
| $6.20 \times 10^{13}$ | | 3.24 | 1.15 | 189–298 | Flow, dischg, MS | 03PER[251] |
| $2.42 \times 10^7$ | 2.4 | 0 | 1.1[1.2] | 220–300 | Flow, dischg, MS | 95BEI/HAC[255] |
| Experimental (preferred data, 298 K) | | | | | | |
| $1.85 \times 10^{13}$ | | | 1.24 | 298 | Weighted average | *This work* |
| $1.66 \times 10^{13}$ | | | 1.1 | 298 | Flow, dischg, MS | 03PER[251] |
| $2.06 \times 10^{13}$ | | | 1.1 | 298 | Flow, dischg, MS | 95BEI/HAC[255] |
| $1.69 \times 10^{13}$ | | | 1.2 | 298 | Rel rate, photol, FTIR | 95MOO/SMI[261] |
| $2.23 \times 10^{13}$ | | | 1.2 | 295 | Rel rate, laser photol, FTIR | 93WAL/HUR[228] |
| $1.33 \times 10^{13}$ | | | 1.06 | 300 | Rel rate, electron beam, IR | 83MAN/SET[272] |
| $1.82 \times 10^{13}$ | | | [1.1] | 298 | Rel rate, flow, dischg, HF emission | 77SMI/SET[273] |
| $2.16 \times 10^{13}$ | | | [1.1] | 298 | Rel rate, H2+F→HF + H | 75MAN/GRA[274] |
| Experimental (excluded data) | | | | | | |
| $4.00 \times 10^{12}$ | | | 1.23[5] | 298 | Pulse radiolysis, UV detect | 98KOW/JOW[227] |
| $2.41 \times 10^9$ | | | 1.75[1.3] | 298 | Electron beam, ESR, CH | 86JON/MA[85] |
| $5.30 \times 10^{13}$ | | | [2.8] | 298 | Rel rate, fast flow, chemilum | 73POL/JON[275] |
| Theoretical | | | | | | |
| $3.24 \times 10^8$ | 1.75 | −0.91 | | 180–1800 | CC/6–311 VTST | 05WAN/LIU[247] |
| $6.28 \times 10^{14}$ | | 8.60 | | 1200–1800 | High T fit to 05WAN/LIU[247] | This work |

**TABLE 24.** $CH_2F_2 + F \rightarrow CHF_2 + HF$ rate expressions. $k(T) = A\,T^n \exp(-E/RT)$. $k(T)$, temperature-dependent rate constant. $A$, pre-exponential factor. $n$, temperature coefficient. $E$, energy coefficient. $f(2\sigma)$, expanded uncertainty factor. Units: $k$ ($cm^3\,mol^{-1}\,s^{-1}$), $E$ ($kJ\,mol^{-1}$), $T$ (K)

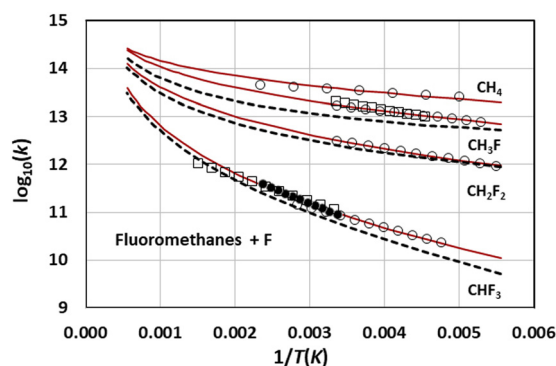| $A$ | $n$ | $E$ | $f$ | $T$ | Method | Reference |
|---|---|---|---|---|---|---|
| Evaluations | | | | | | |
| $2.05 \times 10^8$ | 1.79 | 1.30 | 1.35(1.35) | 180–1800 | Recommend | This work |
| $5.54 \times 10^{14}$ | | 9.77 | 1.35 | 1200–1800 | Recommend, high T fit | This work |
| Experimental (preferred data) | | | | | | |
| $2.23 \times 10^{13}$ | | 4.78 | 1.15 | 182–298 | Flow, dischg, MS | 03PER181[251] |
| Experimental (preferred data, 298 K) | | | | | | |
| $3.03 \times 10^{12}$ | | | 1.35 | 298 | Weighted average | This work |
| $3.25 \times 10^{12}$ | | | 1.1 | 298 | Flow, dischg, MS CH | 03PER181[251] |
| $2.83 \times 10^{12}$ | | | 1.2 | 298 | Rel rate, photol, FTIR | 95MOO/SMI[261] |
| $2.59 \times 10^{12}$ | | | 1.2 | 295 | Rel rate, laser photol, FTIR | 93WAL/HUR[228] |
| $3.44 \times 10^{12}$ | | | 1.05[1.1] | 298 | Electron beam, dischg flow, LIF | 85CLY/HOD[276] |
| $2.34 \times 10^{12}$ | | | 1.33 | 300 | Rel rate, electron beam, IR | 83MAN/SET[272] |
| $4.06 \times 10^{12}$ | | | [1.3] | 298 | Rel rate H2 + F = HF + H | 75MAN/GRA[274] |
| Experimental (excluded data) | | | | | | |
| $1.26 \times 10^{12}$ | | | 1.47[2.5] | 298 | Pulse radiolysis, UV detect | 98KOW/JOW[227] |
| $5.90 \times 10^{12}$ | | | [1.9] | 298 | Rel rate, laser photol, FTIR | 92NIE/ELL82[277] |
| $1.10 \times 10^{13}$ | | | [3.5] | 298 | Rel rate, fast flow, chemilum | 73POL/JON[275] |
| Theoretical | | | | | | |
| $1.54 \times 10^7$ | 2.1 | 0.13 | [1.4] | 180–1800 | CC/6–311 VTST | 08WAN/LIU[248] |
| $5.38 \times 10^{14}$ | | 10.74 | [1.2] | 1500–1800 | High T fit to 05WAN/LIU[247] | This work |

**TABLE 25.** $CHF_3 + F \rightarrow CF_3 + HF$ rate expressions. $k(T) = A T^n \exp(-E/RT)$. $k(T)$, temperature-dependent rate constant. $A$, pre-exponential factor. $n$, temperature coefficient. $E$, energy coefficient. $f(2\sigma)$, expanded uncertainty factor. Units: $k$ ($cm^3$ $mol^{-1}$ $s^{-1}$), $E$ ($kJ$ $mol^{-1}$), $T$ (K)
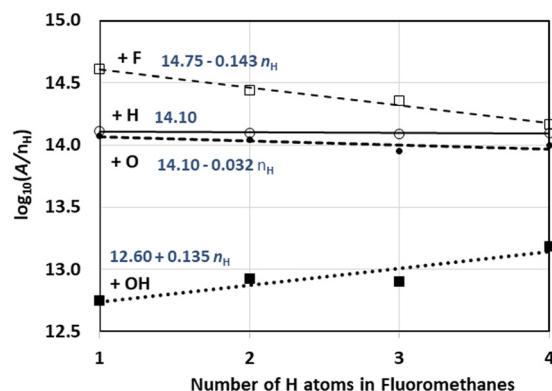
| $A$ | $n$ | $E$ | $f$ | $T$ | Method | Reference |
|---|---|---|---|---|---|---|
| Review | | | | | | |
| $4.57 \times 10^4$ | 2.77 | 3.00 | 1.35(1.2] | 210–1800 | Recommend | This work |
| $4.09 \times 10^{14}$ | | 15.54 | 1.40 | 1200–1800 | Recommend, high T fit | This work |
| Experimental (preferred data) | | | | | | |
| $1.26 \times 10^{13}$ | | 12.22 | 1.5 | 297–421 | Dischg flow, MS | 98LOU/SAW[256] |
| $2.17 \times 10^{12}$ | | 7.90 | 1.55 | 210–353 | Rel rate, flash photol, UV abs | 93MAR/SZE[257] |
| $6.38 \times 10^{12}$ | | 10.00 | [1.4] | 301–667 | Dischg flow, MS | 73CLY/MCK[258] |
| Experimental (preferred data, 298 K) | | | | | | |
| $8.49 \times 10^{10}$ | | | 1.20 | 298 | Weighted average | This work |
| $8.13 \times 10^{10}$ | | | 1.2 | 298 | Rel rate, photol, FTIR | 95MOO/SMI[261] |
| $7.23 \times 10^{10}$ | | | 1.35 | 294 | Photol, chemilum | 94MOO/SMI[262] |
| $8.43 \times 10^{10}$ | | | 1.3 | 295 | Rel rate, laser photol, FTIR | 93WAL/HUR[228] |
| $7.23 \times 10^{10}$ | | | [1.2] | 298 | Rel rate CH | 92NIE/ELL1009[278] |
| $7.23 \times 10^{10}$ | | | [1.2] | 298 | Rel rate, flash photol, UV abs CH | 92MAR/SZE[279] |
| $9.03 \times 10^{10}$ | | | [1.05] | 298 | Dischg flow LIB | 83CLY/HOD[280] |
| $8.99 \times 10^{10}$ | | | [1.05] | 298 | Pulse radiolysis, ESR | 76GOL/SCH[281] |
| Experimental (excluded data, 298 K, some duplicates) | | | | | | |
| $9.08 \times 10^{10}$ | | | 1.5 | 298 | Dischg flow, MS | 98LOU/SAW[256] |
| $4.88 \times 10^{12}$ | | | 1.2[60] | 298 | Pulse radiolysis, UV detect | 98KOW/JOW[227] |
| $7.23 \times 10^{10}$ | | | [1.2] | 298 | Rel rate, flash photol, UV abs CH | 92MAR/SZE[279] |
| $9.03 \times 10^{10}$ | | | [1.05] | 298 | Dischg flow LIB | 83CLY/HOD[280] |
| $4.35 \times 10^{11}$ | | | [5] | 298 | Rel rate, H2+F=HF + H | 75MAN/GRA[274] |
| $1.90 \times 10^{11}$ | | | [2] | 298 | Rel rate, fast flow, chemilum | 73POL/JON[275] |
| $1.13 \times 10^{11}$ | | | [1.3] | 298 | Dischg flow, MS | 73CLY/MCK[258] |
| Theoretical | | | | | | |
| $7.11 \times 10^4$ | 2.69 | 4.14 | | 180–1800 | CC/6–311 VTST | 08WAN/LIU[248] |
| $3.28 \times 10^{14}$ | | 15.63 | | 1200–1800 | High T fit to 08WAN/LIU[248] | This work |
| | | n/a | | | G2MP2, found no barrier | 00OKA/TOM[282] |
| n/a | | 16.1 | | | MP2/6–311 barrier | 99LOU/RAY[283] |

expressions could be provided that are statistically equivalent, but our intent in this work was to provide well-behaved rate expressions allowing for accurate interpolation and extrapolation.



**FIG. 20.** Fluoromethanes + F $\rightarrow$ fluoromethyls + HF rate constants. $k$ ($cm^3$ $mol^{-1}$ $s^{-1}$). Red solid lines represent recommended rate expressions. Dashed lines represent the calculations by Wang et al. (05WAN/LIU,[247] 08WAN/LIU[248]). Experimental data: $CH_4$ circles (06PER[252]), $CH_3F$ circles (03PER[251]), squares (95BEI/HAC[255]), $CH_2F_2$ circles (03PER[251]), $CHF_3$ circles (93MAR/SZE[257]), filled circles (98LOU/SAW[256]), and squares (73CLY/MCK[258]).



**FIG. 21.** Normalized $A$ factors (per H atom) (on a logarithmic scale) at high temperatures as a function of the number of H atoms for the different reactants H, O, OH, and F. $A$ ($cm^3$ $mol^{-1}$ $s^{-1}$).

We now discuss the systematic trends we have observed and provide a basis for our claim that the rate expressions are self-consistent.

## 8.2. Correlations for rate constant $A$ factors

It was found that the relative $A$ factors for abstractions by H and O atoms for rate constants at high temperatures (1200–1800 K) roughly scaled (within about 30%) with the number of hydrogens in the molecule (reaction path degeneracy), while the relative A factors for abstractions by OH and F changed upon fluorine substitution. This included both $A$ factors derived from our rate expressions and from TSs derived from reliable *ab initio* quantum chemical calculations. The $A$ factors, of course, should not scale exactly with the number of hydrogens for a number of reasons: (a) TSs will move along the reaction coordinates in a homologous series, changing the shapes of the PESs; (b) the addition of heavy F atoms to replace light H atoms will impact the enthalpic differences between the TS and the reactants; and (c) the large electronegativity of additional F atoms will, of course, change the nature of the TSs. Figure 21 shows the normalized $A$ factors (per H atom) at high temperatures for all of the H abstraction reactions from the fluoromethanes by H, O, OH, and F. We see that for abstraction by H and O, the normalized $A$ factors are very nearly independent of the degree of fluorination (within about 10%–20%). This is less than the assigned uncertainties of $f = (1.3–1.5)$ for the rate constants. The independence of the normalized $A$ factors is unsurprising since abstractions are simple reactions—bond breaking concurrent with bond formation, relatively tight (closer) TSs, and only slight changes expected in the structure and bond frequencies involving spectator atoms (those not involved in the reaction). In contrast, we see that the normalized $A$ factors for H abstraction by OH decrease by a factor of about (2.5–3) from $CH_4$ to $CHF_3$, and the opposite trend is observed for abstraction by F atoms, where the normalized $A$ factors increase by about a factor of (2.5–3) from $CH_4$ to $CHF_3$.

The deviations of the normalized $A$ factors (per H atom) from the linear correlations illustrated in Fig. 21 are about factors of 1.01, 1.12, 1.20, and 1.08 (1%, 12%, 20%, and 8%) for abstractions by H, O, OH, and F. Thus, there is a high degree of correlation between the $A$ factors and the number of H (or F) atoms. Although these deviations $(10 \pm 10)$% are the optimized *a posteriori* derived factors, nevertheless, they are significantly less than the assigned uncertainty factors that are on the order of $(40 \pm 20)$%.

The *absolute* values of the normalized $A$ factors for the series of reactions $CH_4 + (O, H, F)$ only differ by a small amount, about $(1.0 \times 10^{14}, 1.25 \times 10^{14}, 1.5 \times 10^{14})$ cm$^3$ mol$^{-1}$ s$^{-1}$, respectively, while the $A$ factor for $CH_4 + OH$ is about (6–8) times less at about $1.5 \times 10^{13}$ cm$^3$ mol$^{-1}$ s$^{-1}$, suggesting a much tighter TS. The decrease in the normalized $A$ factor for abstractions by OH with fluorine substitution from $CH_4$ to $CHF_3$ is a valid systematic trend since the rate constants for these two reactions at high temperatures are relatively well-known ($f = 1.3$). The change in the normalized $A$ factors for these reactions with OH is likely a consequence of several factors involving interaction between the electropositive O–H bond and the very electronegative C–F bonds in the TS. The hindered rotor in the TS involving the OH with a barrier that will depend upon the number of fluorine atoms in the molecules, and consequently a factor of about $1/2R$ in the entropy or a factor of 1.65 in the $A$ factor, might be expected considering that the OH in the $CH_4 + OH$ TS
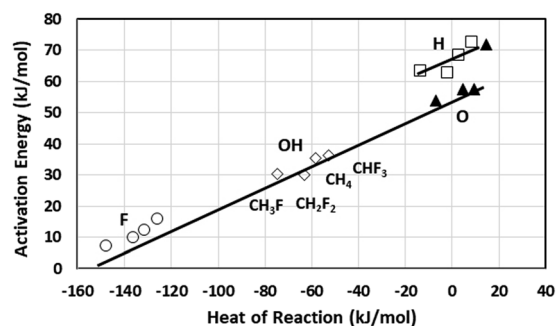


**FIG. 22.** Evans–Polanyi[55] plot of activation energy $E_a$ at high temperatures (1200–1800 K) as a function of heat of reaction $\Delta_r H$. The correlation is approximately $E_a = 55.79 + 0.356 \Delta_r H$. The barriers for H and F atoms are about (8–11) kJ mol$^{-1}$ and (4–5) kJ mol$^{-1}$ higher, respectively, than the trend for O atoms and OH radicals. The barrier for $CHF_3 + O \rightarrow CF_3 + OH$ is about 10 kJ mol$^{-1}$ higher than the trend for other abstractions by O atoms. See discussion in text.

is significantly less constrained (essentially a free rotor) compared to the OH in $CHF_3 + OH$, which is much more constrained (hindered rotor) and closer to a vibration. In addition, both the magnitude and anharmonicity of the bending normal modes involving the OH bond will be significantly impacted by the electrostatics of any O–H/C–F interactions. The consequences of these factors are that the $A$ factors do not scale roughly with the number of hydrogens like for abstractions by H and O atoms; instead, the ratios are about (1.0, 3.0, 4.3, 10.9), indicating that the TSs become increasingly more constrained with fluorine substitution.

There is also an apparent increase in the normalized $A$ factor for the fluoromethanes + F abstractions upon fluorine substitution, changing by about a factor of (2.5–3.0) from $CH_4$ to $CHF_3$. This is a consequence of the semi-ionic nature of this class of reactions involving a highly electronegative F atom with molecules where the charge distribution drastically changes depending upon the number of fluorine substitutions. This is a complicated series of reactions. They are very nearly barrierless reactions (see the references in Tables 21–24), and the temperature dependences of the rate constants are due to the turning point for the reactions moving along the reaction coordinate with temperature (energy), due to quantum dynamical effects, and due to the semi-ionic nature of these reactions. The "TS" for $CHF_3 + F$ is earlier and looser (higher entropy), while that for $CH_4 + F$ is later and tighter (closer).

Such changes in the rate constants are to be expected because of the large changes in the electronegativity of the central carbon atom with fluorine substitution impacting the PES involving the attacking highly electronegative F atom. A much different type of barrier is to be expected for $CHF_3 + F$ with a large positive charge on the carbon atom, compared to that for $CH_4 + F$ where there is a substantial negative charge on the carbon atom. $CHF_3$ has a large dipole moment (positive pointing toward the reaction site) along the reaction coordinate due to the electronegative fluorine substitutions, and consequently, a long-range (loose) semi-ionic interaction with the attacking electronegative F atom is available. In contrast, H atoms are electropositive, and the effective dipole moment along the reaction coordinate for the $CH_4$ reaction is pointing away from the reaction site. Somewhat equivalently, the fluorine substitutions in $CHF_3$ make the central carbon atom

highly electropositive, which makes the H atom being abstracted less electropositive than in $CH_4$, and consequently will have more electron density to react with the attacking F atom (and a higher rate constant).

## 8.3. Activation energies

In Fig. 22, we provide an Evans–Polanyi type relationship[55] showing a correlation between the activation energy $E_a$ at high temperatures (1200–1800 K) determined from the recommended rate expressions and the experimental heats of reaction $\Delta_r H$. The reactions involving F, OH, O, and H with the fluoromethanes follow the relation $E_a = 55.79 + 0.356\Delta_r H$ (kJ mol$^{-1}$) with an expanded uncertainty factor $f(2\sigma)$ of about 2.1 kJ mol$^{-1}$ in the barrier with a "correction" of $-(8–11)$ kJ mol$^{-1}$ and $-(4–5)$ kJ mol$^{-1}$ for H and F atoms, respectively. The uncertainty of about 2.1 kJ mol$^{-1}$ corresponds to uncertainties of only about (10–30)%, or $f = (1.1–1.3)$ in the rate constants at 1500 K, and well within our assigned uncertainties for these reactions of about $f = 1.4 \pm 0.2$. The barriers for abstraction by H and F atoms are likely higher because of electronegativity effects. The other reactive species (O atoms and OH radical) are electronegative, while H atoms are more electropositive and F atoms are highly electronegative. Consequently, the interaction between the attacking H and F atoms and the H atom being abstracted will be less attractive (more repulsive) than for the reaction involving O atoms and OH radical. There is significant uncertainty in the barriers for abstraction by F atoms at high temperatures (which were derived using correlations) since there are no experimental rate constants for any of the fluoromethanes (and methane) above about 450 K. Undoubtedly, there are some differences in the attractiveness of the abstraction potentials for these electronegative species; however, with uncertainties on the order of (2–5) kJ mol$^{-1}$ and over a large range of heats of reaction (about 100 kJ mol$^{-1}$), any effect is likely masked. There are undoubtedly competing factors related to polarization of the reactant molecule and polarization effects in the TS due to substitution of highly electronegative fluorine atoms.

The barrier for $CHF_3 + O \rightarrow CF_3 + OH$ is about 10 kJ mol$^{-1}$ higher than the trend for other abstractions by O atoms. $CHF_3$ is a special case—with three fluorine atoms withdrawing electrons, the electron density on the carbon atom is small. This low electron density on the carbon atom in $CHF_3$ is evident by considering the radical product $CF_3$ in this reaction, which is nearly sp$^3$ hybridized with near tetrahedral angles—we calculate (B3LYP/6-31G$^{**}$) that it has a principal moment of inertia of about 91.1 amu Å$^2$ compared to 90.0 amu Å$^2$ for $CHF_3$. The combination of this electronegativity effect with the triplet oxygen atom (biradical) likely affects the polarization of electrons during the reaction.

Substitution of H atoms by F atoms in methane results in a withdrawal of electron density from the carbon, thus lowering the bond order in the remaining C–H bonds and making them weaker. In general, lowering the C–H bond strength will *decrease* the activation energy for the corresponding H abstraction. However, although the withdrawal of electron density by fluorine weakens the remaining C–H bonds, it also makes the starting molecule more polarized and therefore less able to transfer electron density that would contribute to the formation of a new bond in an abstraction reaction (i.e., in the TS).
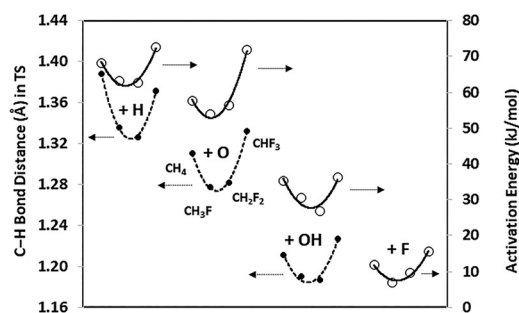


**FIG. 23.** Activation energies (open circles) for hydrogen abstraction by H, O, OH, and F, and TS bond distances (filled circles) vs fluorine substitution in the fluoromethane series. The lines are only to guide the eyes. Activation energies are from this work and bond distances are from Matsugi and Shiina.[59] The four points for each curve are left-to-right for $CH_4$, $CH_3F$, $CH_2F_2$, and $CHF_3$, respectively.
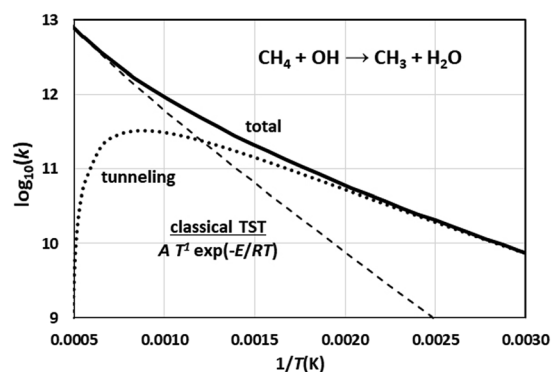


**FIG. 24.** Contribution of tunneling to the rate constants for $CH_4 + OH \rightarrow CH_3 + H_2O$.

This latter effect tends to *increase* the activation energy for abstraction. The first is a static effect in the reactant molecule, while the latter is a dynamic effect in the TS.

In Fig. 23, we see the competition between these two effects and see a correlation between the C–H bond distance in the TS and the activation energy (which is correlated with bond strengths/heats of reaction; see Fig. 22). Shorter C–H bonds indicate more bond energy and thus a more stabilized lower-energy TS. The data suggest that the bond weakening effect dominates for the first two fluorine substitutions ($CH_4$ to $CH_3F$ to $CH_2F_2$) but that this is overshadowed by electronic effects in the extremely polarized $CHF_3$. The activation energies in Fig. 23 are from our recommended rate expressions at high temperatures (1200–1500 K), while the C–H bond distances are from the *ab initio* calculations of Matsugi and Shiina.[59] They did not calculate abstraction by fluorine, and consequently, those bond distances are not contained in the figure.

## 8.4. Tunneling rates

These abstraction reactions involve H atom transfer, and consequently, the rates of reaction at low temperatures are dominated by

FIG. 25. Correlation between activation energies $E_a$ at low temperatures (300 K) and activation energies $E_a$ at high temperatures (1200–1800 K). $E_a$ (kJ mol$^{-1}$). Black squares are reactions involving H atoms, red dots are reactions involving O atoms, blue triangles are reactions involving OH radicals, and green circles are reactions involving F atoms. The activation energies were derived from our recommended rate expressions.
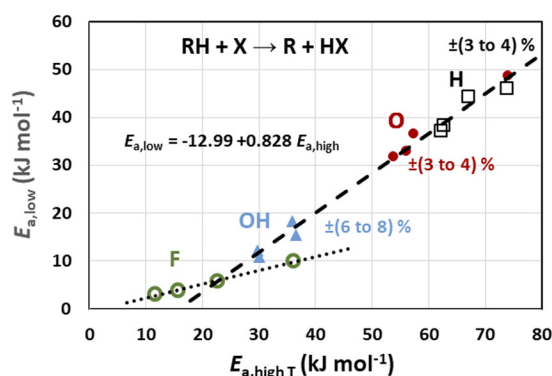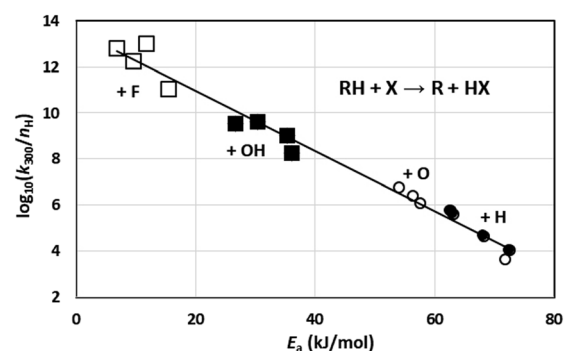


FIG. 26. Normalized (per H atom) rate constant $k$ (cm$^3$ mol$^{-1}$ s$^{-1}$) at 300 K as a function of activation energy $E_a$ (kJ mol$^{-1}$) for H abstractions in the fluoromethane series. Correlation between rate constants with tunneling and activation energies at high temperatures (1200–1800 K). The rates at 300 K and the activation energies at high temperatures were derived from our recommended rate expressions.

quantum chemical tunneling. The tunneling rate is, to first order, a function of the height of the barrier through which the H atom tunnels (to second order, it is also a function of the width and asymmetry of the barrier).

It is well beyond the subject of this chemical kinetic evaluation to go into any detail on the subject of tunneling. There are many theories, treatments, PESs, and computer programs utilized in this field including variational transition state theory,[284] semiclassical TS theory,[285,286] large curvature tunneling approximation,[287] zero curvature tunneling,[288] centrifugal dominant small curvature semiclassical tunneling,[289] multidimensional tunneling,[290–292] Wigner potentials,[293–295] Eckart barriers,[296,297] unsymmetrical Eckart barriers,[134] Polyrate,[298,299] and TheRate.[300]

A generic example of a potential energy curve and barrier was shown in Fig. 1. Here, we present a complementary figure (Fig. 24) to illustrate the contribution of tunneling to these types of H abstraction reactions for the case of CH$_4$ + OH → CH$_3$ + H$_2$O. In this figure, the solid curve is the total rate constant from our recommended rate expression, while the dashed and dotted lines are the contributions from the classical PES and from quantum chemical tunneling, respectively. The classical rate is represented by a rate expression considering an activated complex in TS theory,[301,302] which corresponds to an extended Arrhenius expression with $n = 1$ that asymptotes to the total rate constant at high temperatures. Here, we derived the tunneling contribution by simply subtracting the classical rate from the total rate. In Fig. 24, we see that the contribution of tunneling extends over a wide temperature range, that the rate constant is dominated by tunneling up to about 500 K, that it becomes equal to the classical rate at about 800 K, that the tunneling rate maximizes at about 1200 K, and that it does not finally drop to 10% of the classical rate until above about 1600 K.

Figure 25 shows a strong correlation between $E_a$ at high (1200 K–1800 K) and low temperatures (300 K). These were derived from our recommended rate expressions. There should be a strong correlation since it can be derived analytically from an extended Arrhenius expression, $E_a(T_{\text{high}}) - E_a(T_{\text{low}}) = nR(T_{\text{high}} - T_{\text{low}})$, where

$R$ is the gas constant and $n$ is the temperature coefficient. For example, using a high temperature of 1440 K (1/$T$ average of 1200 K and 1800 K) and a low temperature of 300 K, one calculates the difference between $E_a$ at high and low temperatures to be about $n*9.5$ kJ/mol from this simple equation. Using the four data for OH abstractions in Fig. 25, one calculates on the average $E_a$(high) and $E_a$ (low) to be about 32.8 kJ mol$^{-1}$ and 14.2 kJ mol$^{-1}$ or a difference of about 18.7 kJ mol$^{-1}$. Thus, $n$ should be about 1.97, in excellent agreement with the roughly (1.9–2.0) for OH abstractions in Fig. 27. Similarly, using the three lowest data for abstractions by O (excluding CHF$_3$), one calculates on the average $E_a$ (high) and $E_a$ (low) to be about 56.6 kJ mol$^{-1}$ and 35.0 kJ mol$^{-1}$, respectively, or a difference of about 21.6 kJ mol$^{-1}$. Thus, $n$ should be about 2.27, in excellent agreement with the roughly (2.3–2.4) in Fig. 27. The exact values here are not important—other than to demonstrate that the activation energies $E_a$ at high and low temperatures and the temperature coefficients $n$ are all well-correlated and thus are valid for use in our least-squares optimization with additional constraints.

We find uncertainties in $E_a$ at low temperatures to be about (3–4)% for reactions involving H and O atoms and about (6–8)% for OH where the barriers are about half as much. From these data, we estimate uncertainty factors of about $f = (1.4–2.0)$ for these rate constants, which are consistent with our assigned uncertainty factors of about $f = (1.2–2.3)$. Although barriers for H, O, and OH follow this trend very well, those for F atoms do not. These reactions involving F atoms have very low barriers, and the interactions are much less covalent and much more ionic in nature and thus do not have similar PESs to those for H, O, and OH.

A reaction with a large barrier will have much less tunneling. This is illustrated in Fig. 26, which shows the reaction rates (entirely due to tunneling) at low temperatures $k$(300 K) derived from our recommended rate expressions, on a log$_{10}$ scale, as a function of the effective barrier $E_a$ at high temperatures. The values for $k_{300}$ and $E_a$ were all derived from our recommended rate expressions. The tunneling rates $k$(300 K) were normalized to the number of H atoms (reaction path degeneracy). These effective barriers were derived from the recommended rate expressions for reaction of all of the fluoromethanes (and methane) with H, O, F, and OH over the range
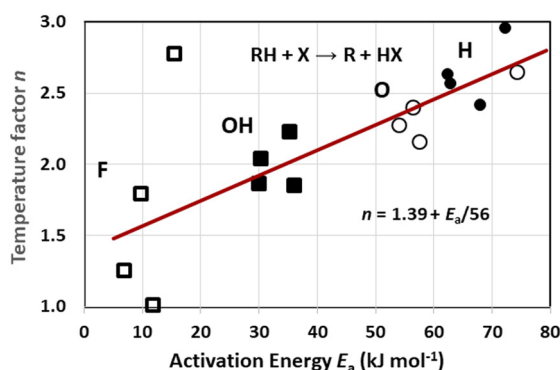
**FIG. 27.** The compensation effect correlation of the temperature coefficient $n$ with energy coefficient $E$ in expressions $k = A\,T^n \exp(-E/RT)$ for H abstractions in the fluoromethane series.

1200–1800 K. We see that abstraction by F atoms has the smallest barriers (near 10 kJ mol$^{-1}$) and largest rate constants, while abstraction by H atoms has the largest barriers (near 65 kJ mol$^{-1}$) and smallest rate constants. Abstraction by OH (near 30 kJ mol$^{-1}$) and by O (near 60 kJ mol$^{-1}$) have intermediate barriers and rate constants.

The correlation in Fig. 26 corresponds to $(k_{300}/n_H) = 4.70 \times 10^{13}$ $\exp(-0.306\,E_a)$, or the changes in the rate constants (per H atom) at 300 K scale as about 31% of the activation energies at high temperatures (1200–1800 K).

The deviations of $k_{300}$ from this correlation with $E_a$ are relatively large—about a factor of $f = 3.5$. However, we found that if we applied a correction of $+(5-7)$ kJ mol$^{-1}$ to $E_a$ for the reactions involving CHF$_3$ (an outlier, see Figs. 7, 22, and 23), the uncertainty factor for this correlation was on the order of $f = 2.0$, not an unreasonable value (consistent with our assigned uncertainties). On the other hand, this is

actually a dependent correlation since there are relatively strong correlations (see Sec. 8 elsewhere) between the $A$ factors, the number of H atoms, the temperature coefficients $n$, and the activation energies $E_a$ at high and low temperatures. Thus, the correlation between $k_{300}$ and $E_a$ at high temperatures should also be satisfactory. In any case, Fig. 25 illustrates that there is a correlation between the rate constant at low temperatures and the activation energy at high temperatures.

A consequence of the correlation between the enhanced rate constant at low temperatures due to tunneling and the activation energy at high temperatures means that there should also be a correlation between the temperature coefficient $n$ and the activation energy $E_a$—this is shown in Fig. 27, where the temperature coefficient $n$ ranges from about $2.6 \pm 0.3$ to $2.4 \pm 0.2$ to $2.0 \pm 0.2$ for H, O, and OH reactions, respectively, or uncertainties in $n$ of about $(10 \pm 2)$%. Note that the temperature coefficient $n$ for F atom reactions does not follow this correlation because of compensation with the very low energy coefficients $E$. Considering the compensation effect between $n$ and $E_a$, we estimate expanded uncertainty factors $f(2\sigma)$ of about $f = 1.25$ for rate constants optimized utilizing the correlation shown in Fig. 27, well within our assigned uncertainty factors of about $f = 1.4 \pm 0.2$. Consequently, we can conclude that recommended values of $n$ and $E_a$ are fully self-consistent.

## 9. Summary

We have complied and critically evaluated rate constants from the literature for abstraction of H from the fluoromethanes (CH$_3$F, CH$_2$F$_2$, CHF$_3$) and methane (CH$_4$) by the radicals H atom, O atom, OH, and F atom. We provide about 350 determinations of rate constants abstracted from the literature for these 16 reactions from just over 200 references. Based on our evaluation, we provide self-consistent recommended rate expressions for these reactions over a wide range of temperatures (about 300–1800 K). We provide expanded uncertainty factors $f(2\sigma)$ for abstractions by H atoms, O

**TABLE 26.** Recommended rate expressions for H abstraction from the fluoromethanes by H, O, OH, and F. $k(T) = A\,T^n \exp(-E/RT)$. $k(T)$, temperature-dependent rate constant. $A$, pre-exponential factor. $n$, temperature coefficient. $E$, energy coefficient. The expanded uncertainty factor $f(2\sigma)$ is at high temperatures with the uncertainty factor at low temperatures (300–500) K given in parentheses. $k_{300}$ is the rate constant at 300 K. Units: $k$ (cm$^3$ mol$^{-1}$ s$^{-1}$), $E$ (kJ mol$^{-1}$), $T$ (K).

| Reaction | $A$ | $n$ | $E$ | $f$ | $T$ | $\log_{10}(k_{300})$ |
|---|---|---|---|---|---|---|
| CH$_4$ + H → CH$_3$ + H$_2$ | $9.01 \times 10^5$ | $2.41 \pm 0.31$ | $38.21 \pm 2.13$ | 1.4(1.6) | 300–1950 | 5.28 |
| CH$_3$F + H → CH$_2$F + H$_2$ | $2.13 \times 10^5$ | $2.56 \pm 0.42$ | $31.98 \pm 2.34$ | 1.5(1.8) | 300–1800 | 6.11 |
| CH$_2$F$_2$ + H → CHF$_2$ + H$_2$ | $8.29 \times 10^4$ | $2.63 \pm 0.45$ | $30.65 \pm 2.41$ | 1.6(1.8) | 300–1800 | 6.09 |
| CHF$_3$ + H → CF$_3$ + H$_2$ | $2.89 \times 10^4$ | $2.95 \pm 0.28$ | $38.61 \pm 2.28$ | 1.1(2.0) | 300–1800 | 4.05 |
| CH$_4$ + O → CH$_3$ + OH | $6.63 \times 10^6$ | $2.16 \pm 0.24$ | $31.42 \pm 1.91$ | 1.18(1.5) | 300–1800 | 6.70 |
| CH$_3$F + O → CH$_2$F + OH | $1.66 \times 10^6$ | $2.28 \pm 0.39$ | $26.34 \pm 2.44$ | 1.4(2.0) | 300–1800 | 7.28 |
| CH$_2$F$_2$ + O → CHF$_2$ + OH | $4.10 \times 10^5$ | $2.40 \pm 0.41$ | $27.19 \pm 2.52$ | 1.4(2.0) | 300–1800 | 6.72 |
| CHF$_3$ + O → CF$_3$ + OH | $2.70 \times 10^4$ | $2.65 \pm 0.58$ | $42.17 \pm 3.52$ | 1.7(2.3) | 300–1800 | 3.65 |
| CH$_4$ + OH → CH$_3$ + H$_2$O | $6.19 \times 10^5$ | $2.23 \pm 0.09$ | $9.84 \pm 1.54$ | 1.12(1.05) | 200–2025 | 9.62 |
| CH$_3$F + OH → CH$_2$F + H$_2$O | $1.06 \times 10^6$ | $2.04 \pm 0.26$ | $5.70 \pm 1.93$ | 1.5(1.22) | 240–1800 | 10.08 |
| CH$_2$F$_2$ + OH → CHF$_2$ + H$_2$O | $3.29 \times 10^6$ | $1.86 \pm 0.24$ | $7.52 \pm 1.90$ | 1.5(1.17) | 220–1800 | 9.82 |
| CHF$_3$ + OH → CF$_3$ + H$_2$O | $1.20 \times 10^6$ | $1.85 \pm 0.19$ | $13.71 \pm 1.78$ | 1.3(1.22) | 250–1800 | 8.27 |
| CH$_4$ + F → CH$_3$ + HF | $2.93 \times 10^{11}$ | $0.91 \pm 0.21$ | $0.79 \pm 1.51$ | 1.35(1.23) | 180–1800 | 13.58 |
| CH$_3$F + F → CH$_2$F + HF | $1.91 \times 10^{10}$ | $1.25 \pm 0.29$ | $0.81 \pm 1.49$ | 1.35(1.24) | 180–1800 | 13.24 |
| CH$_2$F$_2$ + F → CHF$_2$ + HF | $2.05 \times 10^8$ | $1.79 \pm 0.25$ | $1.30 \pm 1.65$ | 1.35(1.35) | 180–1800 | 12.52 |
| CHF$_3$ + F → CF$_3$ + HF | $4.57 \times 10^4$ | $2.77 \pm 0.20$ | $3.00 \pm 1.47$ | 1.35(1.20) | 180–1800 | 11.00 |

atoms, OH radicals, and F atoms at higher temperatures (1200–1800 K) that range about (1.4–1.6), (1.2–1.5), (1.2–1.5), and (1.3–1.5), respectively. Uncertainty factors for these reactions at lower temperatures (300–500 K) are also provided—and are slightly lower (for OH) or slightly higher (for H, O, and F atoms).

For a number of reactions, the reported rate constants in the literature are available only over a limited temperature range, or there are no reliable measurements. In these cases, we predicted the rate constants and their temperature dependencies in a self-consistent manner employing relative rates based on the rate constants and expressions that are established for other reactions in the homologous series. In these cases, we utilized empirical SARs correlating changes in rate constants with characteristics of the reaction, used empirical correlations between the rate constants at room temperature and the activation energy at high temperatures, and also used relative rates derived from *ab initio* quantum chemical calculations to guide (but not force) the rate constant predictions. We found that the relative $A$ factors generally scaled with the reaction path degeneracies (number of H atoms) with some systematic differences due to (a) changes in the PESs from changes in polarizabilities due to substitution by the highly electronegative F atoms and (b) changes from free-rotor to hindered-rotor TSs for the reactions involving OH radicals. We also found that there was a strong correlation between the activation energy $E_a$ at high temperatures where the rate constants can be considered at the classical limit and the activation energy $E_a$ at low temperatures where the rate constants are dominated by quantum mechanical tunneling.

A summary of the evaluated rate constants that are recommended in this study and the uncertainties in the parameters for these reactions is provided in Table 26.

## 10. Notation Used

| Notation | Description |
|---|---|
| Acronyms | |
| EPR | Electron paramagnetic resonance spectroscopy |
| ESR | Electron spin resonance spectroscopy |
| FTIR | Fourier transform infrared spectroscopy |
| GC | Gas chromatography |
| IR | Infrared spectroscopy |
| LIF | Laser induced fluorescence |
| LMR | Laser magnetic resonance spectroscopy |
| MS | Mass spectrometry |
| MW | Microwave excitation |
| UV | Ultraviolet light |
| VUV | Vacuum ultraviolet light |
| Abbreviations | |
| abs | absorption |
| chemilum | chemiluminescence |
| detect | detection |
| dischg | discharge |

(Continued.)

| Notation | Description |
|---|---|
| emiss | emission spectroscopy |
| fast flow | fast flow reactor |
| flame | flame measurements |
| flow | flow reactor |
| fluor | fluorescence |
| fwd/rev rxn | forward/reverse reaction |
| heat recomb | heat of recombination |
| High T fit | High-temperature fit |
| ignition | ignition measurement |
| model | complex chemical kinetic model |
| photodissoc | photodissociation |
| photol | photolysis |
| plasma excit | plasma excitation |
| pulse photol | pulse photolysis |
| Recommended | Recommended value |
| Rel rate | Relative rate |
| reson | resonance |
| rev rxn | reverse reaction |
| Review | Evaluation based on literature review |
| shock | shock tube measurement |
| static | static reactor |
| stirred | stirred reactor |
| thermal | thermal reactor |
| ultrasonic | ultrasonic chemical kinetic method |
| Theoretical methods | |
| BEBO | Bond energy bond order theory |
| Semi-empirical | Semi-empirical theoretical method |
| TST | Transition state theory |
| VTST | Variational transition state theory |
| Quantum chemical methods | |
| BAC-MP4 | BAC-MP4 quantum chemical theory |
| CBS-QB3 | CBS-QB3 composite quantum chemical method |
| CBS-RAD | CBS-RAD composite quantum chemical method |
| CC | Coupled cluster quantum chemical theory |
| CCSD | CC theory with single and double excitations |
| CVT | Canonical variational transition state theory |
| DFT | Density functional theory quantum chemical methods |
| Eckart | Eckart tunneling approximation |
| G2 | G2 composite quantum chemical method |
| G2MP2 | G2MP2 composite quantum chemical method |
| G3B3 | G3B3 composite quantum chemical method |
| MP2 | MP2 quantum chemical theory |
| MP4 | MP4 quantum chemical theory |

*(Continued.)*

| Notation | Description |
|---|---|
| PES | Quantum chemical potential energy surface |
| Quant | Quantum chemical method |
| Quant dynamics | Quantum dynamical method |
| SCT | Small curvature tunneling approximation method |
| Wigner | Wigner tunneling approximation |
| Quantum chemical basis sets | |
| 6-311 | 6-311 quantum chemical basis set |
| KKMLYP | KKMLYP quantum chemical basis set |
| pVQZ | pVQZ quantum chemical basis set |
| pVTZ | pVTZ quantum chemical basis set |

## 11. Supplementary Material

See the supplementary material for __. all the tables in the paper in Excel format.

## 12. Data Availability

The data that support the findings of this study are available within the article.

## 13. References

[1]V. Masson-Delmotte, P. Zhai, H.-O. Pörtner, D. Roberts, J. Skea, P. R. Shukla, A. Pirani, W. Moufouma-Okia, C. Péan, R. Pidcock, S. Connors, J. B. R. Matthews, Y. Chen, X. Zhou, M. I. Gomis, E. Lonnoy, T. Maycock, M. Tignor, and T. Waterfield, IPCC, 2018: Global warming of 1.5 °C. An IPCC Special Report on the impacts of global warming of 1.5 °C above pre-industrial levels and related global greenhouse gas emission pathways, in the context of strengthening the global response to the threat of climate change, sustainable development, and efforts to eradicate poverty, International Panel on Climate Change, Geneva, Switzerland, 2018.

[2]M. O. McLinden, J. S. Brown, R. Brignoli, A. F. Kazakov, and P. A. Domanski, "Limited options for low-global-warming-potential refrigerants," Nat. Commun. **8**, 14476 (2017).

[3]S. Sekusak, K. R. Liedl, B. M. Rode, and A. Sabljic, "Reaction-path dynamics of hydroxyl radical reactions with ethane and haloethanes," J. Phys. Chem. A **101**, 4245 (1997).

[4]H. Sun, H. He, H. Gong, X. Pan, Z. Li, and R. Wang, "Theoretical investigation into the hydrogen abstraction reaction of $CH_3CH_2F$ (HFC-161) with OH," Chem. Phys. **327**, 91 (2006).

[5]M. A. Ali and B. Rajakumar, "Computational study on OH radical reaction with $CHF_2CHFCHF$ (HFC-245ea) between 200 and 400 K," Int. J. Chem. Kinet. **43**, 418 (2011).

[6]B. Rajakumar, R. W. Portmann, J. B. Burkholder, and A. R. Ravishankara, "Rate coefficients for the reactions of OH with $CF_3CH_2CH_3$ (HFC-263fb), $CF_3CHFCH_2F$ (HFC-245eb), and $CHF_2CHFCHF_2$ (HFC-245ea) between 238 and 375 K," J. Phys. Chem. A **110**, 6724 (2006).

[7]M. A. Ali, B. Upendra, and B. Rajakumar, "Kinetic parameters of abstraction reactions of OH radical with ethylene, fluoroethylene, *cis*- and *trans*-1,2-difluoroethylene, and 1,1-difluoroethylene, in the temperature range of 200–400 K: GAUSSIAN-3/B3LYP theory," Chem. Phys. Lett. **511**, 440 (2011).

[8]C. M. Tovar, M. B. Blanco, I. Barnes, P. Wiesen, and M. A. Teruel, "Gas-phase reactivity study of a series of hydrofluoroolefins (HFOs) toward OH radicals and Cl atoms at atmospheric pressure and 298 K," Atmos. Environ. **88**, 107 (2014).

[9]Y. Zhang, K. Chao, X. Pan, J. Zhang, Z. Su, and R. Wang, "Mechanism and kinetic study of 3-fluoropropene with hydroxyl radical reaction," J. Mol. Graph. Model. **48**, 18 (2014).

[10]Y. Zhang, R. Song, Y. Sun, Z. Wang, B. Huang, and J. Sun, "Computational study on the mechanisms and kinetics of the $CH_2$=CHCH$_2$F with O($^3$P) reaction," Spectrochim. Acta A **206**, 104 (2019).

[11]C. B. Rivela, C. M. Tovar, M. A. Teruel, I. Barnes, P. Wiesen, and M. B. Blanco, "CFCs replacements: Reactivity and atmospheric lifetimes of a series of Hydrofluoroolefins towards OH radicals and Cl atoms," Chem. Phys. Lett. **714**, 190 (2019).

[12]N. K. Gour, K. Borthakur, S. Paul, and R. Chandra Deka, "Tropospheric degradation of 2-fluoropropene ($CH_3CF$=$CH_2$) initiated by hydroxyl radical: Reaction mechanisms, kinetics and atmospheric implications from DFT study," Chemosphere **238**, 124556 (2020).

[13]A. Bonard, V. Daële, J.-L. Delfau, and C. Vovelle, "Kinetics of OH radical reactions with methane in the temperature range 295–660 K and with dimethyl ether and methyl-tert-butyl ether in the temperature range 295–618 K," J. Phys. Chem. A **106**, 4384 (2002).

[14]S. Urata, A. Takada, T. Uchimaru, and A. K. Chandra, "Rate constants estimation for the reaction of hydrofluorocarbons and hydrofluoroethers with OH radicals," Chem. Phys. Lett. **368**, 215 (2003).

[15]V. Kaliginedi, M. A. Ali, and B. Rajakumar, "Kinetic parameters for the reaction of hydroxyl radical with $CH_3OCH_2F$ (HFE-161) in the temperature range of 200–400 K: Transition state theory and *ab initio* calculations," Int. J. Quantum Chem. **112**, 1066 (2012).

[16]S. A. Carr, T. J. Still, M. A. Blitz, A. J. Eskola, M. J. Pilling, P. W. Seakins, R. J. Shannon, B. Wang, and S. H. Robertson, "Experimental and theoretical study of the kinetics and mechanism of the reaction of OH radicals with dimethyl ether," J. Phys. Chem. A **117**, 11142 (2013).

[17]P. R. Dalmasso, R. A. Taccone, J. D. Nieto, P. M. Cometto, C. J. Cobos, and S. I. Lane, "Reactivity of hydrohaloethers with OH radicals and chlorine atoms: Correlation with molecular properties," Atmos. Environ. **91**, 104 (2014).

[18]M. P. S. Andersen, S. B. Svendsen, F. F. Osterstrom, and O. J. Nielsen, "Atmospheric chemistry of $CH_3CH_2OCH_3$: Kinetics and mechanism of reactions with Cl atoms and OH radicals," Int. J. Chem. Kinet. **49**, 10 (2017).

[19]R. J. Hanson, "Linear least-squares with bounds and linear constraints," SIAM J. Sci. Comput. **7**, 826 (1986).

[20]L. Vereecken and J. Peeters, "A structure-activity relationship for the rate coefficient of H-migration in substituted alkoxy radicals," Phys. Chem. Chem. Phys. **12**, 12608 (2010).

[21]L. Vereecken, B. Aumont, I. Barnes, J. W. Bozzelli, M. J. Goldman, W. H. Green, S. Madronich, M. R. Mcgillen, A. Mellouki, J. J. Orlando, B. Picquet-Varrault, A. R. Rickard, W. R. Stockwell, T. J. Wallington, and W. P. L. Carter, "Perspective on mechanism development and structure-activity relationships for gas-phase atmospheric chemistry," Int. J. Chem. Kinet. **50**, 435 (2018).

[22]M. R. McGillen, W. P. L. Carter, A. Mellouki, J. J. Orlando, B. Picquet-Varrault, and T. J. Wallington, "Database for the kinetics of the gas-phase atmospheric reactions of organic compounds," Earth Syst. Sci. Data **12**, 1203 (2020).

[23]M. R. McGillen, A. T. Archibald, T. Carey, K. E. Leather, D. E. Shallcross, J. C. Wenger, and C. J. Percival, "Structure-activity relationship (SAR) for the prediction of gas-phase ozonolysis rate coefficients: An extension towards heteroatomic unsaturated species," Phys. Chem. Chem. Phys. **13**, 2842 (2011).

[24]S. Gupta, N. Basant, D. Mohan, and K. P. Singh, "Modeling the reactivities of hydroxyl radical and ozone towards atmospheric organic chemicals using quantitative structure-reactivity relationship approaches," Environ. Sci. Pollut. Res. **23**, 14034 (2016).

[25]L. N. Farrugia, I. Bejan, S. C. Smith, D. J. Medeiros, and P. W. Seakins, "Revised structure activity parameters derived from new rate coefficient determinations for the reactions of chlorine atoms with a series of seven ketones at 290 K and 1 atm," Chem. Phys. Lett. **640**, 87 (2015).

[26]N. Basant and S. Gupta, "Multi-target QSPR modeling for simultaneous prediction of multiple gas-phase kinetic rate constants of diverse chemicals," Atmos. Environ. **177**, 166 (2018).

[27]S. M. Aschmann and R. Atkinson, "Effect of structure on the rate constants for reaction of $NO_3$ radicals with a series of linear and branched $C_5$-$C_7$ 1-alkenes at 296 ± 2 K," J. Phys. Chem. A **115**, 1358 (2011).

[28]R. Atkinson, "A structure-activity relationship for the estimation of rate constants for the gas-phase reactions of OH radicals with organic-compounds," Int. J. Chem. Kinet. **19**, 799 (1987).

[29]E. Kwok and R. Atkinson, "Estimation of hydroxyl radical reaction-rate constants for gas-phase organic-compounds using a structure-reactivity relationship: An update," Atmos. Environ. **29**, 1685 (1995).

[30]M. L. Poutsma, "Evolution of structure-reactivity correlations for the hydrogen abstraction reaction by chlorine atom," J. Phys. Chem. A **117**, 687 (2013).

[31]J. Song, G. Stephanopoulos, and W. H. Green, "Valid parameter range analyses for chemical reaction kinetic models," Chem. Eng. Sci. **57**, 4475 (2002).

[32]M. Saeys, M.-F. Reyniers, V. Van Speybroeck, M. Waroquier, and G. B. Marin, "Ab initio group contribution method for activation energies of hydrogen abstraction reactions," ChemPhysChem **7**, 188 (2006).

[33]M. K. Sabbe, M.-F. Reyniers, M. Waroquier, and G. B. Marin, "Hydrogen radical additions to unsaturated hydrocarbons and the reverse $\beta$-scission reactions: Modeling of activation energies and pre-exponential factors," ChemPhysChem **11**, 195 (2010).

[34]P. D. Paraskevas, M. K. Sabbe, M.-F. Reyniers, N. G. Papayannakos, and G. B. Marin, "Group additive kinetics for hydrogen transfer between oxygenates," J. Phys. Chem. A **119**, 6961 (2015).

[35]R. Van de Vijver, M. K. Sabbe, M.-F. Reyniers, K. M. Van Geem, and G. B. Marin, "Ab initio derived group additivity model for intramolecular hydrogen abstraction reactions," Phys. Chem. Chem. Phys. **20**, 10877 (2018).

[36]H.-H. Carstensen and A. M. Dean, "Rate constant rules for the automated generation of gas-phase reaction mechanisms," J. Phys. Chem. A **113**, 367 (2009).

[37]N. Kungwan and T. N. Truong, "Kinetics of the hydrogen abstraction ·CH$_3$ + alkane → CH$_4$ + alkyl reaction class: An application of the reaction class transition state theory," J. Phys. Chem. A **109**, 7742 (2005).

[38]L. K. Huynh, K. Barrier, and A. Violi, "Kinetics study of the OH + alkene → H$_2$O + alkenyl reaction class," J. Phys. Chem. A **112**, 1436 (2008).

[39]B. Bankiewicz, L. K. Huynh, A. Ratkiewicz, and T. N. Truong, "Kinetics of 1,4-hydrogen migration in the alkyl radical reaction class," J. Phys. Chem. A **113**, 1564 (2009).

[40]C. J. Hayes and D. R. Burgess, "Kinetic barriers of H-atom transfer reactions in alkyl, allylic, and oxoallylic radicals as calculated by composite ab initio methods," J. Phys. Chem. A **113**, 2473 (2009).

[41]A. Ratkiewicz and T. N. Truong, "Kinetics of the hydrogen abstraction R–OH + H → R–O· + H$_2$ reaction class," Int. J. Chem. Kinet. **42**, 414 (2010).

[42]D. R. Burgess, J. A. Manion, and C. J. Hayes, "Data formats for elementary gas phase kinetics. Part 3: Reaction classification," Int. J. Chem. Kinet. **47**, 361 (2015).

[43]A. Ratkiewicz, L. K. Huynh, and T. N. Truong, "Performance of first-principles-based reaction class transition state theory," J. Phys. Chem. B **120**, 1871 (2016).

[44]T. N. Truong, "Reaction class transition state theory: Hydrogen abstraction reactions by hydrogen atoms as test cases," J. Chem. Phys. **113**, 4957 (2000).

[45]A. Violi, T. N. Truong, and A. F. Sarofim, "Kinetics of hydrogen abstraction reactions from polycyclic aromatic hydrocarbons by H atoms," J. Phys. Chem. A **108**, 4846 (2004).

[46]Q.-D. Wang, X.-J. Wang, and G.-J. Kang, "An application of the reaction class transition state theory to the kinetics of hydrogen abstraction reactions of hydrogen with methyl esters at the methoxy group," Comput. Theor. Chem. **1027**, 103 (2014).

[47]S. S. Tratch and N. S. Zefirov, "A hierarchical classification scheme for chemical reactions," J. Chem. Inf. Comput. Sci. **38**, 349 (1998).

[48]V. D. Knyazev, "Isodesmic reactions for transition states: Reactions of Cl atoms with methane and halogenated methanes," J. Phys. Chem. A **107**, 11082 (2003).

[49]V. D. Knyazev, "Reactivity extrapolation from small to large molecular systems via isodesmic reactions for transition states," J. Phys. Chem. A **108**, 10714 (2004).

[50]C. W. Coley, W. Jin, L. Rogers, T. F. Jamison, T. S. Jaakkola, W. H. Green, R. Barzilay, and K. F. Jensen, "A graph-convolutional neural network model for the prediction of chemical reactivity," Chem. Sci. **10**, 370 (2019).

[51]A. V. Zeigarnik, O. N. Temkin, and D. Bonchev, "Application of graph theory to chemical kinetics. 3. Topological specificity of multiroute reaction mechanisms," J. Chem. Inf. Comput. Sci. **36**, 973 (1996).

[52]M. H. Holmes and J. Bell, "The application of symbolic computing to chemical kinetic reaction schemes," J. Comput. Chem. **12**, 1223 (1991).

[53]C. A. Grambow, L. Pattanaik, and W. H. Green, "Deep learning of activation energies," J. Phys. Chem. Lett. **11**, 2992 (2020).

[54]N. Sikalo, O. Hasemann, C. Schulz, A. Kempf, and I. Wlokas, "A genetic algorithm-based method for the optimization of reduced kinetics mechanisms," Int. J. Chem. Kinet. **47**, 695 (2015).

[55]M. G. Evans and M. Polanyi, "Further considerations on the thermodynamics of chemical equilibria and reaction rates," Trans. Faraday Soc. **32**, 1333 (1936).

[56]R. G. Susnow, A. M. Dean, W. H. Green, P. Peczak, and L. J. Broadbelt, "Rate-based construction of kinetic models for complex systems," J. Phys. Chem. A **101**, 3731 (1997).

[57]R. Sumathi and W. H. Green, Jr., "Oxygenate, oxyalkyl and alkoxycarbonyl thermochemistry and rates for hydrogen abstraction from oxygenates," Phys. Chem. Chem. Phys. **5**, 3402 (2003).

[58]J. M. Anglada, E. Besalu, J. M. Bofill, and R. Crehuet, "Prediction of approximate transition states by Bell-Evans-Polanyi principle: I," J. Comput. Chem. **20**, 1112 (1999).

[59]A. Matsugi and H. Shiina, "Kinetics of hydrogen abstraction reactions from fluoromethanes and fluoroethanes," Bull. Chem. Soc. Jpn. **87**, 890 (2014).

[60]B. N. Taylor and C. Kuyatt, "Guidelines for evaluating and expressing the uncertainty of NIST measurement results," NIST Techn. Note **1297**, 1 (1994).

[61]M. Schwartz, P. Marshall, R. J. Berry, C. J. Ehlers, and G. A. Petersson, "Computational study of the kinetics of hydrogen abstraction from fluoromethanes by the hydroxyl radical," J. Phys. Chem. A **102**, 10074 (1998).

[62]B. Ruscic, R. E. Pinzon, M. L. Morton, G. von Laszevski, S. J. Bittner, S. G. Nijsure, K. A. Amin, M. Minkoff, and A. F. Wagner, "Introduction to active thermochemical tables: Several "key" enthalpies of formation revisited," J. Phys. Chem. A **108**, 9979 (2004).

[63]Á. Ganyecz, M. Kállay, and J. Csontos, "High accuracy quantum chemical and thermochemical network data for the heats of formation of fluorinated and chlorinated methanes and ethanes," J. Phys. Chem. A **122**, 5993 (2018).

[64]A. Bodi, M. Johnson, T. Gerber, Z. Gengeliczki, B. Sztáray, and T. Baer, "Imaging photoelectron photoion coincidence spectroscopy with velocity focusing electron optics," Rev. Sci. Instrum. **80**, 034101 (2009).

[65]J. A. Blush, P. Chen, R. T. Wiedmann, and M. G. White, "Rotationally resolved threshold photoelectron-spectrum of the methyl radical," J. Chem. Phys. **98**, 3557 (1993).

[66]B. Ruscic, "Active thermochemical tables: Water and water dimer," J. Phys. Chem. A **117**, 11940 (2013).

[67]Q. J. Hu and J. W. Hepburn, "Energetics and dynamics of threshold photoion-pair formation in HF/DF," J. Chem. Phys. **124**, 074311 (2006).

[68]Y. P. Zhang, C. H. Cheng, J. T. Kim, J. Stanojevic, and E. E. Eyler, "Dissociation energies of molecular hydrogen and the hydrogen molecular ion," Phys. Rev. Lett. **92**, 203003 (2004).

[69]B. Ruscic, D. Feller, and K. A. Peterson, "Active thermochemical tables: Dissociation energies of several homonuclear first-row diatomics and related thermochemical values," Theor. Chem. Acc. **133**, 1415 (2013).

[70]O. V. Boyarkin, M. A. Koshelev, O. Aseev, P. Maksyutenko, T. R. Rizzo, N. F. Zobov, L. Lodi, J. Tennyson, and O. L. Polyansky, "Accurate bond dissociation energy of water determined by triple-resonance vibrational spectroscopy and ab initio calculations," Chem. Phys. Lett. **568-569**, 14 (2013).

[71]J. Yang, Y. Hao, J. Li, C. Zhou, and Y. Mo, "A combined zero electronic kinetic energy spectroscopy and ion-pair dissociation imaging study of the F$_2^+(X^2\Pi_g)$ structure," J. Chem. Phys. **122**, 134308 (2005).

[72]J. Yang, Y. Hao, J. Li, C. Zhou, and Y. Mo, "Erratum: "A combined zero electronic kinetic energy spectroscopy and ion-pair dissociation imaging study of the F$_2^+(X^2\Pi_g)$ structure" [J. Chem. Phys. 122, 134308 (2005)]," J. Chem. Phys. **127**, 209901 (2007).

[73]K. Takahashi, Y. Yamamori, and T. Inomata, "A kinetic study on the reaction of CHF$_3$ with H at high temperatures," J. Phys. Chem. A **101**, 9105 (1997).

[74]J. W. Sutherland, M.-C. Su, and J. V. Michael, "Rate constants for H + CH$_4$, CH$_3$ + H$_2$, and CH$_4$ dissociation at high temperature," Int. J. Chem. Kinet. **33**, 669 (2001).

[75]H. J. Baeck, K. S. Shin, H. Yang, V. Lissianski, and W. C. Gardiner, "Reaction between CH$_3$ and H$_2$ at combustion temperatures," Bull. Korean Chem. Soc. **16**, 543 (1995).

[76]H. J. Baeck, K. S. Shin, H. Yang, Z. Qin, V. Lissianski, and W. C. Gardiner, "Shock-tube study of the reaction between $CH_3$ and $H_2$," J. Phys. Chem. **99**, 15925 (1995).

[77]P.-M. Marquaire, A. G. Dastidar, K. C. Manthorne, and P. D. Pacey, "Electron-spin-resonance study of the reaction of hydrogen-atoms with methane," Can. J. Chem. **72**, 600 (1994).

[78]M. J. Rabinowitz, J. W. Sutherland, P. M. Patterson, and R. B. Klemm, "Direct rate-constant measurements for $H+CH_4 = CH_3 + H_2$, 897–1729 K, using the flash-photolysis shock-tube technique," J. Phys. Chem. **95**, 674 (1991).

[79]G. Dixon-Lewis and A. Williams, "Some observations on the combustion of methane in premixed flames," Symp. Int. Combust. Proc. **11**, 951 (1967).

[80]M. G. Bryukov, I. R. Slagle, and V. D. Knyazev, "Kinetics of reactions of H atoms with methane and chlorinated methanes," J. Phys. Chem. A **105**, 3107 (2001).

[81]A. Sepehrad, R. M. Marshall, and H. Purnell, "Reaction between hydrogen-atoms and methane," J. Chem. Soc. Faraday Trans. 1 **75**, 835 (1979).

[82]J. Peeters and G. Mahnen, "Reaction mechanisms and rate constants of elementary steps in methane-oxygen flames," Symp. Int. Combust. Proc. **14**, 133 (1973).

[83]M. J. Kurylo, G. A. Hollinden, and R. B. Timmons, "ESR study of kinetic isotope effect in reaction of H and deuterium atoms with $CH_4$," J. Chem. Phys. **52**, 1773 (1970).

[84]N. I. Gorban and A. B. Nalbandyan, "Determination of the rate constants of elementary reactions between atomic hydrogen and simple saturated hydrocarbons," Zh. Fiz. Khim. **36**, 1757 (1962).

[85]W. E. Jones and J. L. Ma, "An electron-spin-resonance study of the reactions of hydrogen-atoms with halocarbons," Can. J. Chem. **64**, 2192 (1986).

[86]P. Roth and T. Just, "Atom-Resonance absorption-measurements at thermal-decomposition of methane after shock-waves," Ber. Bunsenges. Phys. Chem. **79**, 682 (1975).

[87]R. R. Baker, R. R. Baldwin, and R. W. Walker, "The use of the $H_2 + O_2$ reaction in determining the velocity constants of elementary reactions in hydrocarbon oxidation," Symp. Int. Combust. Proc. **13**, 291 (1971).

[88]M. J. Kurylo and R. B. Timmons, "ESR study of the kinetics of the reaction of H atoms with methane," J. Chem. Phys. **50**, 5076 (1969).

[89]V. V. Azatyan, "Combustion limitation method in the heterogeneous termination of chains in diffusion range," Arm. Khim. Zh. **20**, 577 (1967).

[90]R. H. Lawrence and R. F. Firestone, "Kinetics of thermal deuterium atom reactions with methane and ethane," J. Am. Chem. Soc. **88**, 4564 (1966).

[91]J. W. S. Jamieson and G. R. Brown, "Kinetics of reaction of atomic hydrogen with methane," Can. J. Chem. **42**, 1638 (1964).

[92]C. P. Fenimore and G. W. Jones, "Rate of reaction of methane with H atoms and OH radicals in flames," J. Phys. Chem. **65**, 2200 (1961).

[93]M. R. Berlie and D. J. Le Roy, "Kinetics of the reaction $H + CH_4 = CH_3 + H_2$," Can. J. Chem. **32**, 650 (1954).

[94]Z. Konkoli, E. Kraka, and D. Cremer, "Unified reaction valley approach mechanism of the reaction $CH_3 + H_2 \rightarrow CH_4 + H$," J. Phys. Chem. A **101**, 1742 (1997).

[95]R. J. Berry, C. J. Ehlers, D. R. Burgess, M. R. Zachariah, and P. Marshall, "A computational study of the reactions of atomic hydrogen with fluoromethanes: Kinetics and product channels," Chem. Phys. Lett. **269**, 107 (1997).

[96]D. K. Maity, W. T. Duncan, and T. N. Truong, "Direct *ab initio* dynamics studies of the hydrogen abstraction reactions of hydrogen atom with fluoromethanes," J. Phys. Chem. A **103**, 2152 (1999).

[97]A. A. Westenberg and N. Dehaas, "Rates of $H + CH_3X$ reactions," J. Chem. Phys. **62**, 3321 (1975).

[98]J. A. Manion, R. E. Huie, R. D. Levin, D. R. Burgess, Jr., V. L. Orkin, W. Tsang, W. S. McGivern, J. W. Hudgens, V. D. Knyazev, D. B. Atkinson, E. Chai, A. M. Tereza, C.-Y. Lin, T. C. Allison, W. G. Mallard, F. Westley, J. T. Herron, R. F. Hampson, and D. H. Frizzell, *NIST Chemical Kinetics Database*, NIST Standard Reference Database 17 (NIST, 2015), http://kinetics.nist.gov.

[99]J. A. Manion and W. Tsang, "Hydrogen atom attack on 1,2-dichlorotetrafluoro-ethane: Rates of halogen abstraction," J. Phys. Chem. **100**, 7060 (1996).

[100]G. O. Pritchard and M. J. Perona, "Some hydrogen atom abstraction reactions of $CF_2H$ and $CFH_2$ radicals, and the C–H bond dissociation energy in $CF_2H_2$," Int. J. Chem. Kinet. **1**, 509 (1969).

[101]E. Goos, A. Burcat, and B. Ruscic, "Extended third millenium ideal gas thermochemical database with updates from active thermochemical tables," 2020, http://burcat.technion.ac.il/dir (accessed June 23, 2020).

[102]N. I. Parsamyan, V. V. Azatyan, and A. B. Nalbandyan, "Determination of the rate constant for reaction of atomic hydrogen and oxygen with methyl fluoride," Arm. Khim. Zh. **21**, 1003 (1967).

[103]N. I. Parsamyan and A. B. Nalbandyan, "Determination of the rate constants for reactions of hydrogen and oxygen atoms with difluoromethane," Arm. Khim. Zh. **21**, 1003 (1968).

[104]L. W. Hart, C. Grunfelder, and R. M. Fristrom, "Point source technique using upstream sampling for rate constant determinations in flame gases," Combust. Flame **23**, 109 (1974).

[105]W. K. Aders, D. Pangritz, and H. G. Wagner, "Investigations of reactions of hydrogen-atoms with methyl-fluoride, methyl-chloride, and methyl-bromide," Ber. Bunsenges. Phys. Chem. **79**, 90 (1975).

[106]D. L. Baulch, J. Duxbury, S. J. Grant, and D. C. Montague, "Evaluated kinetic data for high-temperature reactions. Volume 4. Homogeneous gas-phase reactions of halogen-containing and cyanide-containing species," J. Phys. Chem. Ref. Data 10, Supplement 1, Volume **4** (1981).

[107]J. Hranisavljevic and J. V. Michael, "Rate constants for $CF_3 + H_2 \rightarrow CF_3H + H$ and $CF_3H + H \rightarrow CF_3 + H_2$ reactions in the temperature range 1100–1600 K," J. Phys. Chem. A **102**, 7668 (1998).

[108]J. C. Amphlett and E. Whittle, "Reactions of trifluoromethyl radicals with iodine and hydrogen iodide," Trans. Faraday Soc. **63**, 2695 (1967).

[109]G. O. Pritchard and J. K. Foote, "Reactions of $C_2F_5 + C_3F_7$ radicals with hydrogen + deuterium," J. Phys. Chem. **68**, 1016 (1964).

[110]V. N. Kondratiev, *Rate Constants of Gas Phase Reactions: Reference Book* (Office of Standard Reference Data, National Bureau of Standards, Washington, DC, 1972), COM-72-10014 1.

[111]H. Richter, J. Vandooren, and P. Van Tiggelen, "Kinetics of the consumption of $CF_3H$, $CF_2HCCl$ and $CF_2O$ in $H_2/O_2$ flames," J. Chim. Phys. PCB **91**, 1748 (1994).

[112]H. Richter, J. Vandooren, and P. J. Van Tiggelen, "Decay mechanism of $CF_3H$ or $CF_2HCl$ in $H_2/O_2/Ar$ flames," Symp. Int. Combust. Proc. **25**, 825 (1994).

[113]P. B. Ayscough, J. C. Polanyi, and E. W. R. Steacie, "The vapor phase photolysis of hexafluoroacetone in the presence of methane and ethane," Can. J. Chem. **33**, 743 (1955).

[114]Y. Yamamori, K. Takahashi, and T. Inomata, in *Proceedings of the Thirty-Fourth Japanese Symposium on Combustion (Hiroshima)* (Combustion Society of Japan, Kyoto, Japan, 1996), Vol. 35, pp. 125.

[115]Y. Hidaka, T. Nakamura, H. Kawano, and T. Koike, "$CF_3Br-H_2$ reaction in shock-waves," Int. J. Chem. Kinet. **25**, 983 (1993).

[116]C. K. Westbrook, "Numerical modeling of flame inhibition by $CF_3Br$," Combust. Sci. Technol. **34**, 201 (1983).

[117]T. Bérces, F. Szilágyi, and I. Szilagyi, "Reactions of $CF_3$ radicals with benzotrifluoride and C–H bond strength in $C_6H_5CF_3$ and $C_6H_6$," J. Chem. Soc. Faraday Trans. 1 **68**, 867 (1972).

[118]C. L. Kibby and R. E. Weston, "Photolysis of hexafluoroacetone in presence of $H_2$ $D_2$ and HD. Kinetic isotope effects in reaction of $CF_3$ with molecular hydrogen," J. Chem. Phys. **49**, 4825 (1968).

[119]M. B. Fargash, F. B. Moin, and V. I. Ocheret'ko, "Effect of $H_2$ and HCl additions on the photolysis of chlorotrifluoromethane," Kinet. Katal. **9**, 762 (1968).

[120]G. B. Skinner and G. H. Ringrose, "Shock-tube experiments on inhibition of hydrogen-oxygen reaction," J. Chem. Phys. **43**, 4129 (1965).

[121]G. B. Skinner and G. H. Ringrose, "Ignition delays of hydrogen-oxygen-argon mixture at relatively low temperatures," J. Chem. Phys. **42**, 2190 (1965).

[122]G. O. Pritchard, H. O. Pritchard, H. I. Schiff, and A. F. Trotman-Dickenson, "The reactions of trifluoromethyl radicals," Trans. Faraday Soc. **52**, 849 (1956).

[123]X. Shan and D. C. Clary, "A reduced dimensionality quantum mechanical study of the $H + HCF_3 \leftrightarrow H_2 + CF_3$ reaction," Phys. Chem. Chem. Phys. **15**, 18530 (2013).

[124]M. Zhang, Z. Lin, and C. Song, "Comprehensive theoretical studies on the $CF_3H$ dissociation mechanism and the reactions of $CF_3H$ with OH and H free radicals," J. Chem. Phys. **126**, 034307 (2007).

[125]F. Louis, C. A. Gonzalez, and J.-P. Sawerysyn, "Direct combined *ab initio*/transition state theory study of the kinetics of the abstraction reactions of halogenated methanes with hydrogen atoms," J. Phys. Chem. A **108**, 10586 (2004).

[126]D. R. Burgess, Jr., M. R. Zachariah, W. Tsang, and P. R. Westmoreland, "Key species and important reactions in fluorinated hydrocarbon flame chemistry," ACS Symp. Ser. **611**, 322 (2007).

[127]N. L. Arthur and T. N. Bell, "An evaluation of the kinetic data for hydrogen abstraction from silanes in the gas phase," Rev. Chem. Intermed. **2**, 37 (1978).

[128]N. L. Arthur, K. F. Donchi, and J. A. McDonell, "BEBO calculations. 4. Arrhenius parameters and kinetic isotope-effects for reactions of $CH_3$ and $CF_3$ radicals with $H_2$ and $D_2$," J. Chem. Soc. Faraday Trans. 1 **71**, 2431 (1975).

[129]K. Glanzer, M. Maier, and J. Troe, "Shock-wave study of the high-temperature UV absorption and the recombination of $CF_3$ radicals," J. Phys. Chem. **84**, 1681 (1980).

[130]G. A. Skorobogatov, V. K. Khripun, and A. G. Rebrova, Kinet. Catal. **49**, 466 (2008).

[131]C. J. Cobos, A. E. Croce, K. Luther, and J. Troe, "Temperature and pressure dependence of the reaction $2CF_3$ ($^+M$) $\leftrightarrow$ $C_2F_6$ ($^+M$)," J. Phys. Chem. A **114**, 4748 (2010).

[132]J. A. Montgomery, M. J. Frisch, J. W. Ochterski, and G. A. Petersson, "A complete basis set model chemistry. VII. Use of the minimum population localization method," J. Chem. Phys. **112**, 6532 (2000).

[133]J.-D. Chai and M. Head-Gordon, "Long-range corrected hybrid density functionals with damped atom-atom dispersion corrections," Phys. Chem. Chem. Phys. **10**, 6615 (2008).

[134]H. S. Johnston and J. Heicklen, "Tunnelling corrections for unsymmetrical Eckart potential energy barriers," J. Phys. Chem. **66**, 532 (1962).

[135]J. Harvey, R. P. Tuckett, and A. Bodi, "A halomethane thermochemical network from iPEPICO experiments and quantum chemical calculations," J. Phys. Chem. A **116**, 9696 (2012).

[136]C. J. Cobos, A. E. Croce, K. Luther, L. Sölter, E. Tellbach, and J. Troe, "Experimental and modeling study of the reaction $C_2F_4$ ($^+M$) $\leftrightarrow$ $CF_2 + CF_2$ ($^+M$)," J. Phys. Chem. A **117**, 11420 (2013).

[137]P. B. Ayscough, "Rate of recombination of radicals. II. The rate of recombination of trifluoromethyl radicals," J. Chem. Phys. **24**, 944 (1956).

[138]M. W. Chase, C. A. Davies, J. R. Downey, D. J. Frurip, R. A. McDonald, and A. N. Syverud, "JANAF Thermochemical Tables, Third Edition, Part II, Cr-Zr," Phys. Chem. Ref. Data 14, Supplement 1 (1985).

[139]M. W. Chase, C. A. Davies, J. R. Downey, D. J. Frurip, R. A. McDonald, and A. N. Syverud, "JANAF Thermochemical Tables, Third Edition, Part I, Al-Co," Phys. Chem. Ref. Data 14, Supplement 1, (1985).

[140]M. W. Chase, Jr., "NIST-JANAF Thermochemical Tables, 4th Edition," J. Phys. Chem. Ref. Data, Monograph 9 (1998).

[141]T. Ogawa, G. A. Carlson, and G. C. Pimentel, "Reaction rate of trifluoromethyl radicals by rapid scan infrared spectroscopy," J. Phys. Chem. **74**, 2090 (1970).

[142]A. Miyoshi, K. Ohmori, K. Tsuchiya, and H. Matsui, "Reaction-rates of atomic oxygen with straight chain alkanes and fluoromethanes at high-temperatures," Chem. Phys. Lett. **204**, 241 (1993).

[143]A. Fernandez and A. Fontijn, "Wide temperature range kinetics of the O + $CHF_3$ reaction," J. Phys. Chem. A **105**, 8196 (2001).

[144]J. W. Sutherland, J. V. Michael, and R. B. Klemm, "Rate constant for the $O(^3P) + CH_4 \rightarrow OH + CH_3$ reaction obtained by the flash-photolysis shock-tube technique over the temperature-range $763 < T < 1755$ K," J. Phys. Chem. **90**, 5941 (1986).

[145]A. A. Westenberg and N. Dehaas, "Reinvestigation of rate coefficients for O + $H_2$ and O + $CH_4$," J. Chem. Phys. **50**, 2512 (1969).

[146]J. Espinosa-García and J. C. García-Bernáldez, "Analytical potential energy surface for the $CH_4 + O(^3P) \rightarrow CH_3$ reaction. Thermal rate constants and kinetic isotope effects," Phys. Chem. Chem. Phys. **2**, 2345 (2000).

[147]E. González-Lavado, J. C. Corchado, and J. Espinosa-Garcia, "The hydrogen abstraction reaction $O(^3P) + CH_4$: A new analytical potential energy surface based on fit to *ab initio* calculations," J. Chem. Phys. **140**, 064310 (2014).

[148]E. Gonzalez-Lavado, J. C. Corchado, Y. V. Suleimanov, W. H. Green, and J. Espinosa-Garcia, "Theoretical kinetics study of the $O(^3P) + CH_4/CD_4$ hydrogen abstraction reaction: The role of anharmonicity, recrossing effects, and quantum mechanical tunneling," J. Phys. Chem. A **118**, 3243 (2014).

[149]D. Troya and E. García-Molina, "Quasiclassical trajectory study of the $O(^3P) + CH_4 \rightarrow OH + CH_3$ reaction with a specific reaction parameters semiempirical Hamiltonian," J. Phys. Chem. A **109**, 3015 (2005).

[150]C. Gonzalez, J. J. W. McDouall, and H. B. Schlegel, "*Ab initio* study of the reactions between methane and OH, H, and $O_3$," J. Phys. Chem. **94**, 7467 (1990).

[151]F. Huarte-Larrañaga and U. Manthe, "Accurate quantum dynamics of a combustion reaction: Thermal rate constants of $O(^3P) + CH_4 \rightarrow OH + CH_3$," J. Chem. Phys. **117**, 4635 (2002).

[152]H.-G. Yu and G. Nyman, "Quantum dynamics of the $O(^3P) + CH_4 \rightarrow OH + CH_3$ reaction: An application of the rotating bond umbrella model and spectral transform subspace iteration," J. Chem. Phys. **112**, 238 (2000).

[153]J. V. Michael, D. G. Keil, and R. B. Klemm, "Theoretical rate-constant calculations for $O(^3P)$ with saturated-hydrocarbons," Int. J. Chem. Kinet. **15**, 705 (1983).

[154]N. Cohen and K. R. Westberg, "The use of transition-state theory to extrapolate rate coefficients for reactions of O-atoms with alkanes," Int. J. Chem. Kinet. **18**, 99 (1986).

[155]N. Cohen, "A reevaluation of low-temperature experimental rate data for the reactions of O-atoms with methane, ethane, and neopentane," Int. J. Chem. Kinet. **18**, 59 (1986).

[156]R. B. Klemm, T. Tanzawa, E. G. Skolnik, and J. V. Michael, "A resonance fluorescence kinetic study of the $O(^3P) + CH_4$ reaction over the temperature range 474 K to 1156," Symp. Int. Combust. Proc. **18**, 785 (1981).

[157]P. Roth and T. H. Just, "Measurements of some elementary hydrocarbon reactions at high temperatures," NBS Spec. Publ. **10**, 1339 (1979).

[158]J. T. Herron and R. E. Huie, "Rate constants for the reactions of atomic oxygen $O(^3P)$ with organic compounds in the gas phase," J. Phys. Chem. Ref. Data **2**, 467 (1973).

[159]J. T. Herron and R. E. Huie, "Rates of reaction of atomic oxygen. 2. Some $C_2$–$C_8$ alkanes," J. Phys. Chem. **73**, 3327 (1969).

[160]A. Miyoshi, K. Tsuchiya, N. Yamauchi, and H. Matsui, "Reactions of atomic oxygen $(^3P)$ with selected alkanes," J. Phys. Chem. **98**, 11452 (1994).

[161]K. Ohmori, M. Yoshimura, M. Koshi, and H. Matsui, "A flash-photolysis study of $CH_4$–$O_2$ mixtures behind shock-waves: Examination of reaction of $CH_3 + O_2$," Bull. Chem. Soc. Jpn. **65**, 1317 (1992).

[162]J. W. Sutherland and R. B. Klemm, "Kinetic studies of elementary reactions using the flash photolysis-shock tube technique," in 16th Symposium (International) on Combustion (1987), p. 395.

[163]W. Felder and S. Madronich, "High-temperature photochemistry (HTP): Kinetics and mechanism studies of elementary combustion reactions over 300–1700 K," Combust. Sci. Technol. **50**, 135 (1986).

[164]W. Felder and A. Fontijn, "High-temperature photochemistry, a new technique for rate coefficient measurements over wide temperature ranges: Initial measurements on the O + $CH_4$ reaction from 525–1250 K," Chem. Phys. Lett. **67**, 53 (1979).

[165]J. W. Falconer, D. E. Hoare, and R. Overend, "Photolysis of carbon dioxide and methane mixtures at 873 and 293 K with 163.3 nm light," J. Chem. Soc. Faraday Trans. 1 **69**, 1541 (1973).

[166]F. W. Froben, "Reaction of oxygen atoms with methane chloroform and carbon tetrachloride," Ber. Bunsenges. Phys. Chem. **72**, 996 (1968).

[167]E. L. Wong and A. E. Potter, "Mass-spectrometric investigation of reaction of oxygen atoms with methane," Can. J. Chem. **45**, 367 (1967).

[168]J. M. Brown and B. A. Thrush, "ESR studies of reactions of atomic oxygen and hydrogen with simple hydrocarbons," Trans. Faraday Soc. **63**, 630 (1967).

[169]R. D. Cadle and E. R. Allen, "Kinetics of reaction of $O(^3P)$ with methane in oxygen nitrogen and argon-oxygen mixtures," J. Phys. Chem. **69**, 1611 (1965).

[170]E. L. Wong and A. E. Potter, "Reaction rates of hydrogen, ammonia, and methane with mixtures of atomic and molecular oxygen," J. Chem. Phys. **39**, 2211 (1963).

[171]H. Zhao, W. Wang, and Y. Zhao, "Thermal rate constants for the $O(^3P) + CH_4 \rightarrow OH + CH_3$ reaction: The effects of quantum tunneling and potential energy barrier shape," J. Phys. Chem. A **120**, 7589 (2016).

[172]D. C. Clary, "Quantum dynamics of the $O(^3P) + CH_4 \rightarrow CH_3 + OH$ reaction," Phys. Chem. Chem. Phys. **1**, 1173 (1999).

[173]J. C. Corchado, J. Espinosa-García, O. Roberto-Neto, Y.-Y. Chuang, and D. G. Truhlar, "Dual-level direct dynamics calculations of the reaction rates for a Jahn-Teller reaction: Hydrogen abstraction from $CH_4$ or $CD_4$ by $O(^3P)$," J. Phys. Chem. A **102**, 4899 (1998).

[174]R. Shaw, "Semiempirical extrapolation and estimation of rate constants for abstraction of H from methane by H, O, HO, and $O_2$," J. Phys. Chem. Ref. Data **7**, 1179 (1978).

[175]S. W. Mayer and L. Schieler, "Activation energies and rate constants computed for reactions of oxygen with hydrocarbons," J. Phys. Chem. **72**, 2628 (1968).

[176]S. W. Mayer and L. Schieler, "Computed activation energies and rate constants for forward and reverse transfers of hydrogen atoms," J. Phys. Chem. **72**, 236 (1968).

[177]W. C. Kreye and P. G. Seybold, "*Ab initio* study of the energetics and thermodynamics of hydrogen abstraction from fluoromethanes by $O(^3P)$. II: $CF_nH_{4-n} + O(^3P) \rightarrow CF_nH_{4-n} \cdots O \rightarrow CF_nH_{3-n} + OH$ (n = 0, 1, 2)," Chem. Phys. Lett. **335**, 257 (2001).

[178]B. Wang, H. Hou, and Y. Gu, "Theoretical investigation of the reactions of $O(^3P)$ with $CH_3F$ and $CH_2F_2$," Chem. Phys. **247**, 201 (1999).

[179]L. J. Medhurst, J. Fleming, and H. H. Nelson, "Reaction rate constants of $OH + CHF_3 \rightarrow$ products and $O(^3P) + CHF_3 \rightarrow OH + CF_3$ at 500–750 K," Chem. Phys. Lett. **266**, 607 (1997).

[180]J. L. Jourdain, G. Poulet, J. Barassin, G. Le Bras, and J. Combourieu, "Mecanismes chimiques de la pollution atmospherique par les composes halogenes: Etude cinetique de reactions elementaires possibles," Pollut. Atmos. **75**, 256 (1977).

[181]M. G. Bryukov, V. D. Knyazev, S. M. Lomnicki, C. A. McFerrin, and B. Dellinger, "Temperature-dependent kinetics of the gas-phase reactions of OH with $Cl_2$, $CH_4$, and $C_3H_8$," J. Phys. Chem. A **108**, 10464 (2004).

[182]J. R. Dunlop and F. P. Tully, "A kinetic-study of OH radical reactions with methane and perdeuterated methane," J. Phys. Chem. **97**, 11148 (1993).

[183]T. Gierczak, R. K. Talukdar, S. C. Herndon, G. L. Vaghjiani, and A. R. Ravishankara, "Rate coefficients for the reactions of hydroxyl radicals with methane and deuterated methanes," J. Phys. Chem. A **101**, 3125 (1997).

[184]G. L. Vaghjiani and A. R. Ravishankara, "New measurement of the rate coefficient for the reaction of OH with methane," Nature **350**, 406 (1991).

[185]D. Amedro, K. Miyazaki, A. Parker, C. Schoemaecker, and C. Fittschen, "Atmospheric and kinetic studies of OH and $HO_2$ by the FAGE technique," J. Environ. Sci. **24**, 78 (2012).

[186]R. P. Overend, G. Paraskevopoulos, and R. J. Cvetanović, "Rates of OH radical reactions. 1. Reactions with $H_2$, $CH_4$, $C_2H_6$, and $C_3H_8$ at 295 K," Can. J. Chem. **53**, 3374 (1975).

[187]J. B. Burkholder, S. P. Sander, J. P. D. Abbat, J. R. Barker, R. E. Huie, C. E. Kolb, M. J. Kurylo, V. L. Orkin, D. M. Wilmouth, and P. H. Wine, *Chemical Kinetics and Photochemical Data for Use in Atmospheric Studies*, Evaluation Number 18 JPL Pub. 15-10, California Institute of Technology, Pasadena, CA, 2015.

[188]N. K. Srinivasan, M.-C. Su, J. W. Sutherland, and J. V. Michael, "Reflected shock tube studies of high-temperature reaction rate constants for $OH + CH_4 \rightarrow CH_3 + H_2O$ and $CH_3 + NO_2 \rightarrow CH_3O + NO$," J. Phys. Chem. A **109**, 1857 (2005).

[189]D. L. Baulch, C. J. Cobos, R. A. Cox, C. Esser, P. Frank, T. Just, J. A. Kerr, M. J. Pilling, J. Troe, R. W. Walker, and J. Warnatz, "Evaluated kinetic data for combustion modeling," J. Phys. Chem. Ref. Data **21**, 411 (1992).

[190]W. Tsang and R. F. Hampson, "Chemical kinetic database for combustion chemistry. 1. Methane and related-compounds," J. Phys. Chem. Ref. Data **15**, 1087 (1986).

[191]N. Cohen and K. R. Westberg, "Chemical kinetic data sheets for high-temperature chemical reactions," J. Phys. Chem. Ref. Data **12**, 531 (1983).

[192]J. Ernst, H. G. Wagner, and R. Zellner, "Combined flash photolysis-shock-tube study of absolute rate constants for reactions of hydroxyl radical with $CH_4$ and $CF_3H$ around 1300 K," Ber. Bunsenges. Phys. Chem. **82**, 409 (1978).

[193]A. Mellouki, S. Téton, G. Laverdet, A. Quilgars, and G. Le Bras, "Kinetic-studies of OH reactions with $H_2O_2$, $C_3H_8$ and $CH_4$ using the pulsed-laser photolysis—Laser-induced fluorescence method," J. Chim. Phys. PCB **91**, 473 (1994).

[194]I. T. Lancar, G. Lebras, and G. Poulet, "New determination of the rate-constant for the reaction $CH_4 + OH$ and its atmospheric implication," C. R. Acad. Sci. **315**, 1487 (1992).

[195]B. J. Finlayson-Pitts, M. J. Ezell, T. M. Jayaweera, H. N. Berko, and C. C. Lai, "Kinetics of the reactions of OH with methyl chloroform and methane-implications

for global tropospheric OH and the methane budget," Geophys. Res. Lett. **19**, 1371, https://doi.org/10.1029/92gl01279 (1992).

[196]G. P. Smith, P. W. Fairchild, J. B. Jeffries, and D. R. Crosley, "Laser pyrolysis laser fluorescence studies of high-temperature reaction-rates: Description of the method and results for $OH + CH_4$, $C_3H_8$, and $C_3H_6$," J. Phys. Chem. **89**, 1269 (1985).

[197]D. Husain, J. M. C. Plane, and N. K. H. Slater, "Kinetic investigation of the reactions of $OH(X^2\Pi)$ with the hydrogen halides, HCl, DC1, HBr and DBr by time-resolved resonance fluorescence $(A^+\Sigma^+)$–$X^2\Pi$)," J. Chem. Soc. Faraday Trans. 2 **77**, 1949 (1981).

[198]T. J. Sworski, C. J. Hochanadel, and P. J. Ogren, "Flash-Photolysis of $H_2O$ vapor in $CH_4$–H and OH yields and rate constants for $CH_3$ reactions with H and OH," J. Phys. Chem. **84**, 129 (1980).

[199]R. A. Cox, R. G. Derwent, and P. M. Holt, "Relative rate constants for reactions of OH radicals with $H_2$, $CH_4$, CO, NO and HONO at atmospheric-pressure and 296 K," J. Chem. Soc. Faraday Trans. 1 **72**, 2031 (1976).

[200]Z. Hong, D. F. Davidson, K.-Y. Lam, and R. K. Hanson, "A shock tube study of the rate constants of $HO_2$ and $CH_3$ reactions," Combust. Flame **159**, 3007 (2012).

[201]P. Sharkey and I. W. M. Smith, "Kinetics of elementary reactions at low-temperatures: Rate constants for the reactions of OH with HCl ($298 \geq T/K \geq 138$), $CH_4$ ($298 \geq T/K \geq 178$) and $C_2H_6$ ($298 \geq T/K \geq 138$)," J. Chem. Soc. Faraday Trans. **89**, 631 (1993).

[202]R. A. Yetter and F. L. Dryer, "Inhibition of moist carbon monoxide oxidation by trace amounts of hydrocarbons," Symp. Int. Combust. Proc. **24**, 757 (1992).

[203]J. F. Bott and N. Cohen, "A shock-tube study of the reaction of the hydroxyl radical with $H_2$, $CH_4$, c-$C_5H_{10}$, and i-$C_4H_{10}$," Int. J. Chem. Kinet. **21**, 485 (1989).

[204]S. Madronich and W. Felder, "Direct measurements of the rate coefficient for the reaction $OH + CH_4 \rightarrow CH_3 + H_2O$ over 300–1500 K," Symp. Int. Combust. Proc. **20**, 703 (1985).

[205]C. D. Jonah, W. A. Mulac, and P. Zeglinski, "Rate constants for the reaction of $OH + CO$, $OD + CO$, and $OH + Methane$ as a function of temperature," J. Phys. Chem. **88**, 4100 (1984).

[206]D. L. Baulch, R. J. B. Craven, M. Din, D. D. Drysdale, S. Grant, D. J. Richardson, A. Walker, and G. Watling, "Rates of hydroxy radical reactions with methane, ethane and propane over the temperature-range 403–696 K," J. Chem. Soc. Faraday Trans. 1 **79**, 689 (1983).

[207]K. M. Jeong and F. Kaufman, "Kinetics of the reaction of hydroxyl radical with methane and with 9 Cl-substituted and F-substituted methanes. 2. Calculation of rate parameters as a test of transition-state theory," J. Phys. Chem. **86**, 1816 (1982).

[208]F. P. Tully and A. R. Ravishankara, "Flash photolysis-resonance fluorescence kinetic-study of the reactions $OH + H_2 \rightarrow H_2O + H$ and $OH + CH_4 \rightarrow H_2O + CH_3$ from 298 to 1020 K," J. Phys. Chem. **84**, 3126 (1980).

[209]R. Zellner and W. Steinert, "Flash-Photolysis study of rate of reaction $OH + CH_4 \rightarrow CH_3 + H_2O$ over an extended temperature-range," Int. J. Chem. Kinet. **8**, 397 (1976).

[210]C. J. Howard and K. M. Evenson, "Rate constants for reactions of OH with $CH_4$ and fluorine, chlorine, and bromine substituted methanes at 296 K," J. Chem. Phys. **64**, 197 (1976).

[211]W. Steinert and R. Zellner, "Rates of reaction of OH with CO and $CH_4$ over an extended temperature range," Deuxieme Symp. Eur. Combust. **2**, 31 (1975).

[212]J. J. Margitan, F. Kaufman, and J. G. Anderson, "The reaction of OH with $CH_4$," Geophys. Res. Lett. **1**, 80, https://doi.org/10.1029/gl001i002p00080 (1974).

[213]D. D. Davis, S. Fischer, and R. Schiff, "Flash photolysis-resonance fluorescence kinetics study: Temperature-dependence of reactions $OH + CO \rightarrow CO_2 + H$ and $OH + CH_4 \rightarrow H_2O + CH_3$," J. Chem. Phys. **61**, 2213 (1974).

[214]N. R. Greiner, "Hydroxyl radical kinetics by kinetic spectroscopy. 6. Reactions with alkanes in range 300–500 °K," J. Chem. Phys. **53**, 1070 (1970).

[215]W. E. Wilson and A. A. Westenberg, "Study of the reaction of hydroxyl radical with methane by quantitative ESR," Symp. Int. Combust. **11**, 1143 (1967).

[216]D. G. Horne and R. G. W. Norrish, "Rate of H-abstraction by OH from hydrocarbons," Nature **215**, 1373 (1967).

[217]R. M. Fristrom, "Radical concentrations and reactions in a methane-oxygen flame," Symp. Int. Combust. Proc. **9**, 560 (1963).

[218]P. Blowers and K. Hollingshead, "Estimations of global warming potentials from computational chemistry calculations for $CH_2F_2$ and other fluorinated methyl species verified by comparison to experiment," J. Phys. Chem. A **113**, 5942 (2009).

[219]J. Korchowiec, "Mechanism of hydrogen abstraction from methane and hydro-fluoromethanes by hydroxyl radical," J. Phys. Org. Chem. **15**, 524 (2002).

[220]L. Masgrau, À. González-Lafont, and J. M. Lluch, "The reactions $CHnD_{4−n}$ +OH → P and $CH_4$ + OD → $CH_3$ + HOD as a test of current direct dynamics multicoefficient methods to determine variational transition state rate constants. II," J. Chem. Phys. **115**, 4515 (2001).

[221]S. El-Taher, "*Ab initio* study of reactions of hydroxyl radicals with chloro- and fluoro-substituted methanes," Int. J. Quantum Chem. **84**, 426 (2001).

[222]J. Korchowiec, S. Kawahara, K. Matsumura, T. Uchimaru, and M. Sugie, "Hydrogen abstraction from methane and hydrofluoromethanes by OH radical: Modified GAUSSIAN-2 study," J. Phys. Chem. A **103**, 3548 (1999).

[223]B. S. Jursic, "Density functional theory study of radical hydrogen abstraction with hydrogen and hydroxyl radicals," Chem. Phys. Lett. **256**, 603 (1996).

[224]W. B. DeMore, "Experimental and estimated rate constants for the reactions of hydroxyl radicals with several halocarbons," J. Phys. Chem. **100**, 5813 (1996).

[225]K.-J. Hsu and W. B. Demore, "Rate constants and temperature dependences for the reactions of hydroxyl radical with several halogenated methanes, ethanes, and propanes by relative rate measurements," J. Phys. Chem. **99**, 1235 (1995).

[226]A. M. Schmoltner, R. K. Talukdar, R. F. Warren, A. Mellouki, L. Goldfarb, T. Gierczak, S. A. McKeen, and A. R. Ravishankara, "Rate coefficients for reactions of several hydrofluorocarbons with OH and O($^1$D) and their atmospheric lifetimes," J. Phys. Chem. **97**, 8976 (1993).

[227]J. Kowalczyk, A. Jówko, and M. Symanowicz, "Kinetics of radical reactions in freons," J. Radioanal. Nucl. Chem. **232**, 75 (1998).

[228]T. J. Wallington, M. D. Hurley, J. Shi, M. M. Maricq, J. Sehested, O. J. Nielsen, and T. Ellermann, "A kinetic-study of the reaction of fluorine-atoms with $CH_3F$, $CH_3Br$, $CH_3Br$, $CF_2H_2$, CO, $CF_3H$, $CF_3CHBr_2$, $CF_3CH_2F$, $CHF_2CHF_2$, $CF_2BrCH_3$, $CHF_2CH_3$, and $CF_3CF_2H$ at 295 ± 2 K," Int. J. Chem. Kinet. **25**, 651 (1993).

[229]R. K. Bera and R. J. Hanrahan, "Investigation of gas-phase reactions of OH radicals with fluoromethane and difluoromethane using Ar-sensitized pulse-radi-olysis," Radiat. Phys. Chem. **32**, 579 (1988).

[230]W. S. Nip, D. L. Singleton, R. Overend, and G. Paraskevopoulos, "Rates of OH radical reactions. 5. Reactions with $CH_3F$, $CH_2F_2$, $CHF_3$, $CH_3CH_2F$, and $CH_3CHF_2$ at 297 K," J. Phys. Chem. **83**, 2440 (1979).

[231]A. S. Petit and J. N. Harvey, "Atmospheric hydrocarbon activation by the hydroxyl radical: A simple yet accurate computational protocol for calculating rate coefficients," Phys. Chem. Chem. Phys. **14**, 184 (2012).

[232]M. Marinkovic, M. Gruber-Stadler, J. M. Nicovich, R. Soller, M. Mülhäuser, P. H. Wine, L. Bache-Andreassen, and C. J. Nielsen, "Experimental and theoretical study of the carbon-13 and deuterium kinetic isotope effects in the Cl and OH reactions of $CH_3F$," J. Phys. Chem. **112**, 12416 (2008).

[233]T. V. Albu and S. Swaminathan, "Hybrid density functional theory with specific reaction parameter: Hydrogen abstraction reaction of fluoromethane by the hydroxyl radical," J. Phys. Chem. A **110**, 7663 (2006).

[234]P.-Y. Lien, R.-M. You, and W.-P. Hu, "Theoretical modeling of the hydrogen abstraction reaction of fluoromethane by the hydroxyl radical," J. Phys. Chem. A **105**, 2391 (2001).

[235]F. Louis, C. A. Gonzalez, R. E. Huie, and M. J. Kurylo, "An *ab initio* study of the kinetics of the reactions of halomethanes with the hydroxyl radical. 2. A comparison between theoretical and experimental values of the kinetic parameters for 12 partially halogenated methanes," J. Phys. Chem. A **104**, 8773 (2000).

[236]J. Espinosa-García, E. L. Coitiño, A. González-Lafont, and J. M. Lluch, "Reaction-path and dual-level dynamics calculations of the $CH_3F$ + OH reaction," J. Phys. Chem. A **102**, 10715 (1998).

[237]R. Talukdar, A. Mellouki, T. Gierczak, J. B. Burkholder, S. A. McKeen, and A. R. Ravishankara, "Atmospheric fate of $CF_2H_2$, $CH_3CF_3$, $CHF_2CF_3$, and $CH_3CFCl_2$: Rate coefficients for reactions with OH and UV absorption cross-sections of $CH_3CFCl_2$," J. Phys. Chem. **95**, 5815 (1991).

[238]M. A. A. Clyne and P. M. Holt, "Reaction-kinetics involving ground $X^2\Pi$ and excited $A^2\Sigma^+$ hydroxyl radicals. 2. Rate constants for reactions of OH $X^2\Pi$ with halogenomethanes and halogenoethanes," J. Chem. Soc. Faraday Trans. 2 **75**, 582 (1979).

[239]I. Szilágyi, S. Dóbé, and T. Bérces, "Rate constant for the reaction of the OH-radical with $CH_2F_2$," React. Kinet. Catal. Lett. **70**, 319 (2000).

[240]T. V. Albu and S. Swaminathan, "Hybrid density functional theory with a specific reaction parameter: Hydrogen abstraction reaction of difluoromethane by the hydroxyl radical," J. Mol. Model. **13**, 1109 (2007).

[241]A. González-Lafont, J. M. Lluch, and J. Espinosa-García, "Variational transition state calculations of the $CH_2F_2$ + OH hydrogen abstraction reaction," J. Phys. Chem. A **105**, 10553 (2001).

[242]A. Bottoni, G. Poggi, and S. S. Emmi, "An *ab initio* study of H-abstraction in halogen-substituted methanes by the OH radical," J. Mol. Struct.: THEOCHEM **279**, 299 (1993).

[243]N. K. Srinivasan, M.-C. Su, J. V. Michael, S. J. Klippenstein, and L. B. Harding, "Reflected shock tube and theoretical studies of high-temperature rate constants for OH + $CF_3H$ → $CF_3$ + $H_2O$ and $CF_3$ + OH → Products," J. Phys. Chem. A **111**, 6822 (2007).

[244]L. Chen, S. Kutsuna, K. Tokuhashi, and A. Sekiya, "New technique for gener-ating high concentrations of gaseous OH radicals in relative rate measurements," Int. J. Chem. Kinet. **35**, 317 (2003).

[245]J. N. Bradley, W. D. Capey, R. W. Fair, and D. K. Pritchard, "Shock-tube study of kinetics of reaction of hydroxyl radicals with $H_2$, CO, $CH_4$, $CF_3H$, $C_2H_4$, and $C_2H_6$," Int. J. Chem. Kinet. **8**, 549 (1976).

[246]T. V. Albu and S. Swaminathan, "Hybrid density functional theory with a specific reaction parameter: Hydrogen abstraction reaction of trifluoromethane by the hydroxyl radical," Theor. Chem. Acc. **117**, 383 (2007).

[247]L. Wang, J.-y. Liu, Z.-s. Li, and C.-c. Sun, "Direct dynamics studies on the hydrogen abstraction reactions of an F atom with $CH_3X$ (X = F, Cl, and Br)," J. Chem. Theory Comput. **1**, 201 (2005).

[248]L. Wang, J.-y. Liu, and Z.-s. Li, "*Ab initio* direct dynamics studies on the hydrogen abstraction reactions of $CF_2H_2$ and $CF_3H$ with F atom," Chem. Phys. **351**, 154 (2008).

[249]A. Persky, "Kinetics of the F + $CH_4$ reaction in the temperature range 184–406 K," J. Phys. Chem. **100**, 689 (1996).

[250]A. Persky, "Kinetics of the reactions F + $H_2S$ and F+$D_2S$ at 298 K," Chem. Phys. Lett. **298**, 390 (1998).

[251]A. Persky, "The temperature dependence of the rate constants for the reactions F + $CH_3F$ and F + $CH_2F_2$," Chem. Phys. Lett. **376**, 181 (2003).

[252]A. Persky, "The temperature dependence of the kinetic isotope effect in the reaction of F atoms with $CH_4$ and $CD_4$," Chem. Phys. Lett. **430**, 251 (2006).

[253]R. Foon and G. P. Reid, "Kinetics of gas phase fluorination of hydrogen and alkanes," Trans. Faraday Soc. **67**, 3513 (1971).

[254]H. G. Wagner, J. Warnatz, and C. Zetzsch, "Reaction of F Atoms with methane," Ann. Asoc. Quim. Argent. **59**, 169 (1971).

[255]T. Beiderhase, W. Hack, and K. Hoyermann, "Elementary reactions in the C–H–F system," Z. Phys. Chem. **188**, 227 (1995).

[256]F. Louis and J.-P. Sawerysyn, "Kinetics and products studies of reactions between fluorine atoms and $CHF_3$, $CHClF_2$, $CHCl_2F$ and $CHCl_3$," J. Chem. Soc. Faraday Trans. **94**, 1437 (1998).

[257]M. M. Maricq and J. J. Szente, "Upper limits for the rate constants of the reactions $CF_3O$ + $O_3$ → $CF_3$ + $O_2$ and $CF_3O_2$ + $O_3$ → $CF_3$ + 2$O_2$," Chem. Phys. Lett. **213**, 449 (1993).

[258]M. A. A. Clyne, D. J. McKenney, and R. F. Walker, "Reaction-kinetics of ground-state fluorine, F($^2$P), atoms. 1. Measurement of fluorine atom concentrations and rates of reactions F + $CHF_3$ and F + $Cl_2$ using mass-spectrometry," Can. J. Chem. **51**, 3596 (1973).

[259]D. Wang and G. Czakó, "Quantum dynamics study of the F + $CH_4$ → HF + $CH_3$ reaction on an *ab initio* potential energy surface," J. Phys. Chem. A **117**, 7124 (2013).

[260]T. Chu, K. Han, and J. Espinosa-Garcia, "A five-dimensional quantum dynamics study of the F($^2$P) + $CH_4$ reaction," J. Chem. Phys. **131**, 244303 (2009).

[261]C. Moore and I. W. M. Smith, "Rate constants for the reactions of fluorine-atoms with alkanes and hydrofluorocarbons at room-temperature," J. Chem. Soc. Faraday Trans. **91**, 3041 (1995).

[262]C. M. Moore, I. W. M. Smith, and D. W. A. Stewart, "Rates of processes initiated by pulsed-laser production of F atoms in the presence of HCl, $CH_4$, and $CF_3H$," Int. J. Chem. Kinet. **26**, 813 (1994).

[263]U. Wörsdörfer and H. Heydtmann, "Bimolecular reactions of fluorine-atoms with $CH_3I$ and $CH_2I_2$," Ber. Bunsenges. Phys. Chem. **93**, 1132 (1989).

[264] P. Pagsberg, J. Munk, A. Sillesen, and C. Anastasi, "UV spectrum and kinetics of hydroxymethyl radicals," Chem. Phys. Lett. **146**, 375 (1988).

[265] D. M. Fasano and N. S. Nogar, "Rate determination for F + CH$_4$ by real-time competitive kinetics," Chem. Phys. Lett. **92**, 411 (1982).

[266] M. A. A. Clyne and W. S. Nip, "Kinetics of fluorine atom reactions using resonance-absorption spectrometry in far vacuum ultraviolet reactions F + HCl, CH$_4$, CHCl$_3$, CHCl$_2$F, and CHClF$_2$," Int. J. Chem. Kinet. **10**, 367 (1978).

[267] K. L. Kompa and J. Wanner, "Study of some fluorine atom reactions using a chemical laser method," Chem. Phys. Lett. **12**, 560 (1972).

[268] J. Espinosa-García, J. L. Bravo, and C. Rangel, "New analytical potential energy surface for the F($^2$P) + CH$_4$ hydrogen abstraction reaction: Kinetics and dynamics," J. Phys. Chem. A **111**, 2761 (2007).

[269] O. Roberto-Neto, F. B. C. Machado, and F. R. Ornellas, "Transition state structure, energetics, and rate constants for the CH$_4$ + F($^2$P) → CH$_3$+HF reaction," Chem. Phys. **315**, 27 (2005).

[270] C. Rángel, M. Navarrete, and J. Espinosa-García, "Potential energy surface for the F($^2$P) + CH$_4$ hydrogen abstraction reaction. Kinetics and dynamics study," J. Phys. Chem. A **109**, 1441 (2005).

[271] D. Troya, J. Millán, I. Baños, and M. González, "*Ab initio* potential energy surface, variational transition state theory, and quasiclassical trajectory studies of the F + CH$_4$ → HF + CH$_3$ reaction," J. Chem. Phys. **120**, 5181 (2004).

[272] A. S. Manocha, D. W. Setser, and M. A. Wickramaaratchi, "Vibrational-energy disposal in reactions of fluorine-atoms with hydrides of group-III, group-IV and group-V," Chem. Phys. **76**, 129 (1983).

[273] D. J. Smith, D. W. Setser, K. C. Kim, and D. J. Bogan, "HF IR chemiluminescence: Relative rate constants for hydrogen abstraction from hydrocarbons, substituted methanes, and inorganic hydrides," J. Phys. Chem. **81**, 898 (1977).

[274] R. G. Manning, E. R. Grant, J. C. Merrill, and J. W. Root, "Hydrogen abstraction reactions of thermal fluorine-atoms with hydrocarbons and fluorinated hydrocarbons," Abstr. Pap. Am. Chem. Soc **168**, 132 (1974).

[275] T. L. Pollock and W. E. Jones, "Gas-Phase reactions of fluorine atoms," Can. J. Chem. **51**, 2041 (1973).

[276] M. A. A. Clyne and A. Hodgson, "Kinetics and detection of F($^2$P) atoms in a discharge flow system," Chem. Phys. **79**, 351 (1983).

[277] O. J. Nielsen, T. Ellermann, E. Bartkiewicz, T. J. Wallington, and M. D. Hurley, "UV absorption-spectra, kinetics and mechanisms of the self-reaction of CHF$_2$O$_2$ radicals in the gas-phase at 298 K," Chem. Phys. Lett. **192**, 82 (1992).

[278] O. J. Nielsen, T. Ellermann, J. Sehested, E. Bartkiewicz, T. J. Wallington, and M. D. Hurley, "UV absorption-spectra, kinetics, and mechanisms of the self reaction of CF$_3$O$_2$ radicals in the gas-phase at 295 K," Int. J. Chem. Kinet. **24**, 1009 (1992).

[279] M. M. Maricq and J. J. Szente, "Flash-Photolysis time-resolved UV absorption study of the reactions CF$_3$H + F = CF$_3$ + HF and CF$_3$O$_2$ + CF$_3$O$_2$ products," J. Phys. Chem. **96**, 4925 (1992).

[280] M. A. A. Clyne and A. Hodgson, "Absolute rate constants for the reaction of fluorine-atoms with H$_2$, CH$_2$Cl$_2$, CH$_2$ClF, CH$_2$F$_2$ and CHCl$_2$," J. Chem. Soc. Faraday Trans. 2 **81**, 443 (1985).

[281] I. B. Goldberg and G. R. Schneider, "Kinetic study of reaction of F with H$_2$ and CF$_3$H by ESR methods," J. Chem. Phys. **65**, 147 (1976).

[282] Y. Okamoto and M. Tomonari, "*Ab initio* calculations on reactions of CHF$_3$ with its fragments," J. Phys. Chem. A **104**, 2729 (2000).

[283] F. Louis, M.-T. Rayez, J.-C. Rayez, and J.-P. Sawerysyn, "*Ab initio* theoretical studies of the reactions between fluorine atoms and halomethanes of type CHCl$_{3-x}$F$_x$ (x = 0, 1, 2 or 3)," Phys. Chem. Chem. Phys. **1**, 383 (1999).

[284] D. G. Truhlar and B. C. Garrett, "Variational transition-state theory," Annu. Rev. Phys. Chem. **35**, 159 (1984).

[285] B. C. Garrett and D. G. Truhlar, "Semi-classical tunneling calculations," J. Phys. Chem. **83**, 2921 (1979).

[286] T. L. Nguyen, J. F. Stanton, and J. R. Barker, "*Ab initio* reaction rate constants computed using semiclassical transition-state theory: HO + H$_2$ → H$_2$O + H and isotopologues," J. Phys. Chem. A **115**, 5118 (2011).

[287] B. C. Garrett, T. Joseph, T. N. Truong, and D. G. Truhlar, "Application of the large-curvature tunneling approximation to polyatomic-molecules: Abstraction of H or D by methyl radical," Chem. Phys. **136**, 271 (1989).

[288] F. Zhang and T. S. Dibble, "Impact of tunneling on hydrogen-migration of the *n*-propylperoxy radical," Phys. Chem. Chem. Phys. **13**, 17969 (2011).

[289] A. G. Vandeputte, M. K. Sabbe, M.-F. Reyniers, V. Van Speybroeck, M. Waroquier, and G. B. Marin, "Theoretical study of the thermodynamics and kinetics of hydrogen abstractions from hydrocarbons," J. Phys. Chem. A **111**, 11771 (2007).

[290] A. F. Wagner, "Improved multidimensional semiclassical tunneling theory," J. Phys. Chem. A **117**, 13089 (2013).

[291] J. Pu, J. C. Corchado, and D. G. Truhlar, "Test of variational transition state theory with multidimensional tunneling contributions against an accurate full-dimensional rate constant calculation for a six-atom system," J. Chem. Phys. **115**, 6266 (2001).

[292] T. N. Truong, "A direct *ab initio* dynamics approach for calculating thermal rate constants using variational transition-state theory and multidimensional semiclassical tunneling methods. An application to the CH$_4$ + H ↔ CH$_3$ + H$_2$ reaction," J. Chem. Phys. **100**, 8014 (1994).

[293] R. P. Bell, "The tunnel effect correction for parabolic potential barriers," Trans. Faraday Soc. **55**, 1 (1959).

[294] E. Wigner, "On the quantum correction for thermodynamic equilibrium," Phys. Rev. **40**, 749 (1932).

[295] C. A. Gonzalez, T. C. Allison, and F. Louis, "General expression for the effective mass in the one-dimensional treatment of tunneling corrections," J. Phys. Chem. A **105**, 11034 (2001).

[296] R. L. Brown, "A method of calculating tunneling corrections for Eckart potential barriers," J. Res. Nat. Bur. Stand. **86**, 357 (1981).

[297] C. Eckart, "The penetration of a potential barrier by electrons," Phys. Rev. **35**, 1303 (1930).

[298] R. Steckler, W.-P. Hu, Y.-P. Liu, G. C. Lynch, B. C. Garrett, A. D. Isaacson, V. S. Melissas, D.-H. Lu, T. N. Truong, S. N. Rai, G. C. Hancock, J. G. Lauderdale, T. Joseph, and D. G. Truhlar, "Polyrate-6.5: A new version of a computer-program for the calculation of chemical-reaction rates for polyatomics," Comput. Phys. Commun. **88**, 341 (1995).

[299] A. D. Isaacson, D. G. Truhlar, S. N. Rai, R. Steckler, G. C. Hancock, B. C. Garrett, and M. J. Redmon, "Polyrate: A general computer-program for variational transition-state theory and semiclassical tunneling calculations of chemical-reaction rates," Comput. Phys. Commun. **47**, 91 (1987).

[300] W. T. Duncan, R. L. Bell, and T. N. Truong, "The Rate: Program for *ab initio* direct dynamics calculations of thermal and vibrational-state-selected rate constants," J. Comput. Chem. **19**, 1039 (1998).

[301] H. Eyring, "The activated complex and the absolute rate of chemical reactions," Chem. Rev. **17**, 65 (1935).

[302] H. Eyring, "The activated complex in chemical reactions," J. Chem. Phys. **3**, 107 (1935).